

吉林大学仪器科学与电气工程学院

**College of Instrumentation & Electrical Engineering, Jilin University**

科技学术实践“六个一”训练项目

**Academic Practice “Six in One” Training Project**

论文集  
**Proceedings**

2016 年下半年

2016 (Second Half)



# 目录

## CONTENTS

### 第一部分 中文论文集

#### Part I Chinese Proceedings

|                                       |    |
|---------------------------------------|----|
| 基于温湿度检测的大型园艺场自动监控系统 .....             |    |
| ..... 陈祖斌; 杨宛瑾; 周 琪; 包家鑫              | 1  |
| 基于自适应窗宽的航空电磁剖面数据噪声压制技术 .....          |    |
| ..... 刘子铭; 高殿尧; 刘学英                   | 5  |
| 基于 ZigBee 的路灯管理系统 .....               |    |
| ..... 丁 芑; 施 斌; 王雅新                   | 10 |
| 基于贝叶斯算法电梯运行效率的研究* .....               |    |
| ..... 张思雨; 周 炆; 任桂莹                   | 14 |
| 一种基于 GPS 与 GPRS 的便携式酒精检测仪的设计与实现 ..... |    |
| ..... 温雪君; 刘小晗; 蔡 瑶                   | 20 |
| 基于 PZT 的多方向风能收集装置设计与应用 .....          | 26 |
| ..... 苟 鑫; 陈玉达; 刘丽佳                   | 26 |
| 基于 QR 码扫描的智能冰箱食品管理系统的设计 .....         | 31 |
| ..... 张碧兰; 杜俊岐; 赵 佐                   | 31 |

## 第二部分 英文论文集

### Part II English Proceedings

|   |     |
|---|-----|
| The Automatic Monitoring System of Large-Scale Horticultural Field Based on Temperature and Humidity Detection..... |     |
| .....Chen Zubin; Yang Wanjin; Zhou Qi; Bao Jiaxin   | 35  |
| Study on Noise suppression of Airborne Electromagnetic Profiles Data Based on Adaptive width Filtering.....         |     |
| .....Liu Ziming   | 40  |
| The streetlight management system based on ZigBee .....   |     |
| ..... Peng Ding; Bin Shi; Yaxin Wang  | 46  |
| Research and design on improving the operation efficiency of elevator .....   |     |
| ..... Zhang Si-yu; Zhou Yang; Ren Gui-ying  | 50  |
| The design and implementation of a portable alcohol detector based on GPS & GPRS.....                               |     |
| ..... Wen Xue-jun; Cai Yao; Liu Xiao-han  | 57  |
| Design and application of multi direction wind energy collection device based on PZT .....                          |     |
| .....ZHOU Xiao-hua; GOU Xin; Chen Yu-da; Liu Li-jia   | 63  |
| Design of intelligent refrigerator food management system based on QR code scanning .....                           |     |
| ..... Zhang Bilan; Du Junqi; Zhao Zuo   | 68  |
| Research of intelligent vehicle lock based on RFID.....   |     |
| .....ZHANG Ruo-xi; SHI Jia-qing; ZHU Wu-fang  | 73  |
| Research of Wireless Remote Video Surveillance System Based on FPGA .....   |     |
| ..... Wang Ning; Fan Meng-xuan; Wang En-hui   | 78  |
| The Design and Implementation of an intelligent lighting System of energy-saving .....                              |     |
| ..... ZHANG Jie; ZHAO Liang; ZHANG Sheng-yu   | 84  |
| Based on ERT Electromagnetic Simulation and Optimization Design on ANSYS.....                                       |     |
| .....JI Yanju; WU Yonghong; SONG Shuang   | 91  |
| Design of Greenhouse's Humiture Measurement and Control System Based on GSM.....                                    |     |
| .....DUAN Qing-ming; ZHANG Ya-ru; CUI Zhen-shu; ZENG Ling-qi  | 96  |
| Design of portable noninvasive blood glucose instrument based on near infrared optics.....                          |     |
| ..... LING Zhen-bao; HOU Yang; YANG Yue; ZHAO Peng-fei  | 100 |

第一部分 中文论文集

**Part I Chinese Proceedings**



# 基于温湿度检测的大型园艺场自动监控系统\*

陈祖斌；杨宛瑾；周 琪；包家鑫

(吉林大学 仪器科学与电气工程学院, 长春 130061)

**摘要：**针对现代农业自动化的需求设计一款根据土壤温湿度实现自动灌溉的控制系统。通过土壤水分温度传感器，检测土壤的湿度和温度；通过微控制器进行处理与分析，在液晶屏上显示数据，并根据设定的阈值进行自动灌溉；通过 ZigBee 组网进行远程通信，在上位机上实时显示数据，实现对大型园艺场的远程实时监测。本系统能够满足当前农业的发展要求，其功能齐全、实用性强、自动化程度高，具有较为乐观的市场潜力。

**关键字：**大型园艺场 温度 湿度 ZigBee 组网 远程监控

## The automatic monitoring system of large-scale horticultural field based on temperature and humidity detection

CHEN Zu-bin; YANG Wan-jin; ZHOU Qi; BAO Jia-xin

(College of Instrumentation & Electrical Engineering, Jilin University, Changchun 130061, China)

**Abstract:** According to the demand of modern agricultural automation, a control system of automatic irrigation is designed according to the temperature and humidity of the soil. This system detects the soil humidity and temperature through the soil temperature and humidity sensors; the data is displayed on the liquid crystal screen, and the automatic irrigation is carried out according to the set threshold through the processing and analysis of the single chip microcomputer; real-time data displays on the host computer, to realize the remote real-time monitoring of large horticultural field through the ZigBee network for remote communication. This system can satisfy the requirements of the development of agriculture, its function is complete, practical, high degree of automation, with a more optimistic market potential.

**Key words:** large-scale horticultural field temperature humidity ZigBee network remote control

## 0 引言

随着经济的发展，我国对园艺的市场需求逐年增长。温室是现代大型园艺场的主要部分，它能调控生产环境，使生产方式更加高产与高效<sup>[1]</sup>。但是，与很多发达国家相比，我国在温室监控系统的自动化程度上有明显的差距<sup>[2]</sup>。目前我国大部分园艺场仍然采用传统的人工灌溉方式<sup>[3]</sup>，不但浪费人力，而且浪费水资源。因此，发展适合中国国情的自动化温室灌溉技术有着重大的意义。传统的自动监控系统往往采用有线连接的方式，此类监控系统往往布线复杂，不易移动<sup>[4]</sup>。本系统针对传统监控系统

中的各种缺点进行了优化设计，采用 ZigBee 技术设计了一个针对大型园艺场的远程智能灌溉系统。通过 ZigBee 技术和无线传感器网络技术的结合，可以实现系统的远程监控。该系统的布线非常简单，不但提高了可靠性，而且降低了成本。

## 1 系统总体设计

基于温湿度检测的大型园艺场自动监控系统主要包括控制模块、电源模块、浇灌模块、远程监控模块。系统的总体设计框图如图 1 所示。

\*指导教师：陈祖斌

项目类型：大学生创新项目（2015651012）

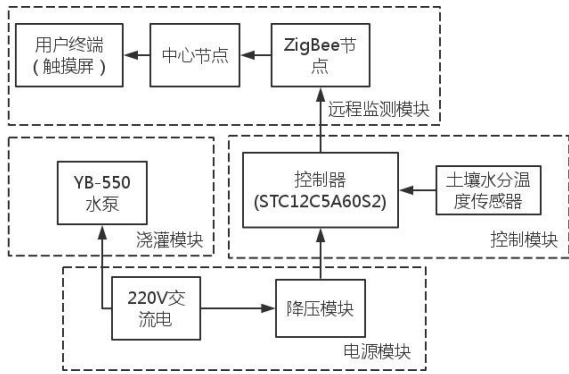


图 1 系统整体结构框图

Fig.1 The overall structure of the system

系统通过土壤水分温度传感器采集信息，经微控制器处理后，通过 ZigBee 组网向上位机发送数据并在触摸屏上显示数据，当数据值低于设定的阈值下限时，微控制器控制水泵工作，直到数据值达到阈值上限，水泵停止工作。

## 2 系统硬件设计

该系统的各个模块工作情况说明如下：

(1)控制模块：控制模块是整个系统的核心，是将整个系统的各个模块连接在一起的控制中心。控制模块由控制器和传感器构成，其中控制器采用 STC12C5A60S2 微控制器，传感器采用 SMTS-II-485 土壤水分温度传感器。

STC12C5A60S2 型号微控制器价格不高，却又具有高速、超强抗干扰、功耗较低等优点<sup>[5]</sup>，十分适合用作该系统的主控芯片。与传统的 8051 微控制器相比，此型号的微控制器在完全兼容传统 8051 微控制器指令代码的基础上，速度要快出 8 至 12 倍<sup>[6]</sup>。因此，采用此型号微控制器作为本系统的主控芯片。

SMTS-II-485 土壤水分温度传感器是一种新型的土壤水分温度传感器。该型号的土壤水分温度传感器具备许多传统土壤水分温度传感器所不具备的优点，该传感器输出信号的稳定性极高，不会发生漂移和跳动<sup>[7]</sup>。最重要的是，该传感器的测量精度很高，性能可靠，从而在信号采集阶段保证了整个系统的精度。此外，该传感器受泥土含盐量的影响很小，因此可以适应在各种土质中的测量。

(2)远程监控模块：通过 ZigBee 节点和中心节点，利用触摸屏实现远程监控。

通讯主机选用 RS485 转 ZigBee，从机选用 RS232 转 ZigBee。通讯距离可达 1600m<sup>[8]</sup>。

触摸屏选用型号为 TPC7062KX 的昆仑通态触

摸屏。TPC7062KX 型号的昆仑通态触摸屏核心是嵌入式低功耗 CPU，一体化、高性能。该触摸屏的显示部分采用 7 英寸高亮度的 TFT 液晶显示屏，触摸部分为四线电阻式<sup>[9]</sup>。此种触摸屏理论上可以满足该系统的远程监控。

(3)浇灌模块：由控制模块控制水泵进行浇灌。水泵选用 YB-550 水泵，经实验，可以满足浇灌需求。

(4)电源模块：分为 220V 交流电和降压模块。由于触摸屏不能使用 220V 供电，因此引入了降压模块，采用 24V 供电。

## 3 系统软件设计

该系统采用 STC12C5A60S2 微控制器进行数据处理，采用 C 语言对软件进行开发设计，使软件具有可读性好，可移植性高等优点。模块化设计思想贯穿于整个系统，使各个程序模块相对独立，便于程序的阅读、移植以及后期的完善。系统软件流程图如图 2 所示。

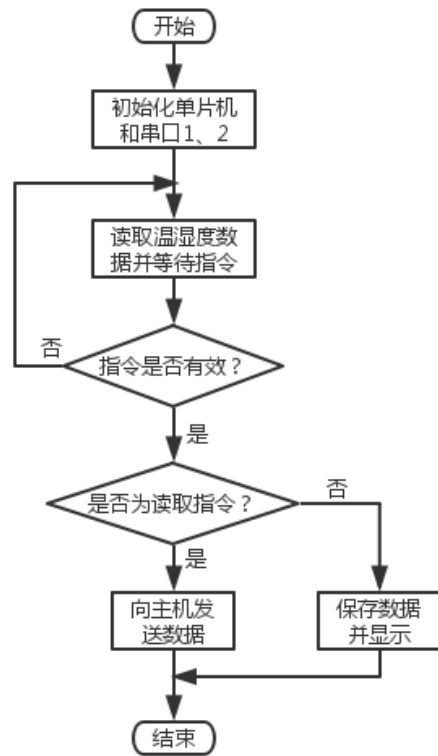


图 2 系统软件流程图

Fig.2 The software flow chart of the system

### 3.1 温湿度采集处理模块

土壤水分温度传感器采集的温湿度数据经 A/D 转换后，通过 RS-485 接口输出，经过 485 转 TTL 模块后，从单片机的串口中输入单片机中进行相应



的处理。

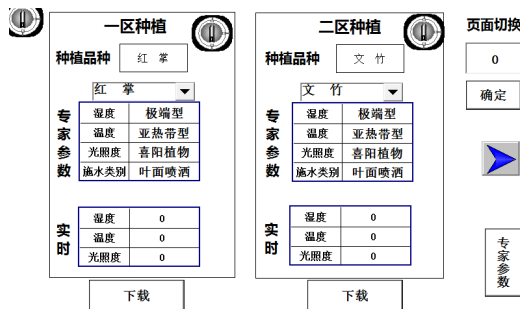
数据传送的通信协议 MODBUS-RTU 协议，该协议是主从协议，一个总线上有一个主站和多个从站，各个站点之间的通讯参数必须一致，包括数据位数、校验位校验方式、波特率及停止位数<sup>[10]</sup>。因此需要在程序中，将各个站点的这些参数设置成一致。此外，每个从站设置的站地址必须不同，否则会引起从站之间的冲突<sup>[11]</sup>。

### 3.2 上位机触摸屏显示模块

运用 MCGS 嵌入版组态软件进行设计，将程序及画面通过 USB 下载到 TPC7062KX 触摸屏上<sup>[12]</sup>。

#### (1) 触摸屏界面设计：

图 3(a)为监控及参数下载界面。左上角的按钮确定是否进行对单片机数据采集，图示是在原始的位置上。界面分为两个板块，每个板块中有各自区域的种植品种所对应的各种参数，包括专家参数和实时温度、湿度和光照度的显示。每个版块下方为下载按钮。右侧为页面切换按钮、翻页按钮以及专家参数按钮。



(a) 监控及参数下载界面



(b) 配方编辑界面

图 3 触摸屏界面

Fig.3 The interface of touch screen

#### (2) 触摸屏画面动作设计：

在每一个区域种植的白色框上，都有一个旋钮，这个是决定是否对相应区域进行数据采集，起到了方便用户对采集区域选择的功效。

在种植品种框中显示当前所选的作物品种，用

户可以根据自身需求在下拉菜单中选择所需要的作物品种。进行选择后，专家参数改变为所选作物品种所对应的数值，这个数值是由前期的数据设置决定的。下载按钮，作用是将当前的专家参数下载到相应的单片机中。在实时表格中，显示传感器采集到的实时参数。

右上角的页面切换部分可以根据用户的要求切换到相应的画面中，可以通过点击切换按钮或输入页数切换页面。

选择专家参数后，会弹出如图 3(b)所示的配方编辑界面。用户可以根据不同品种的作物，设置不同的湿度，温度，阳光度和施水类别。

设置完毕后，点击保存键及退出键，此时会再次回到图 3(b)所示界面。重新在下拉菜单中选择就可以显示最新数据所对应的级别。分级如表 1 所示。

表 1 分级列表

Table1 Hierarchical list

| 赋值 | 湿度  | 温度   | 光照度  |
|----|-----|------|------|
| 0  | 极端型 | 亚热带型 | 喜阳植物 |
| 1  | 中湿型 | 温带型  | 耐阳植物 |
| 2  | 喜湿型 | 寒带型  | 喜阴植物 |
| 3  | 喜旱型 | 热带型  | 耐阴植物 |

### 3.3 浇灌模块

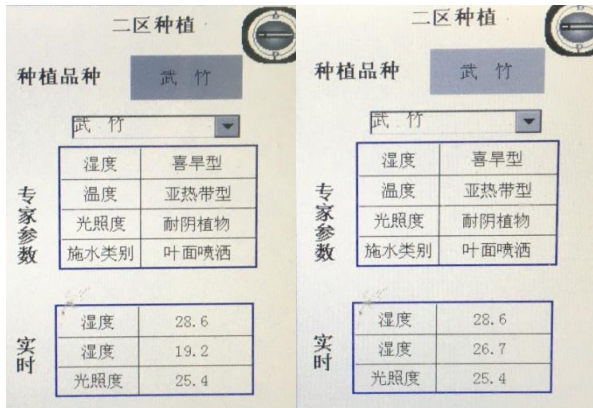
该模块将采集到的温湿度数据反馈至单片机处，然后单片机将数据通过 ZigBee 组网发送至上位机进行显示，与上位机所设定的植物类型所对应的湿度上下限值进行比对。当土壤湿度低于所选植物对应的湿度下限时，启动水泵对土壤进行浇灌。随着土壤湿度的逐渐上升，土壤湿度达到所选植物对应的湿度上限时，关闭水泵。

## 4 测试与分析

温湿度控制测试结果：将土壤水分温度传感器插入待测土壤中，开启电源，显示屏显示当前温度、湿度，且当前湿度低于预定湿度下限，喷头开始向土壤中喷水，显示屏显示实时土壤湿度，土壤湿度逐渐上升。当土壤湿度高于预定湿度上限时，喷头停止喷水，显示屏显示当前土壤湿度。经过多次重复测试，该系统可以实现温湿度控制的功能。

上位机实时数据采集测试结果：浇灌前，微控制器将土壤水分温度传感器采集到的数据通过

ZigBee 传送给上位机,并在上位机上显示,如图 4(a)所示。因为该湿度值低于下限值,水泵开始工作,对土壤进行浇灌,到达上限值时,水泵停止工作,此时的土壤温湿度值如图 4(b)所示。从该图可以看出,上位机可以清晰、直观地反映当前土壤的情况。经过多次实验测试,系统稳定性良好,可以实现预期目标。



(a) 浇灌前界面 (b) 浇灌后界面

图 4 上位机界面

Fig.4 Touch screen interface after

## 5 结论

本文提出一种基于温湿度检测的大型园艺场自动监控系统的设计方案,采用 STC12C5A60S2 为主控芯片,结合 SMTS-II-485 土壤水分温度传感器实现对土壤温湿度的测量,通过 TPC7062KX 触摸屏设置不同种类作物的阈值,选择一种植物后,检测土壤中温湿度,并且利用 ZigBee 组网技术,在 LCD 和上位机上实时显示,利用水泵对湿度进行调节,保持土壤处于一定温湿度范围内,提高作物的生产质量和产量。

## 参考文献

1. 丁晓蕾. 20 世纪中国蔬菜科技发展研究[D].南京农业大学,2008.
2. 袁洪波. 日光温室封闭式栽培系统关键技术研究[D].中国农业大学,2015.
3. 杨丹妮,常丽英,沈海斌,等. 上海市设施番茄水肥管理现状与发展建议[J]. 中国蔬菜,2016,02:11-16.
4. 周益明. 基于无线传感器网络的温室群监测与控制系统

的关键技术研究是实现[D].浙江大学,2009.

5. 罗浩,刘尚武,王书易,等. 基于 STC12C5A60S2 多路温度监控系统设计[J]. 信阳师范学院学报(自然科学版),2014,01:106-110.
6. 秦相林,张海兵,张盈盈. 基于 STC12C5A60S2 的无线温度采集系统设计[J]. 哈尔滨商业大学学报(自然科学版),2011,06:837-840.
7. 蔡文科,俞阿龙,李将,等. 基于 WSN 的大区域农田土壤远程监测系统设计[J]. 农机化研究,2015,09:77-82.
8. 杨京. ZigBee 技术在远程监控系统中的应用研究[D].武汉科技大学,2010.
9. 张博. 基于 ZigBee 技术的农业示范园区沙盘控制系统研究[D].东北农业大学,2014.
10. 沈建培. 基于 PLC 的智能饲喂系统的设计与实现[D].杭州电子科技大学,2014.
11. 何建忠. 基于 MODBUS 协议的工业网关设计与实现[D].内蒙古大学,2013.
12. 江平. PROFIBUS-DP 智能从站关键技术研究及开发[D].天津理工大学,2007.

# 基于自适应窗宽的航空电磁剖面数据噪声压制技术\*

刘子铭；高殿尧；刘学英

(吉林大学 仪器科学与电气工程学院 长春 130022)

**摘要：**利用传统的滤波技术，可以对时间域航空电磁剖面数据进行滤波，但由于窗宽固定，虽然可以清除信号表面的噪声，也会削弱异常幅值。本文提出的自适应滤波去噪方法，根据信号的局部特点，通过自适应窗宽平滑算法判断信号的异常区域，对于非异常的局部信号采用较大窗宽滤波，对于异常的局部信号采用较小的窗宽进行滤波，这样既可以去除噪声，而且维持了原信号的异常幅值。本文通过 FIR 滤波器和 IIR 滤波器对剖面数据进行滤波，与自适应滤波器滤波结果进行对比，通过实测数据的成像结果进一步验证了本文研究的自适应窗宽滤波去噪方法的有效性。

**关键词：**时间域航空电磁；自适应滤波算法；FIR 滤波器；IIR 滤波器

## Study on Noise suppression of Airborne Electromagnetic Profiles Data Based on Adaptive width Filtering

Liu Ziming; Gao Dianyao; Liu Xueying

(The College of Instrumentation and Electrical Engineering, Jilin University, Changchun 130022, China)

**Abstract:** Using the traditional filtering technology, the airborne time-domain electromagnetic data can be filtered, but owing to the fixed window width, it can remove the surface of the noise signal, but weaken anomaly amplitude. Proposed in this paper, the main adaptive filtering denoising method, according to the characteristics of local signal, judges the abnormal signal area based on adaptive window width smooth algorithm, for non anomalous local signals filtering based on larger window wide, for anomalous local signal filtering based on smaller window wide, this method not only removes the noise, but also maintains the abnormal amplitude of the original signal. This paper compares the filtering denoising results using FIR filter, IIR filter and adaptive filter, and verifies the validity of the adaptive filtering denoising method by the imaging results of measured data.

**Keywords:** Airborne Time-domain Electromagnetic Data, Adaptive Filtering Algorithm, FIR Filter, IIR Filter

## 0 前言

时间域航空电磁法是一种有利的矿产工具，随着航空瞬变电磁系统的改进和技术的成熟，越来越多的信息可以在航空电磁数据中取得。因此航空电磁数据处理方法的发展也显得尤为重要。由于其机载的飞行探测方式，发射线圈、接收线圈在探测过程中会产生晃动；同时飞行速度、飞行姿态等变化

会引起探测系统装置参数的不稳定；而且空中飞行探测过程中气压、温度等变化也能够引入系统噪声，严重影响数据质量及成像精度，制约航空电磁探测系统对地下异常体的反演解释，减小勘探深度<sup>[1-4]</sup>。

随着航空电磁探测技术与仪器研究工作的深入，我国学者也开展了航空电磁噪声的背景场去除、数据滤波、叠加、抽道等预处理方法的研究<sup>[5-6]</sup>。虽然时间域航空电磁探测的原始数据，经过多重预处理与滤波后，剖面数据的信噪比得到了极大提高，

\* 指导教师：朱凯光

项目类型：大学生创新项目(2015651017)

但晚期道仍然含有残余噪声，影响地下深部的探测能力。

在航空电磁数据的叠加抽道方面，国际上常用的时间域航空电磁探测系统也提出了一些较新的叠加抽道技术 Macnae(1984)年提出裁剪 (pruing) 的方法去除天电干扰；Buselli (1992) 和 Cameron (1996) 提出中值滤波法；Strack (1989,1992) 提出修剪平均法；Sutarno 和 Vozoff (1989) 采用非线性滤波技术抑制天电干扰等。根据 Macnae(1984)、Lane(1998)采用控制着震荡频率低于发射信号频率的技术，Fugro 公司采用陷波的方法；THEM 系统采用多项式拟合去除运动噪声的方法<sup>[7]</sup>。

由于工程物探对浅部目标的探测要求，近年来，我国学者也开展了主成分去噪的相关研究，朱凯光等<sup>[8-9]</sup>将祝成功根系引入时间域航空电磁反演，偶遇祝成功去噪声特性，在含噪数据的主成分反演中取得了由于其他方法的反演结果。本文提出基于自适应滤波的航空电磁剖面数据噪声处理技术，分析了空间噪声特点，研究了自适应窗宽平滑算法，设计了自适应低通滤波器，并与 FIR 滤波器和 IIR 滤波器滤波后的波形进行对比，最后通过仿真数据和实测数据的去噪比较，验证了本文去噪算法的有效性。

## 1 FIR 和 IIR 滤波器原理

### 1.1 FIR 滤波器原理

FIR 滤波器，是单位脉冲响应的长度有限的滤波器。具体来讲，FIR 滤波器的突出特点是其单位取样响应  $h(t)$  是一个  $N$  点长的有限长序列， $0 \leq n \leq N-1$ 。滤波器的输出  $y(n)$  可表示为输入序列  $x(n)$  与单位取样响应  $h(t)$  的线性卷积，由于 FIR 滤波器只存在原点上存在极点，所以 FIR 系统具有全局稳定性。FIR 滤波器是由一个“抽头延迟线”加法器和乘法器集合构成的，每一个乘法器的操作系数就是一个 FIR 系数。

### 1.2 IIR 滤波器原理

IIR 滤波器，是单位脉冲响应为无限长的滤波器，IIR 滤波器有几个显著的特性：IIR 滤波器同时存在不为零的极点和零点。要保证滤波器为稳定的系统，需要使系统的极点在单位圆内，也就是说系

统的稳定性由系统函数的极点决定。由于 IIR 滤波器存在不为零的极点，因此只能实现近似的线性相位特性。也正是因为 IIR 滤波器的非线性相位特性限制了其应用范围。

## 2 自适应滤波方法

### 2.1 自适应滤波的去噪原理

根据自适应窗宽平滑算法<sup>[10]</sup>，设计了低通滤波器组，以第  $k$  道剖面数为例，具体算法如下：

设自适应窗宽调整范围为  $W_L - W_U$ ， $W_L$ 、 $W_U$  分别为最小、最大窗宽值。先以最大窗宽对剖面数据  $\hat{x}_k$  进行平滑滤波，得到  $\hat{x}_{jk}$ ，并计算其二阶差分

$\Delta_k(j)$  (式(1))，

$$\Delta_k(j) = \left( \frac{2}{W_U - 1} \right) \sum_{i=1}^{[(W_U-1)/2]} 2\hat{x}_{jk}(j) - \hat{x}_{jk}(j+i) - \hat{x}_{jk}(j-i) \quad (1)$$

式中， $j = 1, 2, \dots, n$ ， $[\cdot]$  表示向下取整。 $\hat{x}_k$  计算的二阶差分  $\Delta_k(j)$  反映平滑滤波后的  $\hat{x}_{jk}$  剖面数据的

局部梯度变化率，在剖面  $\hat{x}_{jk}$  的异常处绝对值较大，在平坦部分则趋近于零。

利用公式 (2) 将剖面上各测点的二阶差分  $\Delta_k(j)$  线性转换成各测点平滑滤波器的自适应窗宽

$W_k(j)$ ，在最小窗宽与最大窗宽之间：

$$W_k(j) = [W_U - (W_U - W_L) \left( \frac{|\Delta_k(j)|}{\Delta_T} - \frac{1}{2} \right)] \quad (2)$$

其中， $\Delta_T$  为二阶差分的阈值，若  $\Delta_T$  取值太小得到的窗宽  $W_k(j)$  较小，影响剖面平坦部分的滤波效

果；反之窗宽  $W_k(j)$  较大，不仅会引起异常沿剖面

扩散，还会降低异常幅值。偏移量  $(-\frac{1}{2})$  的设置是为了获取更大的窗宽。常规的低通滤波器带宽固

定，而根据自适应窗宽平滑算法设计的剖面数据低通滤波器组，能够根据信号的局部特性改变滤波器频带，具有明显优势，不仅能够有效去除剖面数据上的高频空间噪声，还可以保证剖面数据异常的幅度。

### 2.2 自适应滤波器的设计

自适应滤波技术是根据局部信号的特点，采用不同的窗宽进行滤波相对于传统的滤波方法，自适应滤波技术可以根据局部信号的特点，采用不同的窗宽进行滤波，判断信号的异常区域，非异常的局部信号采用较大窗宽滤波，异常的局部信号采用较小的窗宽进行滤波，这样既去除了噪声，也维持了原信号的异常幅值。本文设计自适应滤波器的最大窗宽为 51，最小窗宽为 3。

## 3 仿真数据的去噪实例

为观察三种滤波器滤波程度的效果，本文设计了均匀半空间大地模型，电导率为 0.01 S/m，共有 1000 个测点，吊舱式直升机时间域航空电磁探测系统，采用中心回线测量方式，发射线圈半径为 7.5 m，发射电流为 25 Hz 的正负方波，飞行高度为 30 m，归一化发射电流，对大地模型进行一维正演计算，为仿真野外实测数据，在正演数据中加入 10% 的高斯白噪声，抽道后可得到各测点的 16 道 off-time 电磁响应，剖面数据如图 1 所示。

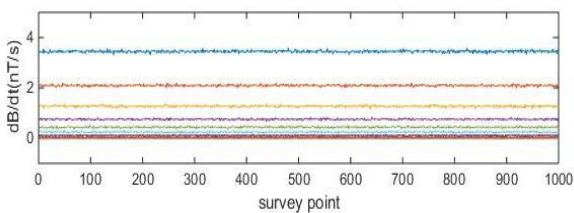


图 1 均匀半空间大地模型 16 道电磁数据剖面曲线

Fig.1 16 channels of homogeneous half space earth model

可以看出，含噪数据大地模型的剖面数据包含高频空间噪声，为对比去噪效果，本文采用 FIR，IIR，自适应窗宽滤波器，分别对其进行滤波。设计的 FIR，IIR 滤波器均为低通滤波器，截止频率在 0-1 之间可调，阶数为任意数值，设计的自适应窗宽滤波器，最大窗宽为 51，最小窗宽为 3。图 2 给出了三种方法去噪后电磁剖面数据的后四道剖面曲线。

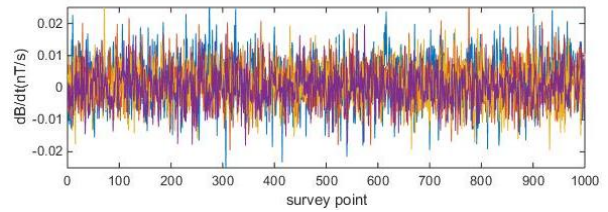


图 2 均匀半空间大地模型后四道剖面曲线

Fig.2 Homogeneous half space the earth model four channels curve after denoising result

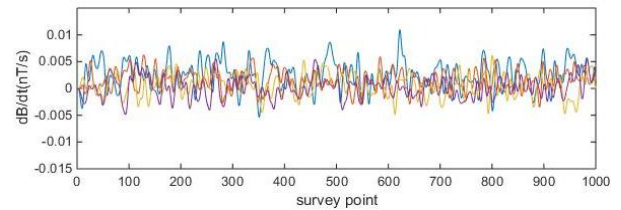


图 2 (a) FIR 滤波结果

Fig.2(a) Result of IIR filtering

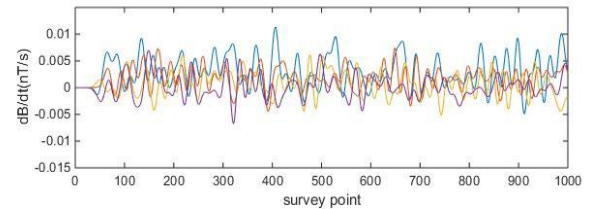


图 2 (b) IIR 滤波结果

Fig.2(b) Result of IIR filtering

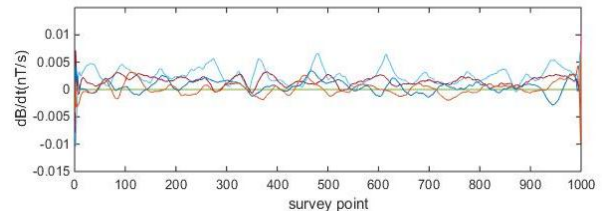


图 2 (c) 自适应算法滤波结果

Fig.2(c) Result of adaptive filtering

对比图 2 (a)，图 2 (b)，图 2(c) 可以看到，经 FIR，IIR 滤波处理后的剖面曲线（图 2(a)，图 2(b)）的晚期道数据无明显异常，而自适应算法滤波处理后的剖面曲线（图 2(c)）的晚期道数据不仅保证了异常的幅值，而且噪声数据明显减小。

## 4 实测数据的去噪实例

在国家高技术研究发展计划重大项目支持下，国土资源航空物探遥感中心与吉林大学仪器科学与电气工程学院研制开发了我国第一套吊舱式直升机时间域航空电磁探测系统 CHTEM(技术指标同上仿

真系统)。2012 年 1 月,该系统在河南省某地首次试飞成功,并进行了面积性矿场勘查,发现该地区大地呈现高阻特性,电阻率为  $3000 \sim 8000 \Omega \cdot m$ 。在此,以河南野外飞行勘查的某测线为例,选取长约 8.5 km 测线的 17 道剖面数据。如图 3 所示,在测点 3000 附近有幅值约为  $1500 \text{ nT/s}$  的异常。

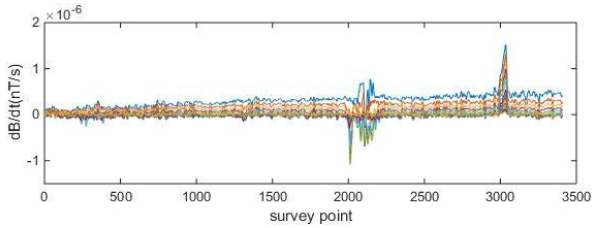


图3 河南野外航空电磁探测的17道剖面曲线

Fig.3 17 channels profile of field data from airborne time domain electromagnetic survey in Henan Province, China

首先对该测线的剖面数据进行 FIR、IIR 和自适应窗宽算法去噪处理,结果分别如图 4 (a)、图 4 (b) 和图 4 (c) 所示。对比三张去噪后的数据剖面,可以看到自适应窗宽滤波算法取得了最好的去噪结果如图 4 (c) 所示,去除了测线上的高频空间噪声。

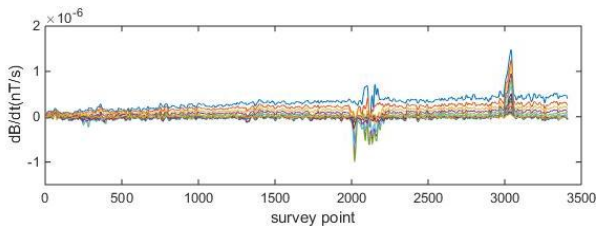


图4 (a) FIR滤波结果

Fig.4(a) Result of FIR filtering

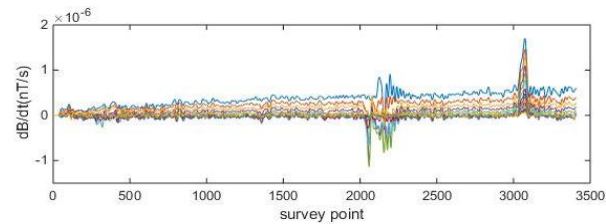


图4 (b) IIR滤波结果

Fig.4(b) Result of IIR filtering

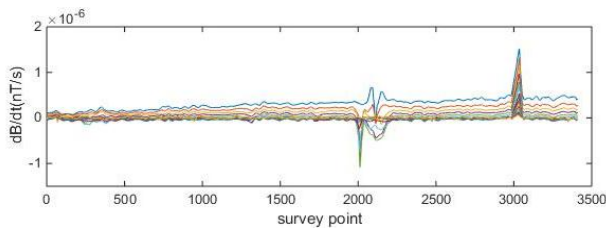


图4 (c) 自适应算法滤波结果

Fig.4(c) Result of adaptive filtering

由图 4 (a), 图 4 (b) 可以看出,两种常规滤波器 FIR, IIR 滤波器去噪效果不明显,噪声水平几乎没有下降。对该测线剖面数据进行自适应窗宽算法滤波处理,设计的滤波器最大窗宽为 51,最小窗宽为 3,滤波结果如图 4 (c) 所示。由图 4 (c) 可以看出,通过自适应算法处理之后,噪声下降比 FIR 和 IIR 滤除的噪声下降明显。

晚期道数据为 17 道剖面数据的最后四道数据,通过对晚期道数据进行滤波处理能更加有效地反映出滤波器的性能。图 5 是原始数据晚期道的图像,图 6 (a), 图 6 (b), 图 6 (c) 分别是三种滤波器对原始数据晚期道滤波的结果。

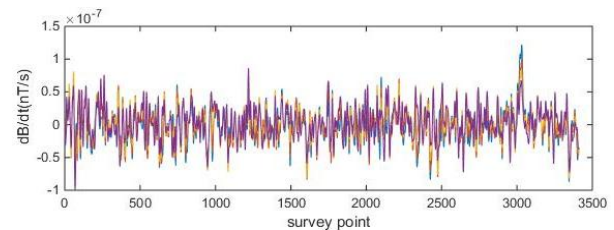


图5 原始数据晚期道图像

Fig.5 The original data terminal image

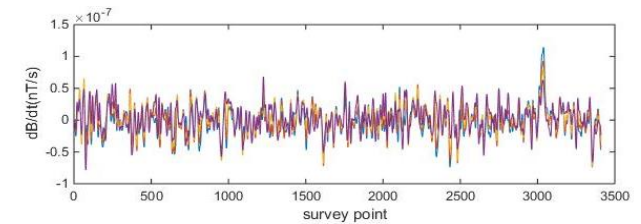


图6 (a) FIR晚期道滤波结果

Fig.6(a) Result of FIR filtering

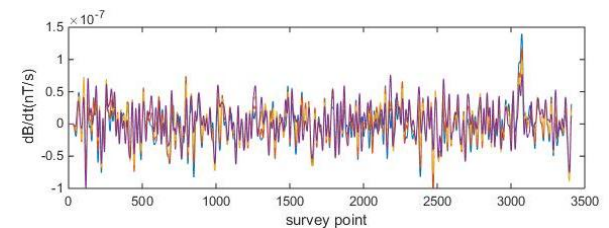


图6 (b) IIR晚期道滤波结果

Fig.6(b) Result of IIR filtering

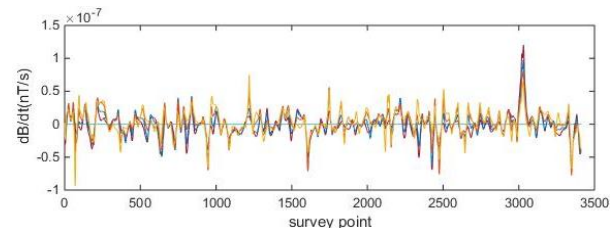


图6 (c) 自适应算法晚期道数据滤波结果

Fig.6(c) Result of adaptive filtering

通过图 6 (a), 图 6 (b), 图 6 (c) 三图对比

可以看出,经常规滤波器 FIR, IIR 滤波处理后的剖面曲线(图 6(a), 图 6(b))晚期道数据无明显异常变化,无法反映大地模型的深部异常体,且仍有较多的高频噪声存在,而自适应窗宽滤波处理(图 6(c))后的晚期道数据保证了异常的幅值,且噪声幅值明显减小,高频噪声明显减少。

## 5 结论

(1) 本文将航空电磁数据处理变换应用到 GUI 界面中进行,经过三种滤波算法对原始剖面数据的处理,既滤除了剖面数据中的高频空间噪声,也去除了剖面数据中的不相关噪声,自适应滤波算法可以提高晚期数据的信噪比,为地球物理探测数据的噪声处理等方面提供了新思路。

(2) 本文采用自适应滤波算法,设计的低通滤波器组可以根据航空电磁剖面数据的局部变换特征,自适应地改变滤波器的带宽,不仅可以有效地滤除高频空间噪声,而且有效地保持了异常的幅值,具有优于 FIR, IIR 滤波器的滤波性能,该滤波算法也可有效地用于测线电磁数据的滤波。

## 参考文献

1. Lane R, Green A, Golding C, et. al. An example of 3D conductivity mapping using the TEMPEST airborne electromagnetic system[J]. Exploration Geophysics, 2000, 31(2):162-172.
2. Macnae, J C, Ltagne Y, West G F. Noise processing techniques for time-domain EM system[J]. Geophysics, 1984, 49(7):934-948.
3. Riddsdill-Smiath T A, Dentith M C. The wavelet transform in aeromagnetic processing[J]. Geophysics, 1999, 64(4):1003-1013.
4. Buselli G, Hwang H S. AEM noise reduction with remote referencing[J]. Exploration Geophysics, 1998, 29(2):71-76.
5. 李楠. 时间域航空电磁数据预处理技术研究[D]. 长春: 吉林大学, 2009.
6. 吕东伟. 吊舱式时间域直升机航空电磁数据处理方法研究[D]. 成都: 成都理工大学, 2011.
7. Auken, E., Westergaard, J. A., Christiansen, A. V., and Sorensen, K. L. Processing and inversion of SkyTEM data for high resolution hydrogeophysical surveys[C]. Australian Society of Exploration Geophysicists, Extended Abstracts. 19th Geophysical Conference and Exhibition..
8. 朱凯光, 王凌群, 谢宾等. 基于主成分分析的航空电磁数据噪声去除方法[J]. 中国有色金属学报, 2013, 23(9):2430-2435.
9. 王凌群, 李冰冰, 林君等. 航空电磁数据主成分滤波重构的噪声去除方法[J]. 地球物理学报, 2015(8):2803-2811.
10. 李修文, 徐金梧, 阳建宏等. 基于梯度自适应窗宽在变速机械阶比分析中的应用[J]. 仪表技术与传感器, 2013(1):68-71.

# 基于 ZigBee 的路灯管理系统\*

丁 芑; 施 斌; 王雅新

(吉林大学, 仪器科学与电气工程学院, 吉林, 长春, 130012)

**摘要:** 该项目设计了一种基于 ZigBee 技术的路灯管理系统, 实现主控端对路灯端的管理和信息采集, 并实时监测各终端的环境条件, 通过电流检测的方法, 对路灯状态进行检测判断其是否故障, 并根据光线情况自动开启或关闭路灯。

**关键词:** ZigBee 技术, 路灯控制, 故障检测

## The streetlight management system based on ZigBee

Ding Peng; Shi Bin; Wang Yaxin

(Jilin university instrumentation and electrical engineering, Changchun, 130012)

**Abstract:** The project is to design a kind of streetlight management system based on the technology of ZigBee, to implement management and information collection of the main control unit from the streetlight unit, and monitoring the environment conditions of each terminal in real time, by using the method of current detection to judge whether the fault detection of streetlight status, and according to the light condition to turn on or off the streetlight automatically.

**Key words:** ZigBee technology Streetlight control Fault detection

## 0 前言

随着城市化建设的深入, 路灯作为城市亮化的重要组成部分, 越来越被政府所重视, 投入了大量的人力及资金建设管理<sup>[1]</sup>, 但随之产生了许多问题, 现有路灯管理系统难以反馈路灯的故障信息, 只能通过人力巡查监测, 故障维修并不及时, 某些路段的照明故障会导致众多不便, 甚至引发交通事故。除此之外, 现有系统不能实现远程管理, 并且多为时间控制, 由于设置的固定性, 往往在一些突发状况比如阴天光照过低时, 不能及时为城市照明。本设计基于 ZigBee 无线通信技术实现远程监控、故障自动检测等功能, 成本低, 可靠性高, 传输速度快。

## 1 总体方案设计

本设计将 ZigBee 技术应用于路灯管理系统中, 实现远距离无线数据传输并控制<sup>[2]</sup>。该系统包括总控制模块和路灯监控模块。总控制模块包括单片机总系统、控制模块、显示模块、ZigBee 总节点模块; 路灯监控模块包括单片机子系统、电流检测模块、传感器模块、开关控制模块、ZigBee 子节点模块。

利用电流检测的方法判断路灯的状态并利用传感器模块检测当时的光线明暗程度, 将信息传输到单片机子系统, 通过 ZigBee 子节点传输到 ZigBee 总节点, 单片机总系统将这些信息进行汇总, 判断路灯当时是否处于故障状态以及是否需要开启路灯, 在 LED 显示模块上显示信息, 再用按键控制将

\* 指导教师: 邱春玲

项目类别: 大学生创新项目 (2016 年校级培育)



控制信号通过 ZigBee 模块反向传输到单片机子系统，通过路灯开关控制模块控制路灯。还需要路灯之间 ZigBee 子模块的通信接力，实现远距离通信。系统总体系统框图如图 1 所示。

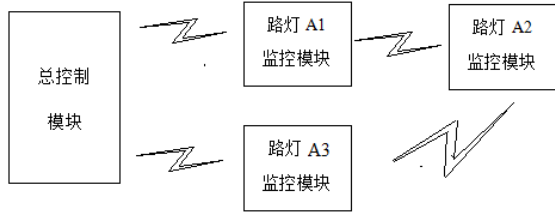


图 1 总系统结构框图

Fig.1 The whole system structure diagram

## 2 硬件设计

### 2.1 总控制模块设计

总控制模块主要包括单片机总系统、按键控制、ZigBee 总节点模块及显示等。单片机采用 STC89C52，具有低功耗高性能的优点。

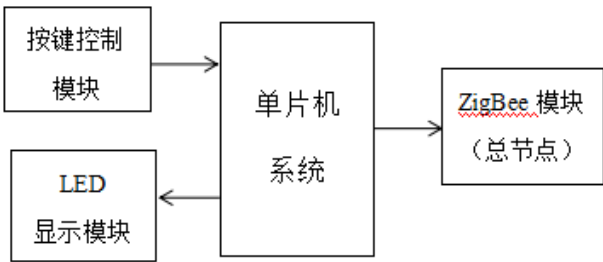


图 2 总控制模块结构框图

Fig.2 The total control module structure diagram

#### 2.1.1 ZigBee 模块

ZigBee 是一种低速短距离传输的无线网络协议。现已有 ZigBee 模块，具体是由射频通信模块+微处理模块（MCU）+ZigBee 无线通信协议构成，一般用来对小数据量的数据进行无线传输，而且 zigbee 通信协议是不收费的，成本低，路灯电流数据和当地光线数据是通过 ZigBee 无线通信协议进行远程传送，接收端也是 ZigBee 协议将数据进行收集并解析，然后再传送给单片机总系统。该设计采用 CC2530 ZigBee 串口传输芯片，可实现节点间 250 米的数据传输，误比特率为 0.5%。

#### 2.1.2 按键控制模块

单独连接在单片机总系统旁边，可以人工对于各种突发情况进行对路灯的控制，可以采用单独按键扫描或者组合按键扫描通过单片机总系统和 ZigBee 模块对不同区域的各个路灯进行远距离无线控制。

#### 2.1.3 显示模块

该设计选择 OLED12864 显示屏，该器件只有 0.96 寸的屏幕，却有 128\*64 的分辨率，一共七个管脚，除去 VCC 和 GND 需要连接到单片机上的只有五个管脚，自动显示从各个子模块采集的温湿度信息以及显示是否故障。

### 2.2 路灯监控模块设计

共设计三个路灯监控模块，模拟三个区域的路灯，其中每个包括电流检测模块，传感器模块，开关控制模块。

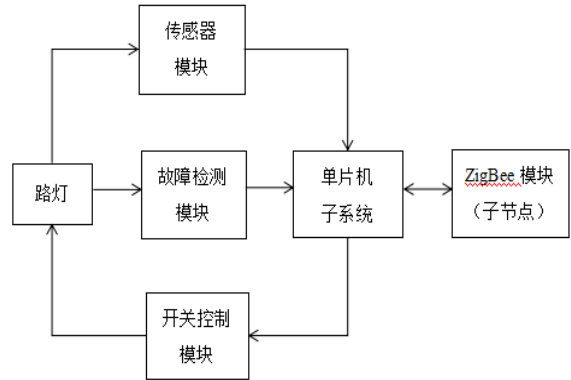


图 3 路灯监控模块结构框图

Fig.3 Streetlight monitoring module structure diagram

#### 2.2.1 电流检测模块

通过检测电流的方法判断故障情况，路灯故障情况包括路灯晚间不亮、亮度过暗、白天不正常亮等情况，路灯不亮或者亮度过暗，都可以通过电流检测出路灯电流为零或很小，白天亮可以检测出电流正常但外界光线亮度很亮。电流检测模块连接在电灯和单片机子系统之间，进行简单的数据处理判定路灯是否故障，并通过 ZigBee 模块传输给单片机总系统故障信息，显示是否故障及故障路灯序号。该设计采用小电阻与灯泡串联并用 ADC0804 单通道 AD 转换芯片检测电阻电压，不仅可以计算出流过路灯的电流，还可以保护路灯电路<sup>[3]</sup>。

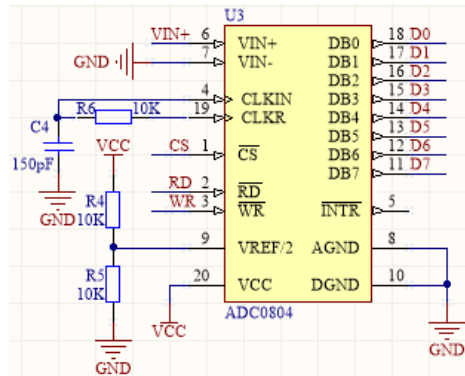


图 4 电流检测 AD 转换电路图

Fig.4 Current detection AD conversion circuit diagram

#### 2.2.2 传感器模块

利用光敏传感器检测当地的光照强度，并输出

高低电平，通过单片机判断当时是否需要打开或关闭路灯，为自动控制提供数据。利用温湿度传感器 DHT11 将各个区域的温湿度环境反馈给总控板并显示。

### 2.2.3 继电器控制模块

连接在单片机子系统和路灯之间，由于单片机电流过小，不能直接将灯泡用单片机高低电平控制，所以采用继电器对路灯进行控制，便于保护电路并且更有效地控制电路，也可以模拟小电流控制 220V 交流电灯的情况。

## 3 软件设计

### 3.1 总控制程序设计

总控制板设定为节点 1，其余三个路灯控制板分别设定为节点 2,3,4，数据传输路径为 1-2-4 和 1-3-4 的网状传递方式<sup>[5]</sup>，这样不仅可以拉长数据传输的距离，还可以在节点 2 故障时仍然可以传递节点 4 的数据，不至于发生大规模的数据丢失<sup>[6]</sup>。总控制电路可以通过按键控制相应路灯的开闭，并显示三个路灯的温湿度采集信息和故障信息，无故障则显示“正常”，故障则显示“故障”。总控制板电路程序一次循环流程图如下：

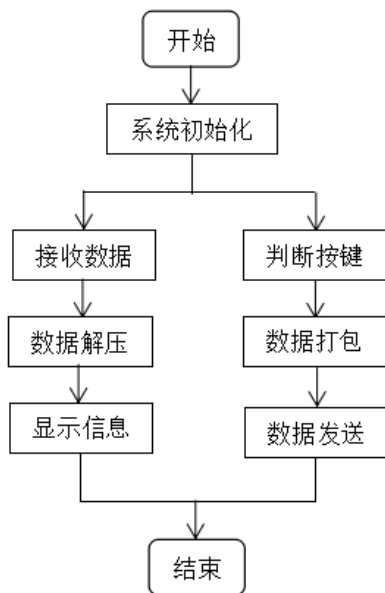


图 5 总控制程序一次循环流程图

Fig.5 total control module program flow chart in one cycle

### 3.2 路灯控制程序设计

路灯控制电路板上温湿度传感器采集温湿度信息，光敏传感器采集亮度信息，将信息打包后发送到主控板并接收主控板传来的控制信息对路灯进行控制<sup>[6]</sup>。节点 2 和节点 3 还需要传递节点 4 打包的信息到主控制板上。路灯控制部分的程序流程在

主控程序的基础上，显示信息改为路灯开闭，判断按键改为采集温湿度、电流、亮度信息和故障判断，一次循环的流程基本相同。

## 4 整体测试

### 4.1 功能测试

硬件电路成品一共有 4 个电路板，其中有 1 个主控板（编号板 1），3 个路灯板（编号板 2,3,4），经测试成品基本完成了以下功能<sup>[4]</sup>：

(1) 能够进行电路板之间的信息传输，信息传输方式为 1←2←4 和 1←3←4 两条传输线路，将 2,3,4 板采集的温湿度环境信息和路灯故障信息传输到板 1 并显示，主控板输出控制信号控制板 2,3,4 路灯的亮灭。两个板间的信息传输距离可以在实验室里达到 12 米。

(2) 板 2,3,4 根据光敏传感器采集的信号白天灭灯，夜晚亮灯，在白天可以通过板 1 控制灯的亮灭。

(3) 板 2,3,4 通过 AD 采集串联电阻电压计算转换为灯泡电流，通过电流以及当前路灯的开闭状态综合判断路灯是否故障并将信息传输给板 1。

### 4.2 数据测试

传输距离测试：在空旷的场地给电路板供电，经过测试可以得到数据，各板之间最远传输距离为 20.5 米，在更空旷的地方测试效果会更好。

电流采集测试：在路灯电路板一侧焊接显示屏插排，通过编写程序在显示屏上显示路灯正常及故障时的电流。三个路灯板故障电流范围为 0~20mA，正常电流范围为 80~113mA。

温湿度采集：通过总控制板上显示屏显示可以观测出三个路灯温差为 ±3℃，湿度差为 ±5%。

## 5 总结

通过对基于 ZigBee 技术的路灯管理系统的研究，分析了在路灯管理系统中 ZigBee 技术的优势<sup>[7]</sup>，给出了系统的具体实现方案，可以实现自动检测故障、远程操控等功能，可根据实际需求，确定各路灯管理系统的规模，若有其他需求可以适当补充功能。

## 参考文献

1. 王权平,王莉.ZigBee 技术简析[J].通讯世界.2003(04)

2. 樊冰,孙文胜.ZigBee 技术及其应用研究[J].大众科技.2007(06)
3. 刘奎.ZigBee 技术与应用[J].科技资讯.2006(06)
4. 喻楚云.ZigBee 在家庭远程遥控管理系统中的应用[J].大连民族学院学报. 2006(03)
5. 王宝英,蔡雪梅,梅春燕,刘鹏.基于 ZigBee 技术的智能交通网络研究 [J]. 重庆邮电大学学报(自然科学版).2007(06)
6. 叶睿.基于 Zigbee 技术的路灯无线控制[J].科技信息(科学教研).2008(02)
7. 刘雅举,蔡振江,张莉,李东明,赵秋霞.基于射频芯片的 ZigBee 无线传感器网络节点的设计[J].微计算机信息.2007(22)
8. 无线龙.ZigBee 无线网络原理[M].北京：冶金工业出版社.2011.9
9. 张天凡.51 单片机 C 语言开发详解[M].北京：电子工业出版社.2008.6
10. 魏东平,朱连章,于广彬.C 程序设计语言[M].北京：电子工业出版社.2009.2

# 基于贝叶斯算法电梯运行效率的研究\*

张思雨; 周 炆; 任桂莹

(吉林大学 仪器科学与电气工程学院, 吉林 长春 130012)

**摘要:** 传统电梯的先到先服务算法实时性较差, 用户平均候梯时间偏长。为了减少电梯能耗, 提高电梯的运行效率, 本文建立基于贝叶斯算法的电梯运行模型, 通过先验概率与条件概率进行分类, 提出不同时段依据概率停靠轿厢的设想, 并结合红外检测技术避免电梯空停现象。为了验证算法的实际运行效率, 本文在电梯模型上进行仿真测试, 基于贝叶斯算法所得平均候梯时间为 47.8 s, 较传统算法提高约 28%。该模型将电梯使用的高峰与低谷时段区别对待, 提高系统的实时效率。

**关键词:** 贝叶斯算法; 概率统计; 运行效率; 后验概率

## Research and Design on Improving the Operation Efficiency of Elevator

Zhang Si-yu; Zhou Yang; Ren Gui-ying;

(College of Instrumentation and Electrical Engineering, Jilin University, Changchun 130012)

**Abstract:** The first-come first service algorithm of traditional elevator is poor real-time performance. The average waiting time of the user is too long. In order to reduce the energy consumption of elevator and improve the operation efficiency of the elevator, the model based on Bayesian algorithm is proposed in this paper, according to the the prior probability and conditional probability Classification, the idea of probability parking at different periods is put forward, and combined with the infrared detection technology to avoid the empty stop of the elevator. In order to verify the actual operation efficiency of the algorithm, the simulation test is carried out on the elevator model. Based on Bayesian algorithm the average waiting time is about 47.8s. The time compared with the traditional algorithm is improved by about 28%. The model will treat peak and valley period of using elevator differently, improving the real-time efficiency of the system.

**Key words:** Bayesian algorithm; Probability statistics; Operating efficiency; Posterior probability

## 0 前言

在快速发展的现代化社会里, 电梯在高层建筑中扮演着不可或缺的角色, 电梯控制算法也渐渐成为研究热点。目前电梯控制多采用先来先服务 (FCFS) 的算法<sup>[1]</sup>, 这种随机服务算法不具有实时性的特点, 影响着用户的使用效率。

本文中提出分时段对每楼层电梯使用次数进行概率统计, 具有基于贝叶斯算法智能统计和学习能力<sup>[2]</sup>, 对大楼内的客流量进行深入分析, 提取出系统的特征信息, 按照期望效用最大化原则生成预测, 控制电梯闲置时停靠在所预测的使用概率最高的楼层<sup>[3-5]</sup>, 根据不同的运行状态, 采用不同的调度方案<sup>[6]</sup>, 从而在最大程度上满足更多的人在最短时间内乘坐上电梯, 一方面提高电梯本身的运行效率, 另

一方面可节省大多数人等待电梯的时间, 提高总体的效益<sup>[7]</sup>。同时将红外检测技术融入到电梯的设计与控制中<sup>[8]</sup>, 避免电梯实际运行中经常会遇到的轿厢停止后电梯外无人的问题, 提高电梯运行效率。

## 1 电梯概率统计模型的建立

### 1.1 建模依据

电梯的乘客流量信息受众多因素影响: (1) 医院、办公楼、居民小区等使用性质不同; (2) 不同楼层间人员分布不同; (3) 人员使用时间段不同如上下班高峰期; (4) 突发事件引起的乘客流量波动等, 上述响因素中前三者是属于有规律的确定的因素, 而后者属于随机因素, 对于有规律的确定的因素影响进行分析, 同时对不确定的随机因素以合适的比例按照平均值的方式处理。同时为统一评价标准, 对电梯

每层呼叫后乘客需要等待的时间来建模研究。

## 1.2 建模过程

以 $n$ 层电梯模型为例,假设电梯单次运行完毕之后,就停留在该楼层等待下一次呼叫,若记停留的楼层序号为 $x$ ,记呼叫楼层序号为 $m$ ,从停留楼层到达呼叫楼层所需要的时间记为 $t$ ,

若假设电梯乘客各楼层的呼叫次数分别为 $N_x$ ,根据经验公式[9]计算 $N_x$ :

$$N_x = \frac{x\{1 - [(x-1)/x]^r\} - 1}{n} \quad (1)$$

$r$ 为电梯有效乘客人数 $r = 0.8 \mu r_c$ ,其中 $r_c$ 为实际呼叫次数, $\mu$ 为修正系数

假设电梯运行数个周期,所有楼层需要等待的总时间记为 $T_n$ ,每个楼层滞留时间记为 $\Delta T$ <sup>[9]</sup>:

$$\Delta T = 0.8 + K(f+1)^{1/3} \quad (2)$$

其中 $K$ 为车厢出入口打开宽度的修正系数, $f$ 为 $N_x$ 的取整值;

采用传统的FCFS方案,闲置时电梯停留在固定楼层(实际中多为1楼),不同状态下乘客需要电梯从停留楼层到达呼叫楼层所需要的总时间关系列写如下:

$$T_n = \sum_{m=1}^n (|1-m| \Delta T) N_x + (n-1) \Delta T \quad (3)$$

若采用本研究方案中依据概率大小确定闲停位置,让电梯停留在使用频率最高的楼层,这里假设 $k$ 楼使用的频率最高,即让电梯闲置时停留在 $k$ 层( $n=k$ ),也即 $N_k \geq \max(N_x)$ 则所有楼层需要等待的总时间记为 $T'$ :

$$T'_n = \sum_{m=1}^n (|n-m| \Delta T) N_x \quad (4)$$

节省时间与总等待时间之和的比例记为

$$\beta = \frac{T_n - T'_n}{T_n} 100\% \quad (5)$$

比例系数 $\beta$ 在一定程度上反映了效率提高的高低,由式(5)可知, $k$ 楼使用电梯的频率越高,即 $N_k$ 值相比其他楼层越大,则比例系数 $\beta$ 越高,从一定程度上说明效率提高的越明显。

由概率论可知,随机模型中任一个单变量处于同等地位,此例中如果其他楼层使用效率最高,采用新的调度算法可以得到同样的结果。

## 1.3 模型结论

该模型通过对各楼层用户对电梯的次数进行统

计,根据经验公式获得每个楼层电梯停留的时间,再结合各个楼层的呼叫次数及电梯运行的调度方案计算出比例系数 $\beta$ , $\beta$ 在一定程度上反映了采用新方案相对于传统电梯调度方案电梯运行总体效率提高的比例,也就是在某个时段如果有楼层使用电梯频率相比其他楼层使用电梯的频率高,让电梯闲置时停留在使用频率最高的楼层,则采用新调度方案将进一步减少平均候梯时间,提高电梯整体的运行效率。

## 2 贝叶斯算法预测电梯呼叫楼层

### 2.1 算法应用构思

根据上述建模结论可知让电梯闲置时停留在使用频率最大的楼层,有利于提高电梯的整体的运行效率,因而在实际的电梯系统中如何根据已有数据得到各个楼层使用电梯频率的概率分布,以及较为准确预测某段时间下一次使用电梯概率最大的楼层是几层尤为重要。贝叶斯算法一方面可以根据某些已有电梯信息对用户呼叫事件做出预测,另一方面可以把新用户的呼叫事件作为样本实时更新下一次的预测结果,而这一预测结果正好可以电梯控制的参考信息以便高效调度电梯。

分析可知该电梯的特征向量可以用向量 $X=\{X_1, X_2, X_3, \dots, X_n\}$ 表示,其中特征属性 $X_n$ 表示不同楼层是否呼叫的度量,从电梯整体的角度考虑,特征属性<sup>[10]</sup>有两个分类 $Y=0$ 表示无呼叫请求, $Y=1$ 表示有呼叫请求,根据贝叶斯定理可以得到最大后验概率<sup>[11]</sup>:

$$P(Y|X_n) = \frac{P(X_n|Y)P(Y)}{P(X_n)} \quad (6)$$

通过比较 $P(Y_n|X)$ 中最选取最大项,就可以得到电梯使用频率最大的楼层 $n$ 。

### 2.2 算法应用设计

设电梯系统的特征函数为 $\psi(x)$ ,样本值来自于一段时间 $T$ 内固定间隔 $t$ 分段获取样本数据

$$\varphi(k) = \begin{cases} 1, & k \text{ 表达式为真} \\ 0, & K \text{ 表达式为假} \end{cases} \quad (7)$$

则通过电梯统计过去的呼叫次数,获得先验概率,即电梯在有呼叫的状态下,相应楼层的呼叫概率如式(8),电梯在某段时刻被呼叫的概率如式(9)

$$P(X_n = h | Y = 1) = \frac{\sum_{m=1}^n \varphi(X_n = h \cap Y = 1)}{\sum_{m=1}^n \varphi(Y = 1)} \quad (8)$$

$$P(Y = 1) = \frac{1}{n} \sum_{m=1}^n \varphi(Y = 1) \quad (9)$$

在固定时间  $T$  内电梯停留在不同楼层的概率如式(10)

$$P(X) = \prod_{m=1}^n P(X_n | Y = 1)P(Y = 1) + \prod_{m=1}^n P(X_n | Y = 0)P(Y = 0) \quad (10)$$

当电梯运行状态改变获得新的统计数据，代入贝叶斯公式获得后验概率<sup>[12]</sup>，即电梯下一次呼叫请求处于某个楼层的概率值如式(11)

$$P(Y = 1 | X) = \frac{\prod_{m=1}^n P(X_n | Y = 1)P(Y = 1)}{\sum_{i=0}^1 \prod_{m=1}^n P(X_n | Y = i)P(Y = m)} \quad (11)$$

### 2.3 数据代入分析

通过实地调研获得某市重点医院上午 8:00--11:00 电梯停留在不同楼层的次数，并统计处理，依据公式 (8) - (11) 处理过程见图1，获得相关概率数据如表1:

表1 电梯停留在不同楼层的概率统计表

Table 1 The probability statistics of the elevator stays in different floors

| 楼层 \ 状态 | 统计值  |      | 后验概率       |
|---------|------|------|------------|
|         | 有呼叫  | 无呼叫  | $P(Y=1 X)$ |
| 1       | 0.10 | 0.15 | 0.15       |
| 2       | 0.16 | 0.04 | 0.24       |
| 3       | 0.07 | 0.03 | 0.11       |
| 4       | 0.08 | 0.04 | 0.12       |
| 5       | 0.12 | 0.03 | 0.18       |
| 6       | 0.05 | 0.02 | 0.08       |
| 7       | 0.06 | 0.02 | 0.09       |
| 8       | 0.02 | 0.01 | 0.03       |
| 总计      | 0.66 | 0.34 | 1          |

数据处理过程如图 1:

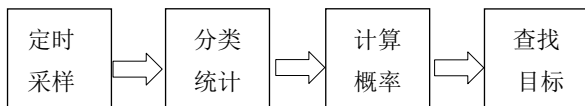


图 1 数据处理过程

Fig.1 Data processing procedure chart

如图 1 所示，在固定时间间隔内进行采样，根据采样结果确定是否有呼叫请求，并根据有无呼叫请求进行分类统计，并利用贝叶斯算法计算出各个楼层有呼叫请求的后验概率记录入表 1，对后验概率进行排序查找最大使用频次的楼层号，获得查找

目标。

根据表 1 中的电梯停留在不同楼层概率的统计值，结合贝叶斯公式计算出后验概率，并绘制后验概率分布图如图 2:

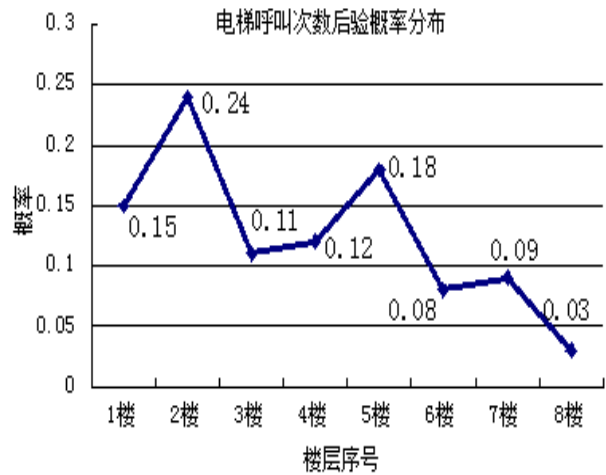


图 2 后验概率分布图

Fig.2 The posterior probability distribution map

由后验概率分布图可知，在电梯有呼叫请求的情况且呼叫楼层在 2 楼的概率最大，实际调研中发现 2 楼设有门诊部，故而人员往来频繁，据此如果控制电梯在该段闲停时自动停到 2 楼，则一方面提高电梯本身的运行效率，另一方面节省大多数人等待电梯的时间，提高总体的效益。

## 3 电梯调度算法的设计与实现

### 3.1 算法流程设计

根据以上的电梯数学模型的建立，以及检测技术的应用研究，在不改变垂直电梯现有的硬件结构基础上模拟其运行方式，并对传统的电梯运行方式进行优化改造，改变其算法结构，设计更加智能高效的运行方式，即依据概率确定闲停位置，通过红外检测技术确定电梯外是否有人，防止轿厢停止后电梯外无人，避免不必要停留等现象。从而大大提高电梯运行效率，为用户节省更多时间。图3为单次电梯运行时的依概率算法流程图:

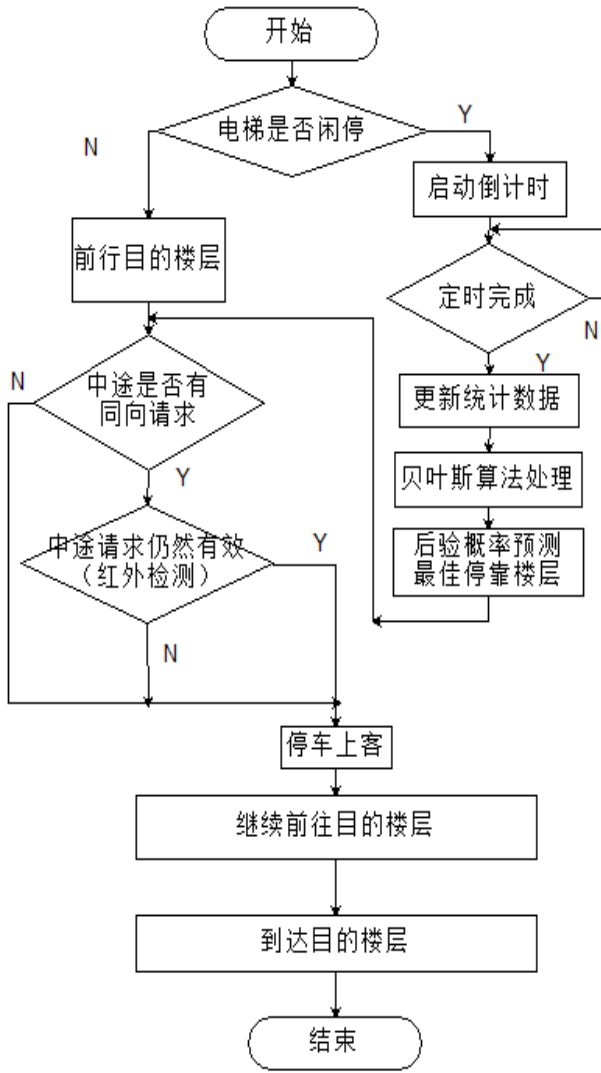


图3 算法流程图  
Fig.3 Algorithm flow chart

根据模型分析，在电梯控制算法里可以把电梯当作一个状态机对待，根据不同的状态给电梯系统不同的控制指令，实现系统的高效有序调度。电梯运行流程如下：

(1)、电梯系统检测当前状态，是否处于闲置状态决定是否启动贝叶斯算法确定最佳停靠楼层，采用依概率停靠轿厢技术；

(2)、系统中还另外加入红外检测技术，防止出现电梯外的用户按下呼叫按键之后，但由于某些原因放弃乘坐电梯，就出现电梯到达该楼层门打开，门外却空无一人的现象（调研这种现象在医院等场所特别常见）；

(3)、该电梯的呼叫请求多采用中断调用机制，任意一个过程都可能被中断打断，去执行级别更高的程序，或者转而重新开始新的循环，前提是不影响正常的运行逻辑。

### 3.2 算法实现与整体系统

图4为模型整体框图，控制器通过各种传感器采集，获得电梯当前运行状态，再结合实际电梯的运行逻辑，并融入依概率停靠轿厢的调度算法和红外检测调度算法对电梯系统进行控制，实现预定功能。

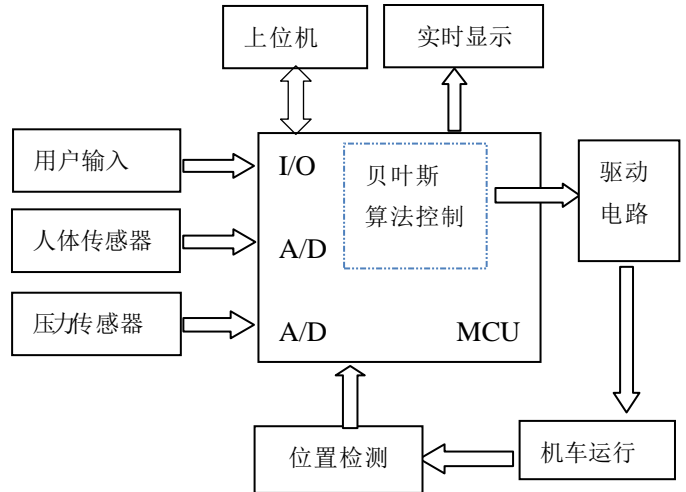


图4 系统框图  
Fig.4 System diagram

## 4 仿真结果对比分析

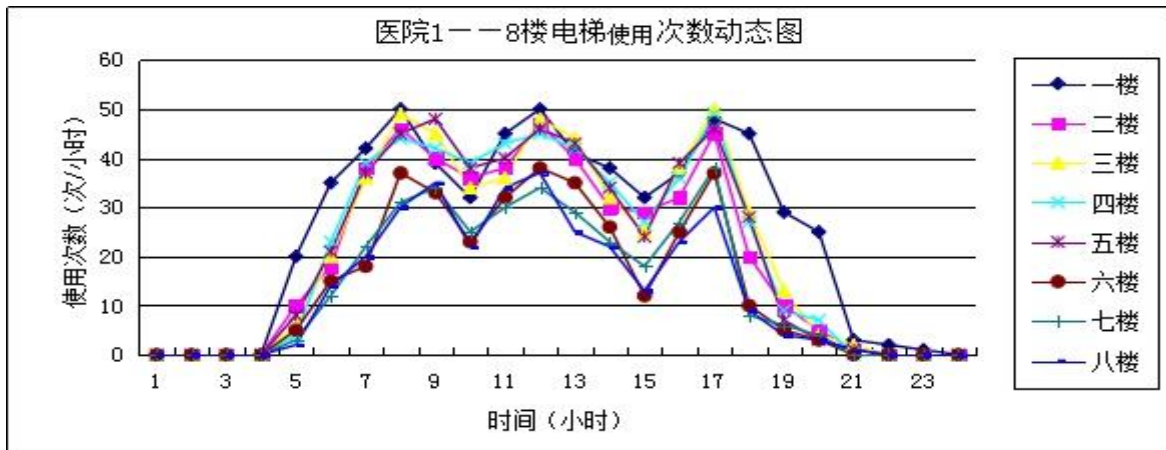


图5 模型测试数据表

Fig5 The model test data sheet

图5为某市重点医院1至8楼电梯使用次数动态图，从中可以看出电梯在上午8点、中午12点，下午17点分别出现客流高峰期，且不同楼层在不同时段各自呼叫次数也有所有同，分布存在差异，将这些数据分别代入式(3)和式(4)中求出传统电梯运行时与基于贝叶斯算法的依概率停靠轿厢算法用户平均等待时间，仿真时根据式(2)取 $\Delta T=20s$ ，依据图中上午8点的数据进行实际模型仿真，测试结果如下：

1至8各楼层仿真数据分别为：20，39，36，30，25，23，22，20

传统运行方式下平均候梯时间

$$t_n = \frac{\sum_{m=1}^8 (|1-m| \Delta T) N_x + (m-1) \Delta T}{\sum_{x=1}^8 N_x} = 66.7s \quad (12)$$

将数据代入公式(8)——(9)获得先验概率，整理代入公式(10)——(11)获得各个楼层有呼叫的后验概率分别如下：0.09、0.18、0.17、0.14、0.12、0.11、0.10、0.09.由此可知有呼叫时的后验概率在 $n=2$ 时取最大，基于贝叶斯算法可知 $n=2$ 平均候

$$\text{梯时间 } t_n' = \frac{\sum_{m=1}^8 (|n-m| \Delta T) N_x}{\sum_{x=1}^8 N_x} = 47.8s \quad (13)$$

$$\text{则等效运行效率提高量 } \beta = \frac{t_n - t_n'}{t_n} \approx 28\%$$

从以上仿真数据对比分析可知，采用贝叶斯算法依概率停靠轿厢技术电梯整体运行效率约提高28%，一定程度上节省用户候梯时间，增加整个系统的实时效率。

## 5 结论与分析

本文中提出分时段对每楼层电梯使用次数进行概率统计、处理分析，根据某些已有电梯信息对用户呼叫事件做出后验预测估计，通过预测结果为执行电梯控制策略提供参考信息以便高效调度电梯。

同时系统引用红外检测技术，确定电梯外是否有人，防止用户途放弃使用电梯，而电梯停靠轿厢后电梯外无人的现象发生，避免不必要停留从而更进一步节省用户乘行时间。

为了验证基于贝叶斯算法的调度算法的可行性和实用性，建立的电梯运行仿真模型，由模型仿真结果及数据可知采用该算法有利于提前预知并削弱客流高峰期，减少用户的候梯时间，提高电梯系统的整体运行效率。

### 参考文献

1. 陈玉仙.新一代电梯的调度算法研究[D].长沙：中南大学，2010.
2. 张轮，杨文臣，刘拓，施奕骋.基于朴素贝叶斯分类的高速公路交通事件检测[J].自然科学版，2014,42(4):2-6.
3. 黄尚君.浅谈超高层建筑的电梯设计[J].科技创新导报，2009(19):1.



4. 李章吕.贝叶斯决策理论研究[D].天津:南开大学,2012.
5. 卿晓霞,王波,段军.考虑等待时间的电梯运行模拟测试与节能分析[J].计算机工程与应用,2012,48(31):232-235.
6. 刘耀武,聂风华,苏强,霍佳震.具有时间约束的电梯节能调度算法[J].系统工程理论与实践,2013,33(9):3-6.
7. 范次猛.教学用电梯模型系统的研究[J].机电工程技术,2009,38(12):52-54.
8. 刘舒祺,施国梁.基于热释电红外传感器的报警系统[J].国外电子元器件,2005(3):5-8.
9. iikonen M L.Customer Service in an Elevator System During Up-peak. Transpn Res, 2001,25(02):27-36.
10. BISHOP C H,SHANLEY K T.Bayesian model averaging problematic treatment of extreme weather and a paradigm shift that fixes it[J].Monthly Weather Review ,2008,136(12) :4641-4652.
11. Raftery A E.Using Bayesian model averaging to calibrate forecast ensembles[D].Washington:University of Washington,2005.
12. OZBAY K,NOYAN N.Estimation of incident clearance times using Bayesian networks approach[J].Accident Analysis & Prevention,2006(38):542-555.

# 一种基于 GPS 与 GPRS 的便携式酒精检测仪的设计与实现\*

温雪君; 刘小晗; 蔡 瑶

(吉林大学 仪器科学与电气工程学院, 长春 130022)

**摘要:** 世界卫生组织在交通事故调查中指出, 一半以上的的车祸与酒后驾驶有关, 酒后驾驶已成为交通事故致死的首要原因。随着“醉酒驾驶”正式入刑, 检测驾驶员是否酒后驾驶的酒精浓度检测仪的设计与应用具有重要意义与价值。为了更有效的减少交通事故的发生, 克服传统监督执法方面的不足, 本项目设计了一种基于 GPS 和 GPRS 的便携式酒精检测仪。该仪器将单片机作为主控芯片, 控制气敏传感器监测呼出气体中的酒精浓度, 并实现 LCD 液晶显示、醉酒阈值设定和声光报警的功能, 是一款实用性较强、安全可靠的便携式气体酒精浓度检测工具, 还可以将检测者的位置信息和酒精检测结果发送到上位机, 在一定程度上可起到监督执法的作用。

**关键词:** 酒后驾驶 酒精检测仪 GPS GPRS 气体酒精浓度

**中图分类号:** X924.3 **文献标识码:** J

## The design and implementation of a portable alcohol detector based on GPS and GPRS

Wen Xue-jun; Liu Xiao-han; Cai Yao

(College of Instrumentation & Electrical Engineering, Jilin University, Changchun 130022, China)

**Abstract:** The world health organization in the traffic accident investigation pointed out that more than half of the car accidents are related to drunk driving, which has become the main cause of traffic accidents. With 'Drunk driving' officially in the sentence, the design and application of alcohol concentration detector to detect whether the driver is drunk driving are become very important. This project designs a portable alcohol detector based on GPS and GPRS to reduce traffic accidents more effectively and to overcome the shortcomings in traditional supervision and law enforcement. The detector uses single chip microcomputer, controlling the gas sensor to monitor the concentration of alcohol in people's breathing, and implements LCD display, threshold setting, sound-light alarm functions. The designed detector is a portable gas alcohol concentration detection tool with strong practicability and safety. It can also send detectors' information of location and alcohol detection results to PC, plays a role in the supervision of law enforcement to a certain extent.

**Key words:** Drunk driving Alcohol concentration detector GPS GPRS Alcohol gas concentration

## 0 前言

近年来, 中国经济高速发展, 人民生活水平不断提高, 中国逐渐步入了“汽车社会”, 酒后驾驶行为所造成的事故也随之越来越多, 对社会的影响也

越来越大。据有关资料统计显示, 酒驾引起的交通事故概率是非酒驾的 16 倍<sup>[1]</sup>。可见, 酒精正在成为越来越凶残的“马路杀手”其检测与预防越来越受到世界各国的重视<sup>[2]</sup>。因此判断驾驶员是否属于酒后驾驶, 准确有效的检测出酒精含量就显得尤为重要, 酒精浓度检测仪也因此具有十分广阔的现实市

\* 指导教师: 李肃义

项目类型: 大学生创新项目 (2015650987)

场和重要意义。

目前国内外检测酒精较为成熟的方法是呼吸式酒精检测法与抽血式检测法<sup>[3]</sup>。现场抽血往往做不到，而事后血检又增加执法时间，并且属于有创检测，过程复杂，成本高，简单可行的是检测驾驶员呼气中的酒精浓度<sup>[4]</sup>。

本项目所设计的是一种基于 STC12C5A16AD 单片机，利用 MQ-3 气敏酒精传感器，对呼气中的酒精浓度进行检测并实现 LCD 显示、醉酒阈值设定、声光报警、GPS 定位和 GPRS 数据传输功能的便携式气体酒精浓度检测仪。

## 1 项目设计理论基础

### 1.1 呼气酒精检测技术

呼气酒精检测技术是一种无创的、对人体呼出的气体进行检测的一种技术。目前用到的呼气检测技术主要分为比色技术、半导体检测技术、电化学检测技术、红外线检测技术<sup>[5]</sup>。由于肺深部气体的酒精浓度与血液酒精浓度存在一定的比例关系，因此，符合国家标准的呼气酒精检测仪在基准条件下的测试结果的准确性还是比较高的<sup>[6]</sup>。本项目就是利用呼气酒精检测技术展开设计的。

### 1.2 GPS 定位技术

全球定位系统 (Global Positioning System-GPS) 是具有海、陆、空全方位实时三维导航与定位能力的新一代卫星导航与定位系统<sup>[7]</sup>。GPS 系统的基本原理是测量出已知位置的卫星到用户接收机之间的距离，然后综合多颗卫星的数据就可知道接收机的具体位置<sup>[8]</sup>。本项目选用了 GPS 模块直接与主控芯片相连通过固定程序知道被测者位置信息。

### 1.3 GPRS 网络通讯技术

GPRS (General Packet Radio Service) 是通用分组无线服务技术的简称，它是 GSM 移动电话用户可用的一种移动数据业务，属于第二代移动通信中的数据传送技术。这项技术位于第二代(ZG)和第三代(3G)移动通讯技术之间<sup>[9]</sup>。本项目是将采集到的酒精含量的数值和 GPS 模块获得的位置坐标信号，一并输入到主控芯片中进行存储，主控芯片再对信息进行处理，之后输入到 SIM900A，SIM900A 对信号进行打包发送，使得目标机得以接收到信息。

## 2 系统总体设计

整体系统包括单片机主控模块、酒精检测模块、GPS 定位模块、阈值设定模块、EEPROM 存储模块、

LCD 显示模块、GPRS 通讯模块、声光报警模块和电源模块。系统整体模块如图 1 所示。

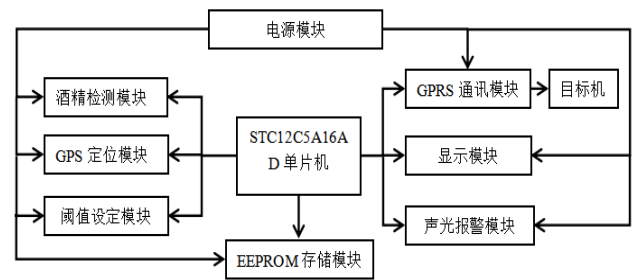


图1 系统框图

Fig. 1 System diagram

本项目主控模块采用 STC12C5A16AD 单片机，酒精检测模块用 MQ-3 气敏酒精传感器。MQ-3 将采集的酒精信号送入单片机内部进行模数转换。单片机对数字信号进行分析处理，并将所得的结果显示在 LCD 上。可以通过按键设置不同的酒精浓度阈值并用 EEPROM 存储，一旦检测出的酒精浓度超过设定的阈值，单片机就会控制蜂鸣器和二极管发出声光报警。GPS 定位模块获得被测者位置信息，传到单片机中，单片机对酒精含量和位置信息进行存储并输入到 GPRS 的 SIM900A 中，以信息的方式打包发送给目标机，起到监督执法的作用。电源模块为整个系统供电。

## 3 系统硬件设计

### 3.1 单片机系统

本系统包括主控模块、阈值设定模块、声光报警模块。主控芯片采用 STC12C5A16AD 单片机，该芯片为 52 内核的 8 位单片机，内存比 51 单片机大 4 倍，最主要的是自带 8 位高速 A/D 转换器，而且烧写程序方便快捷，程序结构完全跟其他 51 一样。主控模块还包括时钟电路和复位电路。声光报警就是在检测的酒精浓度超过阈值时，蜂鸣器响、二极管亮。阈值设定采用按键加减的方式，由程序控制 (见图 2)。

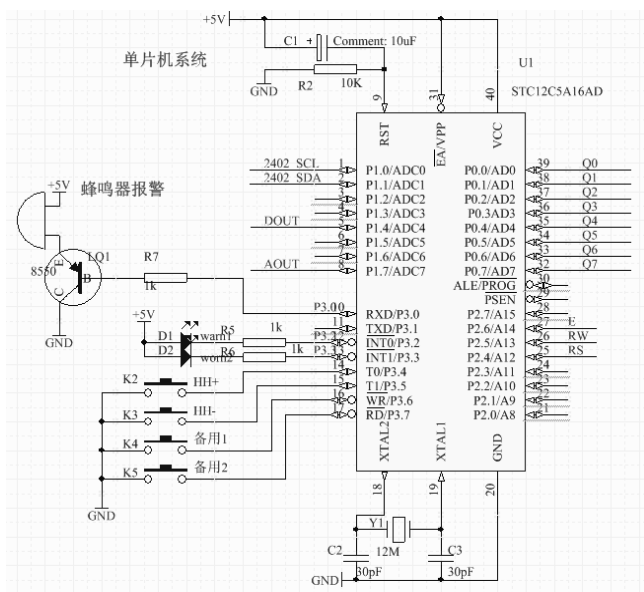


图2 单片机系统原理图

Fig. 2 Schematic diagram of MCU system

### 3.2 酒精检测模块

酒精检测模块包括气体传感器单元和信号调理单元。气体传感器选用了 MQ-3，是考虑到以下几点因素：

- ◆ 对乙醇蒸汽有很高的灵敏度和良好的选择性；
- ◆ 快速的相应恢复特性；
- ◆ 长期的寿命和可靠地稳定性；
- ◆ 简单的驱动电路；

MQ-3 乙醇气体传感器可以看做一个气敏电阻，其阻值随乙醇浓度的变化而变化。通过判断的输出阻值的大小可得到随乙醇气体的浓度。

我们采用 MQ-3 模块来采集气体乙醇信号，其内部包含酒精传感器和将检测信号由电阻值转变成电压值的信号调理电路。原理图如图 3 所示。

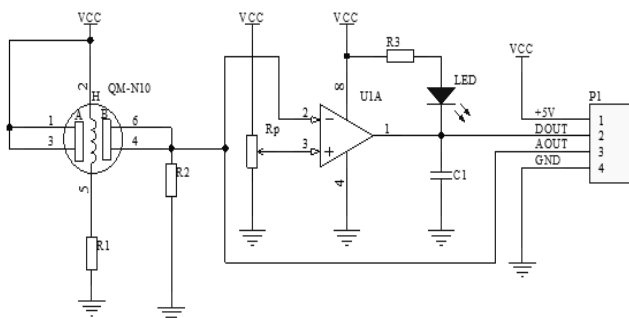


图3 MQ-3模块原理图

Fig. 3 Schematic diagram of MQ-3 module

该模块最终的四个管脚分别对应电源端 (+5V)、TTL高低电平输出端 (DOUT)、模拟电压输出端 (AOUT)、地端 (GND)。AOUT输出的电压检测信号传送到单片机 ADC7 口进行处理，根

据空气中酒精的浓度，数字电平信号DOUT 可以直接输出报警信号。

### 3.3 LCD 显示模块

显示部分采用 LCD1602 液晶屏进行数据显示，与单片机接口电路如图 4 所示。其中 VO 为背光引脚，用电位器调节背光亮度。RS、E/W 和 E 为液晶的控制引脚，其余为数据引脚和电源引脚。

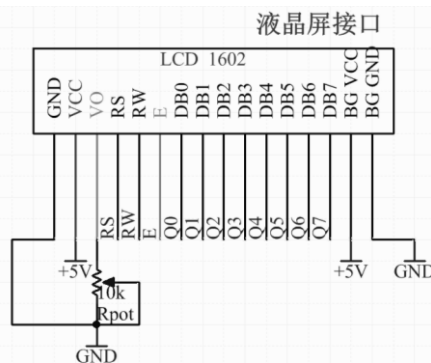


图4 LCD与单片机接口电路

Fig. 4 Circuit of LCD and MCU

### 3.4 EEPROM 存储模块

EEPROM 存储模块采用 I<sup>2</sup>C 接口的 AT24C04 芯片，利用其掉电不失数据的优点实现醉酒阈值的存储。可以通过“增加”、“减少”按键来设定阈值并保存。其原理图如图 5 所示。图中 A0、A1 和 A2 为芯片的地址引脚，一般接地。SCL 和 SDA 为 AT24C04 和单片机 I<sup>2</sup>C 通信的时钟线和数据线。

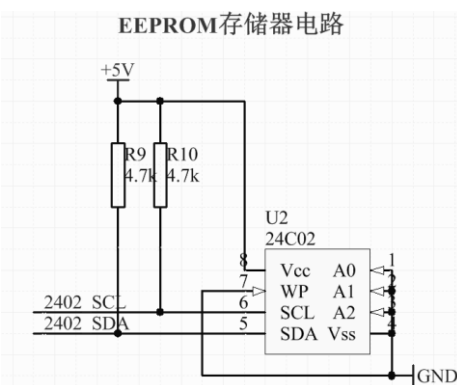


图5 EEPROM存储电路原理图

Fig. 5 Schematic diagram of EEPROM storage circuit

### 3.5 GPS 定位模块

本项目采用集成的 GPS 模块，使用天线更容易接收到位置信息。通过 USB-TTL 工具将单片机接收到的 GPS 定位的信息传给电脑，在串口助手上可接收到时间、经纬度等信息。模块上小灯常亮，表示模块已开始工作，但还未实现定位；灯闪烁则表示模块已经定位成功。其连接图如图 6 所示。

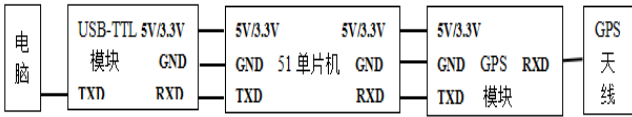


图6 GPS、MCU与上位机连接图

Fig. 6 GPS, MCU and PC connection diagram

### 3.6 GPRS 通讯模块

本项目采用集成的 GPRS 模块，此模块以 SIM900A 为主，将手机 SIM 卡插入插槽，就可以将此模块看作一个手机，可以实现电话语音、短信、彩信、GPRS 数据传输等功能。我们主要是通过 GPRS 模块最终实现信息以短信的方式发送给目标机。MCU 控制 SIM900A 接收到电脑串口助手发送的信息后再发送给目标机。SIM900A 与电脑的连接也同样需要串口转换器。其连接图如图 7 所示。

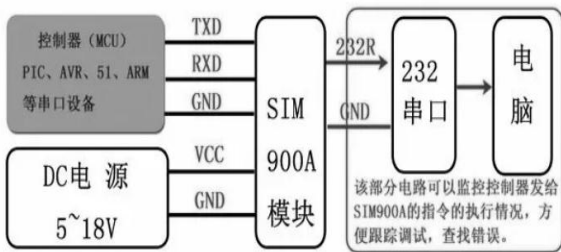


图7 GPRS、MCU与上位机连接图

Fig. 7 GPRS, MCU and PC connection diagram

## 4 软件程序设计

将控制酒精采集、数据处理、显示、阈值设定存储、报警、GPS定位、GPRS数据传输的C代码下载到STC12C5A16AD单片机中。启动电源，进行GPS定位、酒精信号采集处理显示，同时还要通过按键扫描，设定阈值、开启GPRS数据传输。一旦超过阈值，启动报警功能。控制程序流程图如图8所示。

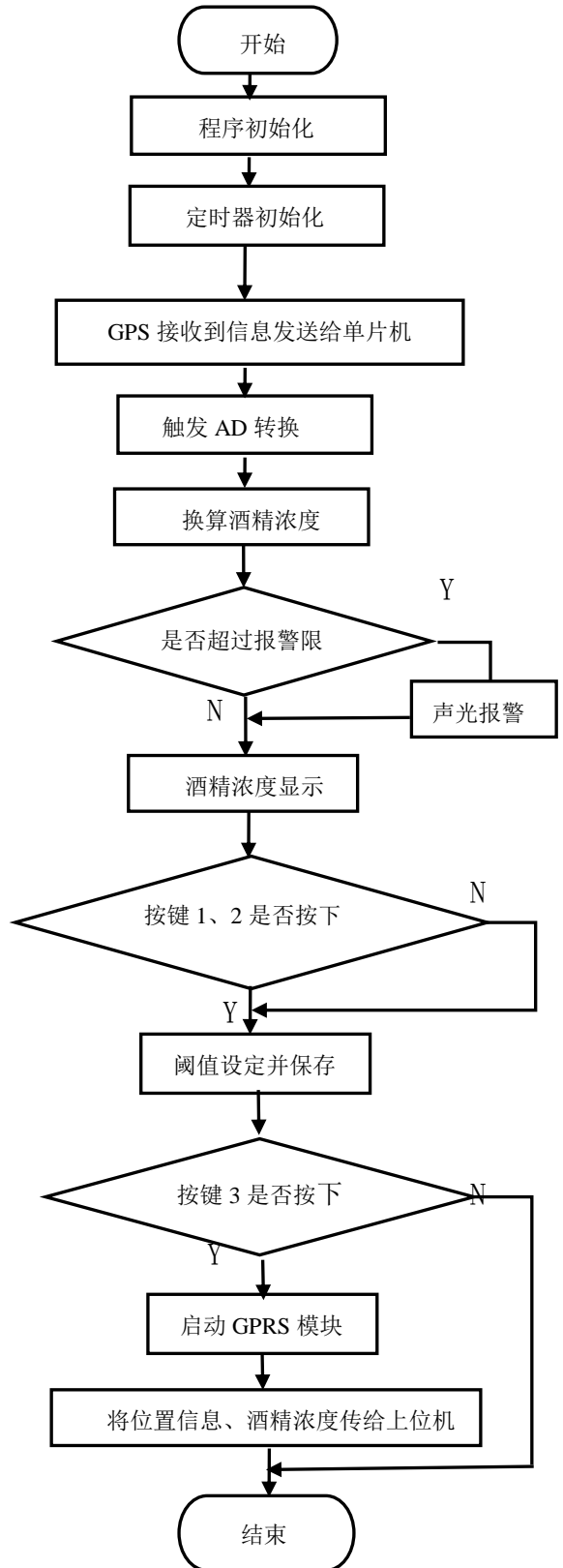


图8 控制程序流程图

Fig. 8 Flow chart of control program

## 5 测试与分析

按照上述硬件和软件设计的方法，进行了分模块调试。首先对GPS模块进行了调试与测试。使用一根USB-TTL线的RXD和GPS模块的TXD口对接，另外一端接在 PC 机上，安装GPS模块的USB驱动后，在串口接收到的位置信息如图9。

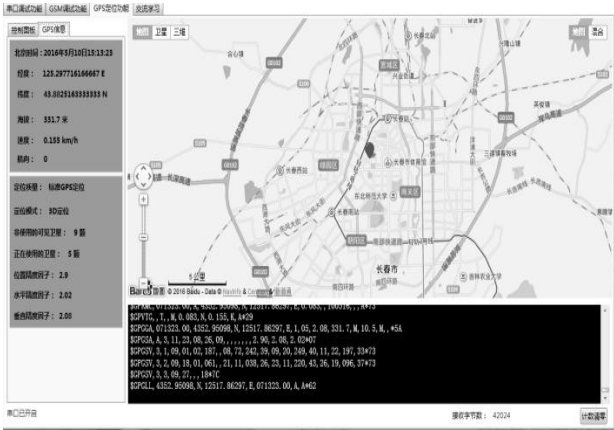


图 9 GPS 串口调试结果

Fig. 9 GPS serial debug results

GPRS也是同样用串口转换器。首先需要插上SIM卡，启动模块，等待模块注册成功即可对模块操作直到看到绿灯慢闪，周期3S，表明模块已经注册到2G网络。然后在串口助手中设置短信形式、接收方手机号码、短信内容等，最终会收到的短信和调试过程图片如图10与图11。

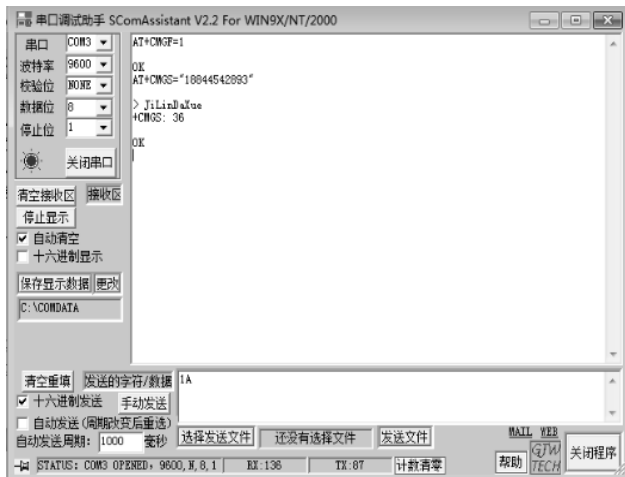


图10 GPRS的初始化设置串口界面

Fig. 10 Initialization settings of GPRS in serial interface



图11 目标机接收的短信

Fig. 11 Message received of the target machine

最后把上述两个模块和酒精检测等所有模块结合起来，观察到的现象如图12所示。

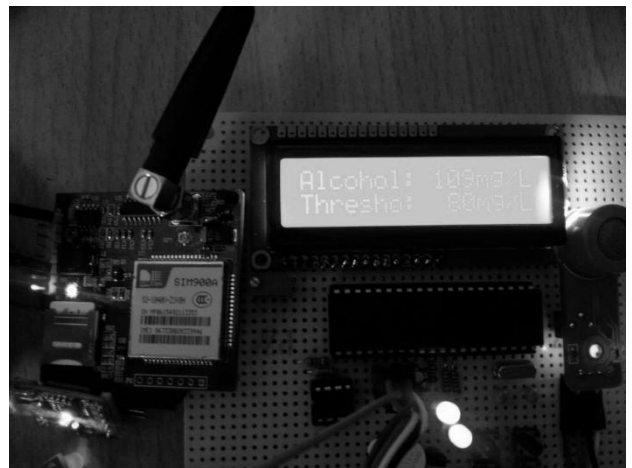


图12 系统运行实物图

Fig. 12 Prototype of the alcohol detector

可见，本系统能够显示被测者的酒精含量，上图酒精含量为109mg/100mL，超过了设定的的阈值80mg/100mL，所以可以看到二极管亮。并且GPS定位，GPRS数据传输，最终将被测者的所在位置（东经125.29、北纬43.88，海拔高度265.8m）以及酒精含量值以短信的形式发送给目标机，目标机接收到的短信如图13所示。



图13 目标机最终接收的短信

Fig. 13 The final message received by the target machine

另外，用这个酒精检测仪做了对比实验，选用酒精含量：4.3（%）麦汁浓度：11（%）的青岛啤

酒。被测者们（体重相差不大）饮不同量的酒精，测量其饮酒后30min酒精含量值来进行对比实验。实验所得数据如表一所示：

表一 酒精检测仪实验数据记录表

Table 1 Experimental data record of alcohol detector

| 饮酒量   | 被测者 | 酒精浓度<br>(mg/100mL) | 平均值   | 血液中理想值 |
|-------|-----|--------------------|-------|--------|
| 300mL | A   | 36                 | 40.67 | 32.25  |
|       | B   | 44                 |       |        |
|       | C   | 42                 |       |        |
| 600mL | A   | 71                 | 74.67 | 64.50  |
|       | B   | 78                 |       |        |
|       | C   | 75                 |       |        |
| 900mL | A   | 103                | 108   | 96.75  |
|       | B   | 109                |       |        |
|       | C   | 112                |       |        |

从实验数据可以看出真实值比呼出气体酒精含量普遍低，并且随着饮酒量增多差值增大，所以需要利用多次实验对比曲线来进行曲线校正。上述图表也可以反映出：本项目设计的基于GPS、GPRS的便携式酒精检测方法在理论和实际中都是可行的，可以作为交警检查酒驾很好地工具，为道路安全提供很好地保障。

## 6 结束语

醉酒驾驶是当前危害公共交通安全的重大社会弊病，是造成交通事故的重要原因。本项目利用呼气法检测酒精浓度，在此基础上增加了GPS定位和GPRS网络数据传输模块，不仅可以根据不同环境设定醉酒阈值，使仪器使用更方便快捷；还可以令交警在巡查酒驾时，能自动发送饮酒者位置与酒精含量信息，实时性强、安全可靠，起到监督执法的作用。在下一步的工作中，要对本项目进行优化，弥补本项目的一些不足。如多次多人进行对比试验，进一步加强和改进传感器，使测量更准确，测量方法更卫生、更人性化。

## 参考文献

1. 邓进,李坤,罗开俭等.贵州省2002年度道路交通事故调查[J].中华创伤杂志,2004,20(10):620-621.
2. 陈国强.汽车驾驶员血液酒精含量的近红外光谱法无损检测[D].山东大学,2012.
3. 卢立倩.基于近红外光谱的血液酒精含量无损检测系统设计[D].山东大学,2014.
4. 林放,周立平.电子酒精检测装置简述[J].科技情报开发与经济,2011(2):214.
5. 卢利强,方学新.在交通执法中呼气酒精检测的应用研究[J].中国公共安全(学术版),2011,No.2504:116-119.
6. 俞春俊,卢利强.呼气酒精浓度检测的合法性研究[J].道路交通管理,2012,05:36-37.
7. 段珺玉.浅析常用导航技术[J].中国电力教育,2010,S1:794-795.
8. 周正兴.GPS全球卫星定位系统组成及原理简析[J].家电维修:大众版,2012,01:51-57.
9. 赵国庆.基于GSM/GPRS的远程列车用电监测系统.太原理工大学硕士论文:43-44.

# 基于 PZT 的多方向风能收集装置设计与应用\*

苟 鑫; 陈玉达; 刘丽佳

(吉林大学 仪器科学与电气工程学院, 长春 130026)

**摘要:** 为解决微功耗设备长时间工作于户外的电源供给问题, 本文提出了一种基于 PZT 的多方向风能收集装置。该装置以压电效应为基础, 利用设计的压电悬臂梁阵列将风能转化为振动机械能, 在压电效应作用下机械能进一步转化为交流电能。通过设计合理的转换电路, 把风致振动产生的电能存储在锂聚合物电池中。此外, 本文还设计了以 MSP430F149 微处理器为核心的无线数据传输系统。经实验测试, 本装置在 6-9m/s 风速环境中达到最佳工作状态, 连续工作 40min 能将一块 25mAh 的锂聚合物电池充满。这一装置具有结构简单, 无污染等优点, 可以广泛应用于野外数据监测、无线数据传输等领域。

**关键词:** 压电效应; 悬臂梁阵列; 转换电路; 无线数据传输

## Design and application of multi direction wind energy collection device based on PZT

GOU Xin; Chen Yu-da; Liu Li-jia

(College of Instrumentation & Electrical Engineering, Jilin University, Changchun 130026, China)

**Abstract:** In order to solve the power supply problem of the micro power equipment which needs long time working in the outdoor, this paper presents a multi direction wind energy collection device based on PZT. Based on the piezoelectric effect, the design of the piezoelectric cantilever beam array is used to convert wind energy into mechanical energy, and mechanical energy can be converted into alternating current energy under the action of piezoelectric effect. Through the rational design of the conversion circuit, the wind-induced vibration produced by the electrical energy stored in the lithium polymer batteries. In addition, wireless data transmission system based on MSP430F149 microprocessor is designed in this paper. The experimental test, the device in the 6-9m/s wind speed environment to achieve the best working state, continuous work 40min can be a 25mAh of lithium polymer battery full. The device has the advantages of simple structure, no pollution, etc, and can be widely used in field data monitoring, wireless data transmission and other fields.

**Key words:** piezoelectric effect; cantilever beam array; energy conversion; wireless data transmission

## 0 引言

随着物联网技术的不断发展, 各种各样的微功耗设备逐渐进入我们的生活, 它们的应用也越来越广泛, 但其长期供电问题却随之而来, 特别是对于长期工作在野外的数据采集与监测设备, 由于所搭配的电池容量有限, 而且不方便及时更换, 需要合理配置其电源供给系统。针对微功耗设备的电源供给问题, 国内外研究人员都青睐于自然环境中普遍

存在的太阳能<sup>[1]</sup>, 热能<sup>[2]</sup>以及振动能<sup>[3-4]</sup>。风能, 作为环境中普遍存在的一种能量形式, 能够很好地与其他能源结合, 形成良性互补。微型风能收集装置的设计思路一般是先将风能转化为振动机械能, 再通过静电式、电磁式或压电式装置将机械能转化为电能<sup>[5]</sup>。压电陶瓷是一类具有压电特性的电子陶瓷材料, 能够将机械能和电能互相转换, 已被广泛应用于医学成像、声传感器、声换能器、超声马达等<sup>[6]</sup>。本文所提出的风能收集装置的换能元件选取锆钛酸铅压电陶瓷(缩写为 PZT)<sup>[7]</sup>, 它是能够对

\* 指导教师: 周晓华

项目类型: 大学生创新项目 (2015650988)



来自不同方向风中蕴含的能量实现有效收集，以实现低功耗设备的自供能。

## 1 机械系统设计

机械系统是整个装置的重要组成部分，它直接与风耦合以进行能量转换，其结构设计的优劣直接影响整个装置的能量转换效率。机械系统主要由壳体和压电悬臂梁阵列构成，其核心是压电悬臂梁，机械系统如图 1 所示。

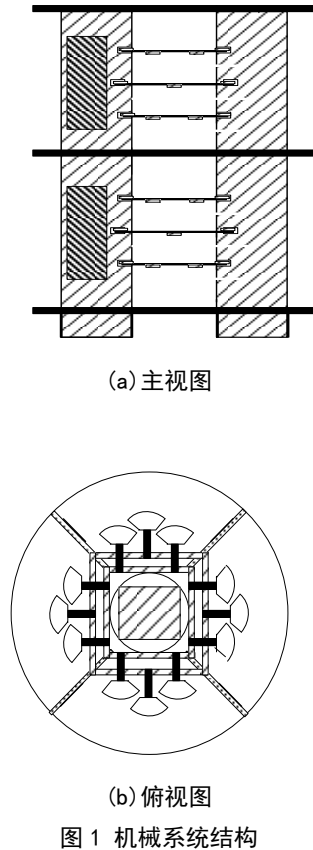


图 1 机械系统结构

### 1.1 壳体

壳体由厚度为 3.0mm 的有机玻璃切割、组装而成，除用于连接、支撑、固定与保护外，还起到约束流体的作用；整个壳体呈圆柱状，分为横向隔板与纵向隔板，纵向隔板与横向隔板各开有小槽，槽与槽之间相互嵌入，构成壳体。壳体的横向隔板为外径 30.0cm、内径 13.0cm 的圆环片状结构，纵向隔板为矩形片状结构，每层高度为 10.0cm，三张横向隔板与四张纵向隔垂直交错排列，将整个圆柱形空间分割成八个张角为 90° 的喇叭口单元。

### 1.2 压电悬臂梁阵列

压电悬臂梁阵列环绕分布在圆柱形装置的八个单元中，每个单元里的压电悬臂梁阵列具有相同的排列方式。仅从一个单元来看，压电悬臂梁阵

列由 5 个压电悬臂梁组成，分上、中、下三层，上层和下层每层并行排列两个压电悬臂梁，中间层仅放置一个，但其距圆柱中心线的距离比上下层压电悬臂梁距圆柱中心线的距离稍远，五个压电悬臂梁的顶端构成一个正四棱锥结构，如图 1 (b) 所示。

压电悬臂梁由电极、压电陶瓷片和扇形柔性梁组成。电极由两片长条形单面覆铜板经螺丝夹紧而成，具有夹持固定压电陶瓷片与引出电流的作用。压电陶瓷片的发电原理基于第一类压电方程：

$$D = dT + \epsilon^T E$$

$$S = S^E T + d' E$$

式中  $D$  为电位移矢量， $d$  为压电应变常数， $d'$  为  $d$  的转置， $S$  为应变变量， $S^E$  为弹性柔顺系数， $T$  为应力， $E$  为电场强度矢量， $\epsilon^T$  为介电常数<sup>[8]</sup>。

扇形柔性梁选用聚对苯二甲酸乙二醇酯薄膜（简称 PET），通过铝片和螺丝夹持，使其与压电双晶片前端紧密连接。利用 ANSYS 进行有限元分析并优化设计得出的模型如图 2 所示，其中压电双晶片的有效尺寸为长 30.0mm、宽 10.0mm、厚 0.7mm，扇形柔性梁的张角为 90°、半径为 25.0mm、厚度 0.1mm。

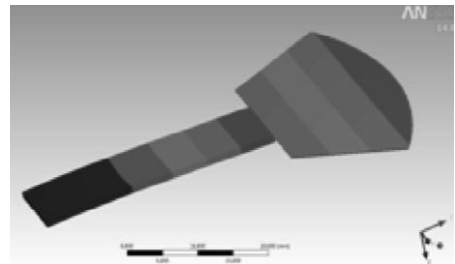


图 2 压电悬臂梁仿真模型

Fig. 2 Simulation model of piezoelectric cantilever beam

## 2 电路系统设计

电路系统的功能是将每个压电悬臂梁阵列产生的不规则交流电能转化为可被各类低功耗设备利用的直流电能，包含整流、并联缓冲、DC-DC 升压变换以及存储环节，其结构如图 3 所示。

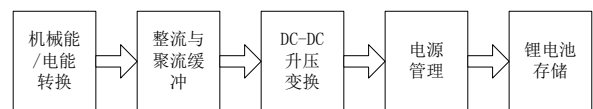


图 3 电路系统结构

Fig. 3 Circuit system structure

### 2.1 倍压整流与聚流缓冲

常用的整流方案有半波、全波、桥式和倍压四种。由于压电悬臂梁输出的交流电压幅值较小，为

有效地将其利用,采用二倍压整流电路<sup>[9]</sup>,如图4所示。与桥式整流电路相比,二倍压整流电路的结压降更小,同时,电路中所用二极管为SD103AWS型肖特基二极管,正向压降 $V_F$ 仅0.4V,能有效降低整流电路的损耗。每个压电悬臂梁均连接一个二倍压整流电路,将产生的无规则交流电压转换为脉动较小的直流电压供后续电路处理。

考虑到单个压电悬臂梁电流输出能力有限,达不到后续处理电路的最低要求,故将一个喇叭口单元中压电悬臂梁阵列的所有输出电流汇聚到超级电容中,当电容中积累的电量达到后续电路的启动电压时,再驱动电路运行。单个二倍压整流电路的输出通过二极管与超级电容相接,能有效避免已经汇聚到超级电容中的电荷倒流至二倍压整流电路的情况。

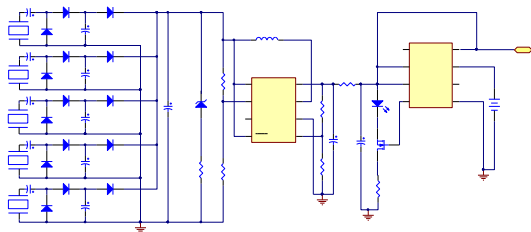


图4 系统电路图

Fig. 4 System circuit diagram

## 2.2 DC-DC 升压与电源管理

电路工作时,超级电容两端的电压较低,达不到一般电子系统所需的5V供电电压,故需要DC-DC升压电路将超级电容两端的低电压泵升到较高的恒定直流电压。MAX1678芯片是一款高效率、低噪音的升压型DC-DC转换器,启动电压低至0.87V,静态工作电流仅37 $\mu$ A<sup>[10]</sup>,满足提出的电路功率损耗低这一要求。此外,MAX1678有固定的3.3V与可调整的2V-5.5V两种输出模式,能极大程度满足电路需要。该DC-DC升压电路以MAX1678芯片为核心,通过调节采样电阻R4和R5的阻值,使输出电压为5.5V,同时,通过调节采样电阻R2和R3的阻值,使升压电路的有效输入电压为2V。

由于MAX1678的输入电压极限值为+6.0V,为保证电路安全可靠工作,在超级电容与DC-DC升压电路之间并联稳压二极管1N4734,防止超级电容端电压在长时间连续充电状态下出现过电压。

为将整个装置的8个单元收集的电能有效存储到锂聚合物电池中,同时避免电池过充和过放,有必要引入电源管理环节。LTC4071芯片能对电池进行断续或连续充电,充电电流范围为550 nA~50 mA,提供4.0V、4.1V、4.2V三种悬浮电压选择<sup>[11]</sup>。此外,该芯片具有接近于零电流的低电池电量断接

功能,能够有效避免锂电池因过放电而受损。如图4所示,LTC4071芯片ADJ端与VCC端相接,编程BAT悬浮电压输出为4.2V;LBSEL端与GND相接,当电池放电电压低于3.2V时将电池与VCC断接;当电池充电电压达到4.2V时,HBO端输出高电平,使N沟道MOSFET导通,点亮LED灯报警,并形成泄流通道,避免电池过充电现象的发生。本装置所选用的锂聚合物电池容量为25mAh,能满足一般应用系统的工作要求。

## 3 应用系统设计

利用上述多方向风能收集装置收集的电能,可以给无线数据传输系统供电,以实现数据采集节点的自供能。无线数据传输系统包含多个数据采集节点和一个基站,互相通信构成网络<sup>[12]</sup>。为叙述方便,仅以单个数据采集节点和基站构成的系统进行阐述,如图5所示。

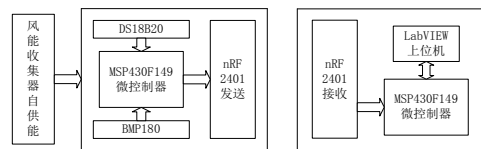


图5 应用系统结构框图

Fig. 5 Structure of application system

### 3.1 数据采集节点

数据采集节点由MSP430F149微控制器、DS18B20温度传感器、BMP180气压传感器和nRF24L01<sup>[13]</sup>组成。MSP430F149微控制器不断将气压和温度传感器测得的数据实时读出,在内部经过校验处理以满足通讯要求后发送给nRF24L01,采集到的数据经nRF24L01无线数据传输模块发送到周围空间,以供基站获取。

### 3.2 数据接收节点

数据接收节点也是整个应用系统的基站,负责收集下属数据采集节点的信息并传输到总机上。基站同样选用MSP430F149微控制器作为主控芯片,采用中断工作方式实时读取nRF24L01接收端获取的数据信息。微控制器将数据整理编号后,通过UART串口与计算机上利用LabVIEW开发的上位机通信<sup>[14]</sup>,将整个系统的数据包传输到上位机上显示并存储,为后续数据分析和研究做准备。

## 4 装置整体测试

为证明本装置的实际应用水平,须进行相关测试。设计完成的多方向风能收集装置实物如图6所

示。在实验室条件下，利用四个同时工作的 AFB0612EHE 型轴流风机，AS836 型数字式风速测量仪以及 GDS-2202A 型数字示波器等测试设备搭建起系统测试环境。

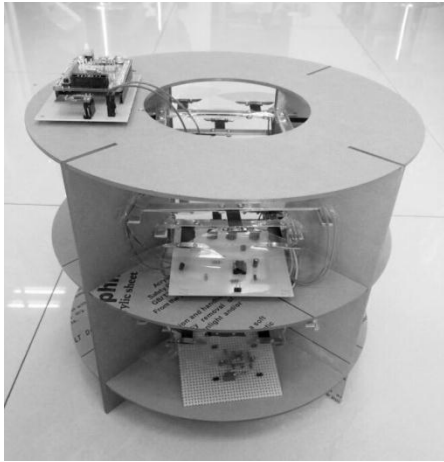


图 6 系统实物图

Figure 6 the real system

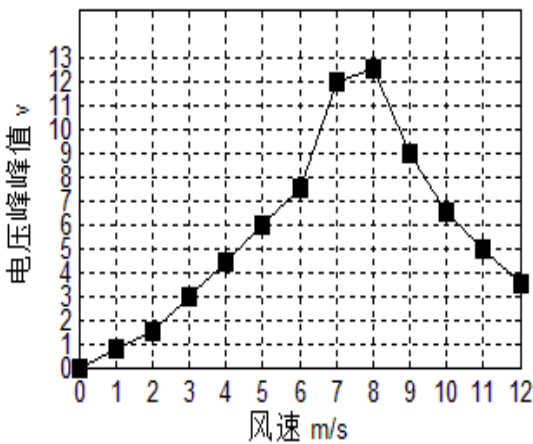


图 7 电压峰值随风速变化曲线

Fig. 7 Voltage peak change with wind speed

从零开始逐渐增加轴流风机的输出功率，测量单片压电悬臂梁输出的交流电压峰峰值，绘制相应变化曲线如图 7 所示。从图中曲线变化波形可知，当风速为 8m/s 时，压电悬臂梁输出的交流电压峰峰值最大；当风速为 6-9m/s 时压电悬臂梁处于高效的工作状态。为反映一个单元中压电悬臂梁阵列的电流输出能力，给压电悬臂梁阵列提供 8m/s 的风速，测量倍压整流后超级电容两端的电压变化情况，两次测量结果如表 1 所示。测量 LTC4071 输出端电压为 4.16V，略低于理想值 4.2V。该装置连续工作 40min，能将 25mAh 的电池充满。同时，将锂电池与数据采集节点连接，数据采集节点正常工作，并能够将实验室温度和气压值发送到上位机上。

## 5 总结与展望

本文所设计的多方向风能收集装置在实验室模拟自然环境中，能够有效收集来自不同方向的风能，达到了最初的设计要求，可以应用在野外数据采集等物联网系统中。在不久的将来，随着压电材料的研究深入和压电悬臂梁制备技术的逐步完善，本文所设计的多方向风能收集装置的能量回收效率必将得到巨大提升，从而推动物联网工程达到新的高度，让人们的生活更加数字化、智能化。

### 参考文献

1. Dittrich T, Belaidi A, Ennaoui A. Concepts of Inorganic Solid-state Nanostructured Solar Cells[J]. Solar Energy Materials and Solar Cells, 2011, 95(6): 1527-1536.
2. Wang Z Y, Leonov V, Fiorini P, et al. Realization of a Wearable Miniaturized Thermoelectric Generator For Human Body Applications[J]. Sensors and Actuators A: Physical, 2009, 156(1): 95-102.
3. Aladwani A, Arafa M, Aldraihem O, et al. Cantilevered Piezoelectric Energy Harvester With a Dynamic Magnifier[J]. Journal of Vibration and Acoustics, Transactions of the ASME, 2012, 134(3): 1-10.
4. 代显智, 张章. 用于自供能传感器的环境能量源研究[J]. 电源技术. 2012(03):440-443.
5. 许卓, 杨杰, 燕乐, 等. 微型振动式能量采集器研究进展[J]. 传感器与微系统. 2015(02): 9-12.
6. 李晓娟, 李全禄, 谢妙霞, 等. 国内外压电陶瓷的新进展及新应用[J]. 硅酸盐通报. 2006(04):101-107.
7. 李涛, 彭同江. 锆钛酸铅压电陶瓷的研究进展与发展动态[J]. 湘南学院学报. 2004(02): 54-57.
8. 孟庆春, 陈光柱. 自供电无线传感网络节点设计[J]. 仪表技术与传感器. 2012(07):102-104.
9. 党自恒. 二倍压整流电路充放电过程解析[J]. 中国市场. 2013(22):30-31.

10. LIU Jun, TAO Jianping, LV Xiaolan .Key Environmental Factors Monitoring System of Low-power Greenhouse Based on WSN Technology[J]. Agricultural Science & Technology, 2016, 17(2): 449-452.
11. 荣训,陈志敏,曹广忠.一种低功耗的微弱能量收集电路设计[J].电子技术应用.2016(07):42-49.
12. 李彦,罗续业.海洋环境无线传感器网络监测体系与应用技术研究[J].海洋技术.2009(01):8-11.
13. 千承辉,杨慧婷,任同阳,等.四旋翼飞行器实时航拍及 GPS 定位系统设计[J]. 吉林大学学报(信息科学版). 2015(04):454-462.
14. 沈文义,秦宁宁,孙顺远,等.基于 MSP430 和 LabVIEW 的瓦斯气体无线远程监测系统[J]. 江南大学学报(自然科学版). 2012(02):142-148.

# 基于 QR 码扫描的智能冰箱食品管理系统的设计\*

张碧兰；杜俊岐；赵 佐

(吉林大学 仪器科学与电气工程学院 长春 130022)

**摘要：** 目前，智能化成为家电发展的潮流。居家生活离不开冰箱，智能冰箱的出现具备良好的创新性、便利性和实用性。本项目基于 Android 系统，结合 SQLite 数据库、51 单片机，蓝牙传输等知识，设计实现一款基于 QR 码扫描的智能冰箱食品管理系统 APP，除扫码记录食物信息，生成食物清单，还具备过期食物提醒、购买清单、菜谱等功能，此外结合 STC89C52 和 HC-05 蓝牙模块，进行蓝牙通信，传递温湿度数据。该系统操作简单，功能丰富，具备一定的市场开发潜力。

**关键词：** Android SQLite 数据库 STC89C52 蓝牙通信

## Design of intelligent refrigerator food management system based on QR code scanning

Zhang Bilan; Du Junqi; Zhao Zuo

(The College of Instrument Science & Electrical Engineering ,Jilin University,ChangChun,130022,China)

**Abstract:** At present, intelligentialize become the trend of the development of household appliances. Home life can not be separated from the refrigerator, so smart refrigerator has good innovation, convenience and practicality. This project is based on the Android system, with SQLite database, 51 microcontroller, Bluetooth and other knowledge, to design and implement smart refrigerator food management system based on QR code scanning. It can not only scan QR code to record food information, generate food list, but also have the function of reminding expired items, producing a shopping list and menu. In addition to combining with STC89C52 and HC-05 Bluetooth module to realize bluetooth communication, temperature and humidity data can be transfered. The system is simple, low-cost, feature-rich , and has a certain market development potential.

**Key words:** Android SQLite database STC89C52 Bluetooth communication

## 0 前言

随着人们生活水平的飞速发展，生活节奏不断加快，冰箱在家庭中起的作用越来越大，大量食物放入冰箱，在很大程度上给人们生活带来方便。但是，随着冰箱存储食物的增多，很多食物经过长期存储而忘记取食，会带来如下两方面的问题：其一，致使食物过期腐败，如果误食，会对健康存在威胁，其二，不能及时更新，在外出购物时不能准确知晓急需采购的商品。

针对这些问题，我们经过研究学习，开发了一款基于 QR 码扫描的智能冰箱食品管理系统，致力将冰箱从一个储存食物的容器变成食物的管理者。该应用将会为工作学习忙碌的人群提供便利。

系统整体运行过程如下：首先，通过对二维码的扫描，将食物信息录入系统，此项操作方便快捷，简单易行。其次，建立 SQLite 数据库，将信息添加到数据库中。最后，通过对数据库的操作，生成食物清单。

此外，可以统计过期食物的名称、过期天数等信息，将这些信息提示给使用者。在系统中对过期食物和已吃完食物进行处理，将其从“食物清单”

\* 指导教师：戴强

项目类型：大学生创新项目（20156510250）

中删除，加入“购物清单”内，以便在购物时，给予使用者参考与提示。随着科学技术的进步，人们获取资料的第一途径早已从纸质书籍变成网络。为了顺应这种变换，方便更多人更高效的利用冰箱，数码逐渐代替纸质的各种材料。该系统汇总了大量的电子菜谱，包含四大菜系、家常菜、凉菜等。此外，采用 DHT11 传感器来模拟获取冰箱温湿度，通过 HC-05 蓝牙模块与 APP 进行蓝牙通信，APP 可以接收并显示温湿度数据。

居家生活离不开冰箱的使用，而且智能化家电也是电器发展的潮流。从扫码、随时查看储物情况到过期提醒，菜谱的推荐，还有食物清单的生成。这些功能在日常生活中是必要的。这些点滴的功能是我们迈向理想生活重要的一步。

## 1 总体设计

借助 Android Studio 开发软件，实现了基于 QR 码扫描的智能冰箱食品管理系统的搭建。首先，利用 ZXing 开源项目，实现二维码的扫描和解析，得到食物信息；通过对 SQLite 数据库的操作，生成食物清单，实现过期食物提醒功能；基于对 SD 卡文件的读写，实现菜谱的推荐；以 STC89C52 为核心，通过 DHT11 传感器测试冰箱温湿度数据，结合 HC-05 蓝牙模块，与平板进行蓝牙通信，实现温湿度数据的传输。整个 APP 的功能模块如图 1 所示：

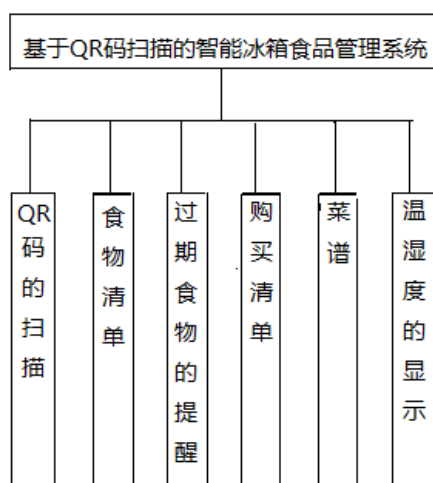


图 1: 系统结构功能图

Fig.1: Structure of system function

## 2. UI 界面设计

主界面共有 4 个区域，界面左侧的三个区域从上至下依次为：接收二维码扫描结果区、用户操作

功能按钮区、温湿度数据显示区。界面右侧区域为一个 FrameLayout，对应于后 4 个功能按钮要显示的内容。UI 界面如图 2:

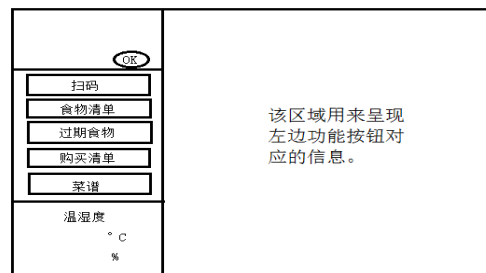


图 2 APP 主界面

Fig2: APP main UI

食物清单界面如图 3:

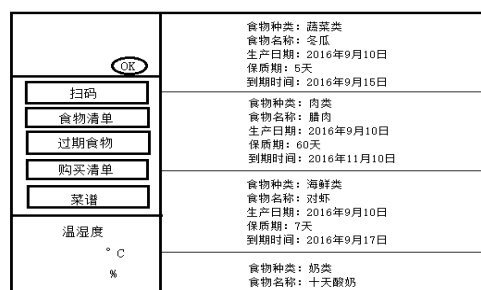


图 3: 食物清单

Fig3: Food list

其它功能按钮对应界面类似，不再赘述。

实现该界面，在 Android studio 项目下的 res 目录下 layout 里建立资源文件，实现布局，在 MainActivity 里注册监听器，添加点击事件，可以初步实现 UI 界面。

## 3 各个功能设计与测试

### 3.1 扫码获取食物信息

QR 码，即二维码，是在代码编制上巧妙地利用构成计算机内部逻辑基础的“0”、“1”比特流的概念，使用若干个与二进制相对应的几何形体来表示文字数值信息<sup>[7]</sup>。相对于只能储存数字的条码来说，应用更加广泛。食物二维码卡片包括食物类别，名称，生产日期，保质期，到期时间等信息。

实现扫码，解码等工作很繁琐，本次开发，直接在 Github 开源网站上下载 ZXing 开源项目，在应用程序中，引用它作为第三方库，即在项目中实现了对 QR 码的扫描。

### 3.2 SQLite 数据库的建立

Android 系统集成了一个轻量级的数据库 SQLite，它是一个嵌入式的数据库引擎，专门适用

于资源有限的设备上适量数据读取<sup>[1]</sup>。Android 提供 SQLiteDatabas 代表一个数据库，一旦应用程序获得了 SQLiteDatabas 对象，就可以管理操作数据库。我们所建立的数据库的结构如表 1 所示：

表 1：数据库结构

Table1: Structure of database

| _id | 食物种类 | 食物名称 | 生产日期       | 保质期 | 到期时间        |
|-----|------|------|------------|-----|-------------|
| 1   | 蔬菜类  | 冬瓜   | 2016年9月10日 | 5天  | 2016年9月15日  |
| 2   | 海鲜类  | 对虾   | 2016年9月10日 | 7天  | 2016年9月17日  |
| 3   | 肉类   | 腊肉   | 2016年9月10日 | 60天 | 2016年11月10日 |

### 3.3 食物信息的录入

食物信息的录入，就是将食物信息添加到数据库中。首先需要完成的工作是将带有换行符的文本分行提取，分别、依次插入到数据库中。针对如何有选择性地提取数据，有两种解决办法：

第一种是手动输入所需信息，将扫码得到的信息进行选择性的复制，然后添加到数据库；

第二种方式是通过 splite()方法，给定分隔符，取出所需信息，以 key-value 形式存储于 ContentValues 变量中；给按钮绑定监听器，设置点击事件，将信息插入到数据库中，即完成了食物信息的录入。

两种方法各有利弊：方式一虽然相对繁琐，有悖于解放双手的初心。但是可以轻松管理没有二维码的食物。方式二简单方便，只需要点击 OK 按钮，后台处理数据，可以将必要信息自动添加到数据库。但是对于没有二维码标签的食物，管理系统不会有任何记录。

虽然二维码标签现在还没有普及，但我们不可否认它是未来的发展趋势，会在生活中扮演越来越重要的角色。第二种方式的研究有充分的必要性。

### 3.4 食物清单的生成

ListView 是最适合呈现食物清单的一种 UI 组件。将数据库与 ListView 联系起来的是 SimpleCursorAdapter。Adapter 是连接后端数据和前端显示的适配器接口，是数据和 UI (View) 之间一个重要的纽带。在常见的 View(ListView,GridView) 等地方都需要用到 Adapter<sup>[5]</sup>。

SimpleCursorAdapter 可以适用于简单的纯文字型 ListView，它需要 Cursor 的字段和 UI 的 id 对应起来。当程序不断地向数据库插入数据时，ListView 可以实时将底层数据库中信息显示出来。

通过对数据库的查询操作，得到食物信息，经由 SimpleCursorAdapter 包装，给 ListView 设置 adapter，即可生成食物清单。

### 3.5 过期食物的统计

对于过期食物统计，需要不断地将当前时间与到期时间进行相减，实时判断食物过期情况。

当前时间用 format.format()得到，到期时间，查询数据库取出即可，但是存在着两个 String 类型的数据无法比较大小的问题。为此，我们提出了如下解决方法：先将 String 类型数据转化为 Data 类型，再通过 getTime()得到 int 型数据。

getTime()函数用于使用当地时间返回当前 Date 对象中的时间值。该时间值表示从 1970 年 1 月 1 日午夜开始，到当前 Date 对象时，所经过的毫秒数，以格林威治时间为准<sup>[2]</sup>。

经过如上操作，即可得到以毫秒为单位的两个需要作比较的日期之差。实际问题中，对于单位的精度要求不必精确到毫秒，故进行单位换算后，将要比较日期之差转为天数，过期食物以 xx 过期 xx 天形式来提醒使用者。

### 3.6 购买清单的生成

对于过期食物，或者已经吃完的食物，在食物清单中将其删除的同时，自动添加到购买清单中。

针对这个要求，我们首先做出了如下尝试：

在系统响应删除操作时同时进行数据传递。两个 fragment，通过 bundle 进行数据传递。但是程序在执行过程中出现了问题：运行中的程序，每当点击购买清单按钮时，就会出现停止运行，APP 闪退。问题在于：除了蓝牙模块，其它部分相当于单线程的工作方式，两个不同布局的按钮同时操作同一个 fragment 必然会存在问题。

因此，我们改进后采用了如下的方法，在删除清单食物时，不进行 fragment 之间的数据传递，而是采用将数据以输入流的形式写文件，主界面的购买清单按钮，打开 fragment,读取文件内容。

第二种方案测试时也存在着问题，文件的内容只能添加不能清除。就算删除 EditText 内容，无法保存文件，这样再次打开应用程序时，仍然会有上次记录。要解决这个问题，主界面的按钮打开 fragment 后，应以 MODE\_WORLD\_WRITEABLE 模式打开文件输入流。这样，设置清空购物清单按钮，也可以起到清空文件的效果。

### 3.7 菜谱的实现

Java 提供了一套完整的 IO 流体系, 包括 `FileInputStream`、`FileOutputStream` 等, 通过这些 IO 流可以非常方便地访问磁盘上的文件内容, Android 同样支持以这种方式来访问手机存储器上的文件。

在 SD 卡上建立电子菜谱, 包含四大菜系, 家常凉菜, 海鲜等等, 一定程度上可以满足人们的需求。系统还为使用者提供个性化扩展的功能: 如果用户想要增加其他菜谱, 只需要将文件添加到菜谱文件夹下即可。

该系统另一个优点在于, 具有良好的人机交互性。使用者可依据自身需要, 个性化修改系统的部分功能, 使其更适应于不同的家庭。

应用程序要读写 SD 卡上的文件, 必须在应用程序的清单文件中添加读写 SD 卡的权限。

仿照手机 Android 手机文件管理器, 将文件形式以 `ListView` 形式呈现, 首先创建一个 `List` 集合, 元素为 `Map`, 再创建一个 `SimpleAdapter`, 为 `ListView` 配置 `Adapter`, 这样, 菜谱就以 `ListView` 形式直观地呈现于 UI, 分类清晰, 方便操作。

### 3.8 温湿度数据的获取, 传输与接收

该项目采用 DHT11 和 STC89C52 单片机来模拟获取冰箱温度, 通过 HC-05 蓝牙模块与平板进行串口通信, APP 打开蓝牙, 开启一个新的线程, 来接收温湿度数据。该方式原理清晰, 并能实时反映冰箱内部温湿度数据。

Android 平台提供的蓝牙 API 去实现蓝牙设备之间的通信, 蓝牙设备之间的通信主要包括了四个步骤: 设置蓝牙设备、寻找局域网内可能或者匹配的设备、连接设备和设备之间的数据传输。连接设备之前需要 UUID, 所谓的 UUID, 就是用来进行配对的, 全称是 `Universally Unique Identifier`, 是一个 128 位的字符串 ID, 用于进行唯一标识。

`BluetoothSocket` 类: 代表了一个蓝牙套接字的接口 (类似于 TCP 中的套接字), 它是应用程序通过输入、输出流与其他蓝牙设备通信的连接点。

初次测试时, APP 无法接收蓝牙模块传递的数据。经过分析得出两种可能错误: 一, 蓝牙源码部分有误。检测方法为, 将 APP 与电脑的串口助手连接进行测试, 结果可以正常接收数据, 排除可能。二, 蓝牙模块设置有误, HC-05 是主从一体蓝牙模块, 但它在此处用于接收单片机发送的数据, 扮演从机的角色。故应将其设置为从机状态, 才可以正常收发数据。修改后问题解决。

该项目是基于 Android 系统开发, 结合 51 单片机以及蓝牙通信相关知识, 设计了一款基于 QR 码扫描的智能冰箱食品管理系统。

提供了扫码记录食物信息, 生成食物清单, 进行过期提醒, 自动生成购买清单, 还有电子菜谱等功能。经过检测, 使用流畅, 响应迅速, 具有一定的便利性和实用性。

### 参考文献

1. 李刚. 疯狂 Android 讲义[M]. 北京: 电子工业出版社, 2015: 1-412
2. Kathy Sierra & Bert Bates. Head First Java[M]. O'Reilly TaiWan 公司, 译. 北京: 中国电力出版社, 2015: 27-165
3. 宋长龙. 大学计算机基础[M]. 北京: 高等教育出版社, 2011: 142-166
4. 李兴华. Java 开发实战经典 (名师讲坛) [M]. 北京: 清华大学出版社, 2009
5. 吴亚峰, 索伊娜. Android 核心技术与实例讲解[M]. 北京: 电子工业出版社, 2010
6. 杨云君. Android 的设计与实现[M]. 北京: 机械工业出版社, 2013
7. 兰龙辉, 邱荣祖. 二维码技术在农产品物流追溯系统中的应用[[J/OL]]. 物流工程与管理, 2013
8. 姜申. 基于物联网的智能电冰箱信息化设计[[J/OL]]. 物联网技术, 2011
9. 谭蓁. 家用电冰箱智能控制技术及发展趋势[[J/OL]]. 家用电器科技, 2000
10. 蔡钧涛. 智能冰箱嵌入式食品管理系统[[D/OL]]. 硕士学位论文, 2008
11. 赵子贤. 智能冰箱食品管理系统的设计与实现[[D/OL]]. 硕士学位论文, 2015

## 4 结论



第二部分 英文论文集

**Part II English Proceedings**



# The Automatic Monitoring System of Large-Scale Horticultural Field Based on Temperature and Humidity Detection

Chen Zubin; Yang Wanjin; Zhou Qi; Bao Jiabin

(College of Instrumentation & Electrical Engineering, Jilin University, Changchun 130061, China)

**Abstract** —To the demand of modern agricultural automation, a control system of automatic irrigation is designed according to the temperature and humidity of the soil. This system detects the soil humidity and temperature through the soil temperature and humidity sensors; the data is displayed on the liquid crystal screen, and the automatic irrigation is carried out according to the set threshold through the processing and analysis of the single chip microcomputer; real-time data displays on the host computer, to realize the remote real-time monitoring of large horticultural field through the ZigBee network for remote communication. This system can satisfy the requirements of the development of agriculture, its function is complete, practical, high degree of automation, with a more optimistic market potential.

**Key words** —large-scale horticultural field temperature humidity ZigBee network remote control

## I. INTRODUCTION

WITH the development of economy, the market demand of horticulture in China is increasing year by year. Greenhouse is the main part of modern large-scale horticultural field, it can control the production environment, so that the production of more high yield and efficient[1]. However, compared with many developed countries, China has a significant gap in the degree of automation of the greenhouse monitoring system[2]. At present, most of our garden still use the traditional way of artificial irrigation[3], not only a waste of human resources, but also a waste of water resources. Therefore, it is of great significance to develop the automatic greenhouse irrigation technology which is suitable for China's national conditions. Traditional automatic monitoring systems often use wired connections, such monitoring systems are often complex wiring, not easy to move[4]. In this system, the optimization design of the traditional monitoring system is carried out, and a remote intelligent irrigation system for large garden is designed based on ZigBee technology. Through the combination of ZigBee technology and wireless sensor network technology, the system can realize the remote monitoring and control system. The wiring of the system is very simple, not only improves the reliability, but also reduces the cost.

## II. OVERALL SYSTEM DESIGN

The automatic monitoring system of large garden field based on temperature and humidity detection mainly includes control module, power supply module, irrigation module and remote monitoring module.

The soil water system through the temperature sensor to collect information, through the microcontroller processing, through the ZigBee network to the host computer to send data and display on the touch screen, when the data value is below the threshold limit set, the micro controller to control the water pump work, until the data reaches the threshold limit value, the water pump stops working.

## III. SYSTEM HARDWARE DESIGN

The various modules of the system are described as follows:

(i) control module: the control module is the core of the whole system, and it is the control center of the whole system. The control module is composed of a controller and a sensor, wherein the controller adopts a STC12C5A60S2 microcontroller, and the sensor adopts a SMTS-II-485 soil water temperature sensor.

STC12C5A60S2 model micro controller price is not high, but it has high speed, strong anti-interference, low power consumption[5], very suitable for the main

control chip for the system. Compared with the traditional 8051 microcontroller, this model is based on the complete compatibility of traditional 8051 microcontroller instruction code, the speed to be faster than 12 to 8 times[6]. Therefore, this type of micro controller is used as the main control chip of the system.

SMTS-II-485 soil moisture temperature sensor is a new type of soil moisture temperature sensor. The model of soil moisture temperature sensor has many traditional soil moisture temperature sensor does not have the advantages of high stability of the output signal of the sensor, will not happen drift and jitter[7]. The most important is that the measurement accuracy of the sensor is very high, reliable performance, thus ensuring the accuracy of the whole system in the signal acquisition stage. In addition, the sensor is affected by soil salt content is very small, so it can be adapted to the measurement in a variety of soil.

(ii) remote monitoring module: through the ZigBee node and the center node, the use of touch screen to achieve remote monitoring.

Communication host select RS485 ZigBee, select RS232 from the machine to turn ZigBee. Communication distance up to 1600m[8].

Touch screen selection model for the TPC7062KX Kunlun state touch screen. TPC7062KX model of the Kunlun state touch screen core is embedded low power CPU, integration, high performance. The display part of the touch screen with 7 inches high brightness TFT LCD screen, touch part of the four line resistance[9]. This kind of touch screen theory can meet the system's remote monitoring and control.

(iii) watering module: the control module to control the water pump for irrigation. Pump selection YB-550 pump, the experiment, you can meet the irrigation needs.

(iv) power module: divided into 220V alternating current and voltage reducing module. Because the touch screen cannot use 220V power supply, so the introduction of the buck module, using 24V power supply.

#### IV. SYSTEM SOFTWARE DESIGN

The system uses STC12C5A60S2 microcontroller for data processing, the use of C language for software

development and design, so that the software has a good readability, portability, etc.. The modular design idea runs through the whole system, so that each program module is relatively independent, which is easy to read, transplant and the improvement of the later period.

##### A. Temperature and Humidity Acquisition and Processing Module

Temperature and humidity data collected by the soil moisture temperature sensor after A/D conversion, through the RS-485 interface output, after 485 to TTL module, the microcontroller from the serial port in the input of the corresponding processing.

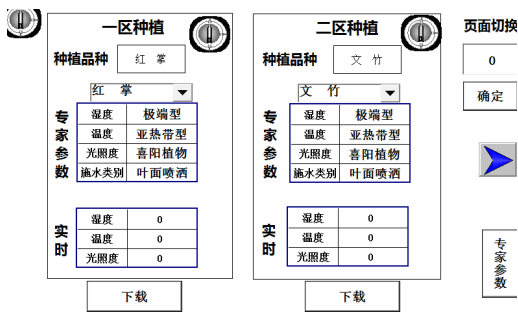
Communication protocol MODBUS-RTU protocol data transmission, the protocol is a master-slave protocol with a master and a number from a bus station, the communication parameters between each station must be consistent, including data bits, parity bit parity, baud rate and the number of stop bits[10]. So it is needed in the program, the various sites of these parameters are set to the same. In addition, each station must be set from the station address must be different, otherwise it will cause the conflict from the station [11].

##### B. Upper Computer Touch Screen Display Module

The use of MCGS embedded configuration software design, the program and the screen through the USB to download to the TPC7062KX touch screen[12].

(i) touch screen interface design:

Figure 1 (a) for monitoring and parameter download interface. The upper left corner of the button to determine whether the microcontroller data collection, the icon is in the original location. The interface is divided into two plates, each of which has a variety of different types of parameters, including the display of expert parameters and real-time temperature, humidity and light intensity. Download buttons below each section. On the right page switching button, flip button and expert parameters button.



(a) Monitoring and parameter Download Interface



(b) Formula editing interface

Fig.1 The interface of touch screen

(ii) touch screen motion design:

In each area planted white box, there is a knob, this is to determine whether the appropriate area for data collection, to facilitate the user to select the effectiveness of the collection area.

Display the current selected crop varieties in the plant variety frame, the user can select the desired crop varieties according to their own needs in the drop-down menu. After selection, the expert parameters are changed to the corresponding values of the selected crop species, which is determined by the data set in the previous period. Download button, the role of the current expert parameters are downloaded to the corresponding microcontroller. In real time table, the real time parameters are displayed.

The upper right corner of the page switching part according to the requirements of the user to switch to the corresponding screen, by clicking on the button or switch input page page.

Select the expert parameters, will pop up as shown in Figure 1 (b) recipe editing interface. The user can set different kinds of crops, set different humidity, temperature, sunlight and water level.

After setting, click the Save button and exit key, this time will be back to Figure 1 (b) shown in the interface. Re select the latest data in the drop-down menu to

select the level corresponding to the latest data. Classification as shown in table 1.

TABLE I  
Hierarchical list

| Value | Humidity          | Temperature  | Illumination   |
|-------|-------------------|--------------|----------------|
| 0     | extreme           | sub tropical | heliophilous   |
| 1     | moderate humidity | temperate    | sun resistant  |
| 2     | hygrophilous      | cold         | skiophilous    |
| 3     | xerophilous       | tropical     | shade tolerant |

### C. Irrigation Module

The module of temperature and humidity data acquisition to the feedback to the microcontroller, and the microcontroller will display data sent to the host computer through the ZigBee network, compared with the corresponding pc set plant type humidity limits. When the soil moisture is lower than the corresponding humidity limit of the selected plants, the water pump is started to water the soil. With the gradual increase of soil moisture, the soil humidity to reach the maximum humidity of the selected plants, close the water pump.

## V. TEST AND ANALYSIS

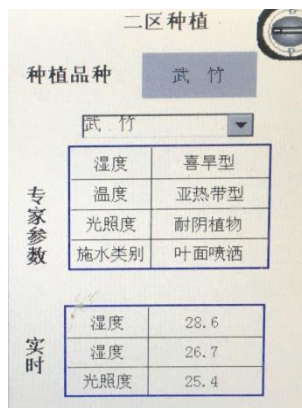
Temperature and humidity control test results: soil water temperature sensor into the power to be measured in the soil, and the display shows the current temperature and humidity, the humidity and humidity below a predetermined limit, the sprinklers went off to the soil, display real-time soil moisture, soil moisture increased gradually. When the soil moisture is higher than the upper limit of the predetermined humidity, the spray head stops spraying water, the display screen displays the current soil moisture. After repeated testing, the system can achieve the function of temperature and humidity control.

Host computer real-time data acquisition test results: before irrigation, the microcontroller will soil moisture temperature sensor data collected through the ZigBee transfer to the host computer, and in the upper computer display, as shown in Figure 2 (a). Because the humidity is lower than the threshold value, the water pump starts to work, the soil is watered, reaching the upper limit value, the water pump stops working,

the temperature and humidity of the soil is shown in Figure 2 (b). Can be seen from the figure, the host computer can clearly and intuitively reflect the current situation of the soil. After several tests, the system stability is good, can achieve the desired goal.



(a) Interface before watering (left)



(b) Interface before watering (right)

Fig.2 Touch screen interface after

## VI. CONCLUSION

This paper presents a design scheme of the automatic monitoring system of large-scale horticultural field temperature and humidity detection based on the STC12C5A60S2 as the main chip, combined with the temperature sensor SMTS-II-485 to realize the measurement of soil moisture on soil temperature and humidity, by setting the threshold of different types of TPC7062KX touch screen for the selection of a plant, soil temperature and humidity detection, and the use of ZigBee network technology, the real time display on LCD and PC, the humidity regulated by pump, keep the soil in a certain range of temperature and humidity, improve crop production quality and yield.

## References

- [1] Ding Xiaolei. Research on the development of Chinese vegetable science and technology in twentieth Century. Nanjing Agricultural University, 2008
- [2] Yuan Hongbo. Study on the key technology of closed cultivation system in sunlight greenhouse. China Agricultural University, 2015
- [3] Yang Danni, Chang Liying, Shen Haibin, et al. The current situation and development of water and fertilizer management in Shanghai city facilities . China vegetables, 2016,02:11-16.
- [4] Zhou Yiming. Research and implementation of key technology of greenhouse group monitoring and control system based on wireless sensor networks. Zhejiang University, 2009
- [5] Luo Hao, Liu Shangwu, Wang Shuyi, et al. Design of multi channel temperature monitoring system based on. STC12C5A60S2 Journal of Xinyang Normal University (NATURAL SCIENCE EDITION), 2014,01:106-110. (in Chinese).
- [6] Qin Xianglin, Zhang Haibing, Zhang Ying. The design of STC12C5A60S2 wireless temperature acquisition system based on. Journal of Harbin University of Commerce (NATURAL SCIENCE EDITION), 2011,06:837-840.
- [7] Cai Wenke, Yu Along, Li Jiang, et al. Design of WSN based remote monitoring system for farmland soil in large area. Agricultural Mechanization Research, 2015,09:77-82.
- [8] Yang Jing. Research on Application of ZigBee technology in remote monitoring system. Wuhan University of Science and Technology, 2010
- [9] Zhang Bo. Agricultural demonstration park sand control. system of Northeast Agricultural University based on ZigBee technology, 2014
- [10] Shen Jianpei. Design and implementation of intelligent feeding system based on. PLC Hangzhou Dianzi University, 2014

- [11] He Jianzhong. Design and implementation of industrial gateway based on MODBUS protocol [D]. Inner Mongolia University, 2013
- [12] Jiang Ping. Research and development of key technology of PROFIBUS-DP intelligent slave station. Tianjin University of Technology, 2007

# Study on Noise suppression of Airborne Electromagnetic Profiles Data Based on Adaptive width Filtering

Liu Ziming

(The College of Instrumentation and Electrical Engineering, Jilin University, Changchun 130022, China)

**Abstract**—Using the traditional filtering technology, the airborne time-domain electromagnetic data can be filtered, but owing to the fixed window width, it can remove the surface of the noise signal, but weaken anomaly amplitude. Proposed in this paper, the main adaptive filtering denoising method, according to the characteristics of local signal, judges the abnormal signal area based on adaptive window width smooth algorithm, for non anomalous local signals filtering based on larger window wide, for anomalous local signal filtering based on smaller window wide, this method not only removes the noise, but also maintains the abnormal amplitude of the original signal. This paper compares the filtering denoising results using FIR filter, IIR filter and adaptive filter, and verifies the validity of the adaptive filtering denoising method by the imaging results of measured data.

**Keywords**—Airborne Time-domain Electromagnetic Data, Adaptive Filtering Algorithm, FIR Filter, IIR Filter

## I. INTRODUCTION

TIME domain electromagnetic method is a favorable tool for mining. With the improvement of the transient electromagnetic system and the maturity of the technology, more and more information can be obtained from the airborne electromagnetic data. Therefore, the development of airborne electromagnetic data processing method is also very important. Because of its machine Flight load detection mode, transmitting coil will swing in the detection process; at the same time, the flight speed and flight attitude change will cause the detection system of device parameter instability and detect changes in pressure and temperature during the flight can also introduce the system noise, affecting the quality of data and imaging precision serious restriction airborne electromagnetic detection system of inversion and interpretation of underground abnormal body, reduce the depth of exploration[1-4].

With the development of the research on the electromagnetic detection technology and instrument, the research of the background field

removal, data filtering, stack and extraction methods of airborne electromagnetic noise[5-6]. Although the original data in time domain airborne electromagnetic exploration, after multiple processing and filtering section, the signal-to-noise ratio of the data has been greatly improved, but still contains advanced residual noise, the detection ability of the deep influence of the underground.

Trace in the superposition of airborne electromagnetic data, the commonly used time domain airborne electromagnetic detection system is also put forward some new extraction technology of Macnae stack(1984) of cutting(pruning) method for removing atmospheric interference; Buselli(1992) and Cameron proposed Strack(median filtering method) proposed pruning averaging method; Sutarno and Vozoff(1989) inhibited the static nonlinear filtering technique is adopted. According to Macnae(1984), Lane(1998) using the technology of controlling the frequency of lower than the transmission signal, Fugro company using the method of notch; THEM system using polynomial fitting method to remove the movement noise[7].

Due to the shallow geophysical exploration project objectives, in recent years, Chinese scholars have



carried out the principal component denoising, Dr Zhu[8][9] will wish success into the root of time domain airborne electromagnetic inversion, the amount of success to encounter the noise characteristics in principal component inversion of noisy data because the inversion results have been achieved in the other methods. This paper puts forward the technology of airborne electromagnetic noise profile data processing based on adaptive filter, analyzes the characteristics of the noise space, the study of adaptive bandwidth smoothing algorithm, designs the adaptive low-pass filter, and compared with FIR filter and IIR filter wave, the denoising by comparing the simulated data and the measured data, verify the effective denoising algorithm in this paper.

## II .PRINCIPLE OF FIR AND IIR FILTERS

### A. Principle of FIR filter

FIR filter, is the length of the unit impulse response limited filter. Specifically, the characteristic of the FIR filter is the unit sampling response  $h(t)$ , it is a finite sequence of a  $N$  long. Filter output  $y(n)$  can be expressed as input sequence  $x(n)$  and the unit sampling response  $h(t)$  linear convolution, because the FIR filter only at the origin of the existence of poles, so the FIR system has a global stability. FIR filter is made up of a "tapped delay line" adder and multiplier set, the operating factor of each multiplier is a FIR coefficient.

### B. Principle of IIR filter

IIR filter, is the unit impulse response for an infinite length of the filter, IIR filter has several significant characteristics: IIR filter at the same time there is not zero poles and zeros. In order to ensure the stability of the filter system, it is needed to make the poles of the system in the unit circle, that is to say, the stability of the system is determined by the poles of the system function. Due to the existence of the IIR filter is not zero poles, it is only possible to achieve the approximate linear phase characteristics. It is the reason why the nonlinear phase characteristic of IIR filter has

limited its application range.

## III. ADAPTIVE FIRTING METHOD

### A. Denoising principle of adaptive filtering

According to the adaptive window width smoothing algorithm[10], a low pass filter bank is designed to take the number of the first section as an example, the specific algorithm is as follows:

The window width value  $W_L$ 、 $W_U$  is the minimum and the maximum window adjustment range. First, use the maximum window width to filter the profile data smoothing  $\hat{x}_k$ , get  $\hat{x}_{jk}$ , and calculate the second order

difference  $\Delta_k(j)$  (type(1)),

$$\Delta_k(j) = \left( \frac{2}{W_U - 1} \right) \sum_{i=1}^{\lfloor (W_U - 1)/2 \rfloor} 2\hat{x}_{jk}(j) - \hat{x}_{jk}(j+i) - \hat{x}_{jk}(j-i) \quad (1)$$

In this type,  $j = 1, 2, \dots, n$ ,  $\lfloor \cdot \rfloor$  indicates the rounding down. Calculated by  $\hat{x}_k$ , the second order difference  $\Delta_k(j)$  reflects the local gradient change rate of  $\hat{x}_{jk}$  and the profile data after smoothing filter, the absolute value of the anomaly  $\hat{x}_{jk}$  in this section is larger, and the flat part is close to zero.

Use type(2) to transform the second order difference  $\Delta_k(j)$  from the adaptive window width  $W_k(j)$  of the smoothing filter of each measurement point. Between the minimum window widths and the maximum window width:

$$W_k(j) = [W_U - (W_U - W_L) \left( \frac{|\Delta_k(j)|}{\Delta_T} - \frac{1}{2} \right)] \quad (2)$$

Among them,  $\Delta_T$  is the two order difference threshold, if  $\Delta_T$  is too small, the window width  $W_k(j)$  is too small, it will have influence on the flat section. If  $W_k(j)$  is too large, not can cause anomalies along the

profile, but reduce the abnormal amplitude. The conventional fixed bandwidth low pass filter, according to the profile data adaptive bandwidth smoothing algorithm designed of low pass filter, not only can effectively remove the high frequency noise on the spatial profile data, but also can ensure the profile data of the amplitude.

*B. Design of adaptive filter*

Adaptive filtering technology is based on the characteristics of the local signals with different window width filtering compared with the traditional filtering method, the adaptive filtering technique according to the characteristics of the local signals with different window width to determine the area of filtering, abnormal signal, non local signal abnormalities with larger bandwidth filter, local abnormal signal by small the width of the window filtering, so as to remove the noise, but also to maintain the original signal amplitude anomaly. In this paper, the maximum window width of the adaptive filter is 51, and the minimum bandwidth is 3.

IV. DENOISING EXAMPLES OF SIMULATION DATA

In order to observe the three degree of filter effect, this paper designs a homogeneous half space earth model, conductivity was 0.01S/m, a total of 1000 measured points, system of helicopter borne time domain airborne electromagnetic detection, the measurement of central loop, the transmitting coil radius is 7.5m, the emission current of 25Hz for positive and negative square wave. Flight height is 30 m, the normalized emission current of the earth model is one-dimensional forward calculation and Simulation for the field data, the forward adding 10% data in the Gauss white noise, can be obtained after the extraction of the measuring point 16 off-time electromagnetic response profile data, as shown in Figure 1.

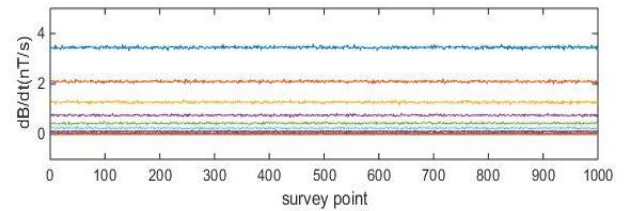


Fig.1 16 channels of homogeneous half space earth model

It can be seen that the data of the model contains high frequency spatial noise, which is used to compare the denoising effect. In this paper, FIR, IIR, adaptive window width filter is used to filter the noise. Design of the IIR, FIR filters are low pass filter, the cut-off frequency between 0-1 adjustable, the number of arbitrary value, the design of adaptive window width filter, the maximum window width of 51, the minimum window width of 3. Three figures shows the four methods for the post profile curves of the electromagnetic profile data. (Figure 2)

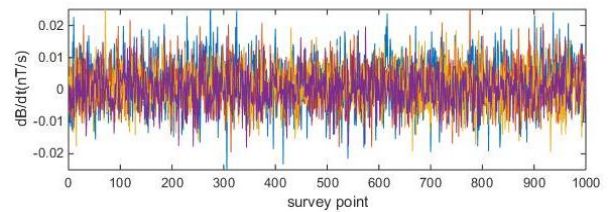


Fig.2 Homogeneous half space the earth model four channels curve after denoising result

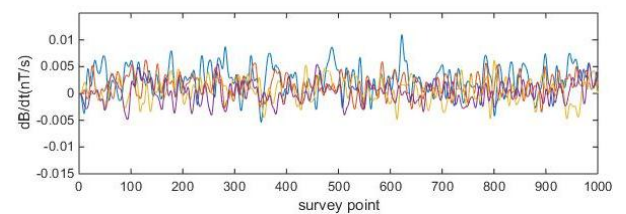


Fig.2(a) Result of IIR filtering

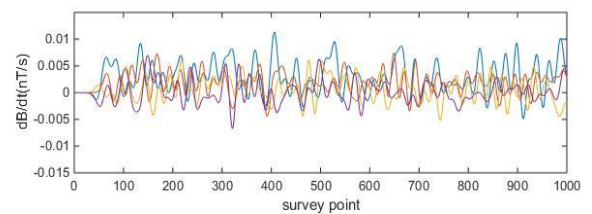


Fig.2(b) Result of IIR filtering

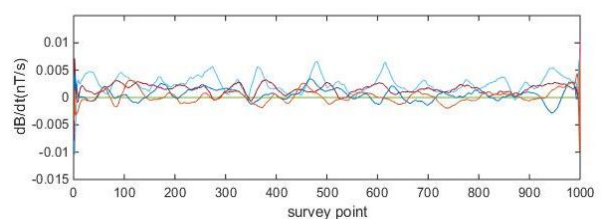


Fig.2(c) Result of adaptive filtering

Contrast to Figure 2(a), Figure 2(b), Figure 2(c) can be seen by FIR, IIR filtered profile curve (Figure 2(a), Figure 2(b)) of the advanced data showed no abnormalities, and the adaptive algorithm filtered profile curve (Figure 2(c)) of advanced data not only ensures the abnormal amplitude, and decreases the noise data.

#### V. DENOISING EXAMPLES OF MEASURED DATA

In the major project of the national high technology research and development program of support, Aero Geophysical Survey and remote sensing center and Jilin University developed China's first set of system of helicopter airborne time domain airborne electromagnetic detection (CHTEM index simulation system.). January 2012, the system in Henan province for the first time in a successful test, and the area of the field survey, found that the region of the earth showed a high resistance characteristics, resistivity of 3000~8000 / m. In this case, taking a survey line of Henan field flight survey as an example, the 17 section data of the length of about 8.5 km measured line is selected. As shown in Figure 3, in the vicinity of the measuring point 3000 with an amplitude of about 1500 nT/s of the anomaly.

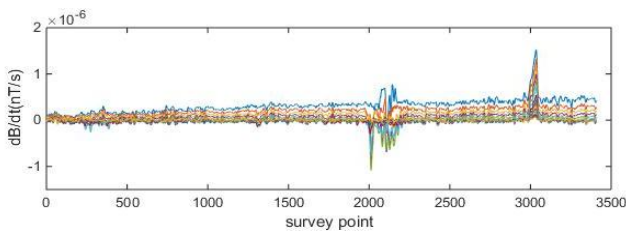


Fig.3 17 channels profile of field data from airborne time domain electromagnetic survey in Henan Province, China

Firstly, the profile data of the measured line are FIR, IIR and adaptive window width algorithm, and the results are shown in Figure 4(a), Figure 4(b) and Figure 4(c). After comparing the three denoising data profiles, we can see that the adaptive window width filtering algorithm has achieved the best denoising results as shown in Figure 4(c), the removal of the measured line of high frequency noise.

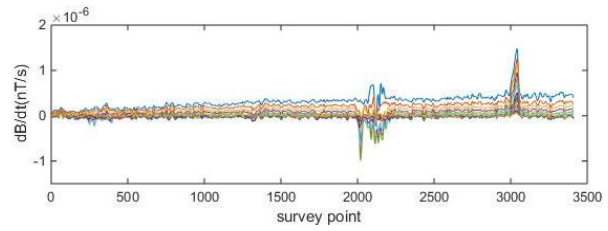


Fig.4(a) Result of FIR filtering

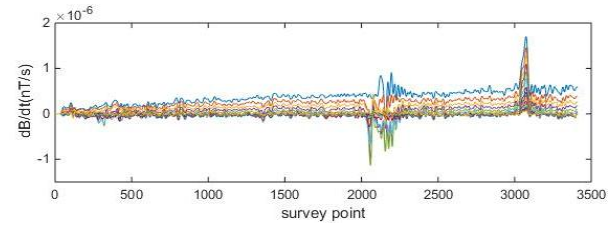


Fig.4(b) Result of IIR filtering

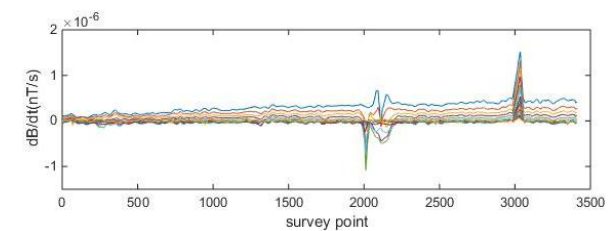


Fig.4(c) Result of adaptive filtering

From Figure 4(a), Figure 4(b) can be seen, the two conventional filter FIR, IIR filter denoising effect is not obvious, the noise level is almost no decline. The data of the measured line is filtered by the adaptive window width algorithm. The maximum bandwidth of the filter is 51, the minimum bandwidth is 3, and the filtering result is shown in Figure 4(c). It can be seen from Figure 4(c), after the adaptive algorithm, the noise reduction than the FIR and IIR filter noise decreased significantly.

The last four data of the late channel data is the last 17 data, and the filter can be more effective to filter the filter. Figure 5 is the original data of the image of the late Tao, Figure 6(a), Figure 6(b), Figure 6(c), respectively, three kinds of filters on the original data channel filter results.

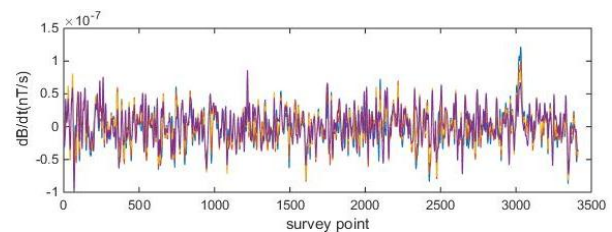


Fig.5 The original data terminal image

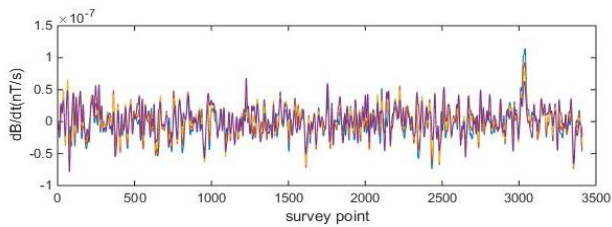


Fig.6(a) Result of FIR filtering

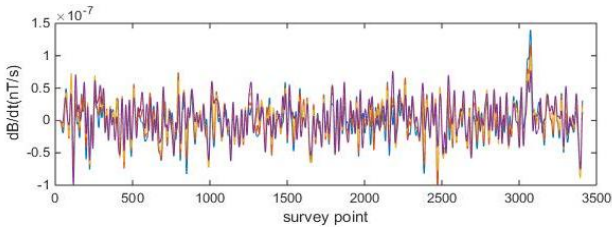


Fig.6(b) Result of IIR filtering

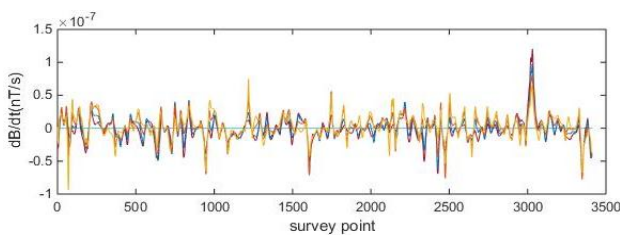


Fig.6(c) Result of adaptive filtering

In Figure 6(a), Figure 6(b), Figure 6(c), the contrast can be seen, the regular FIR filter, IIR filter profile after treatment ( Figure 6(a) ,Figure 6(b)) of advanced data had no obvious abnormalities, can not reflect the deep earth body the model, and there is still more noise with high frequency, and adaptive bandwidth filtering (Figure 6(c)) after the data of late ensure abnormal amplitude, and the amplitude of noise is obviously reduced, the high frequency noise significantly reduced.

## VI. CONCLUSION

1.The airborne electromagnetic data processing transform is applied to the GUI interface, after the original profile data processing of three kinds of filtering algorithm, not only can filter the high frequency noise in spatial profile data, also remove uncorrelated noise profile data, adaptive filtering algorithm can improve the SNR of advanced data, provides a new ideas for geophysical data processing such as noise.

2.This paper adopts adaptive filtering algorithm, low pass filter design can be based on the local characteristics of airborne electromagnetic data transform section, adaptively changing the bandwidth of the filter can not only remove high frequency spatial noise effectively, but also effectively maintain the abnormal amplitude, is better than that of FIR, the filtering performance of IIR filter, the filter can also be for effectively measuring line electromagnetic data filtering.

## Reference

- [1] Lane R, Green A, Golding C, et. al. An example of 3D conductivity mapping using the TEMPEST airborne electromagnetic system[J]. *Exploration Geophysics*, 2000, 31(2):162-172.
- [2] Macnae, J C, Ltagne Y, West G F. Noise processing techniques for time-domain EM system[J]. *Geophysics*, 1984, 49(7):934-948.
- [3] Riddsdill-Smiath T A, Dentith M C. The wavalet transform in aeromagnetic processing[J]. *Geophysics*, 1999, 64(4):1003-1013.
- [4] Buselli G, Hwang H S. AEM noise reduction with remote referencing[J]. *Exploration Geophysics*, 1998, 29(2):71-76.
- [5] Li Nan. Time domain electromagnetic data preprocessing technology research [D]. Changchun: Jilin University, 2009
- [6] Lv Dongwei. Pod time domain helicopter electromagnetic data processing method [D] Chengdu: Chengdu University of Technology, 2011
- [7] Auken, E., Westergaard, J. A., Christiansen, A. V., and Sorensen, K. L. Processing and inversion of SkyTEM data for high resolution hydrogeophysical surveys[C]. Australian Society of Exploration Geophysicists, Extended

Abstracts.19th Geophysical Conference and Exhibition..

- [8] Zhu Kaiguang, Wang Lingqun, Xie bin et al. A method for noise removal from airborne electromagnetic data based on principal component analysis [J]. China Journal of nonferrous metals, 2013, 23 (9): 2430-2435.
- [9] Wang Lingqun, Li Bingbing, Lin Jun et al. The noise removal method for the reconstruction of the main components of airborne electromagnetic data [J]. Journal of Geophysics, 2015 (8): 2803-2811.
- [10] Li Xiuwen, Xu Jinwu, Yang et al. Application of the gradient adaptive window width in the analysis of variable speed mechanical order ratio [J].Instrument technology and Sensor, 2013 (1): 68-71.

# The streetlight management system based on ZigBee

Peng Ding; Bin Shi; Yaxin Wang

(Jilin university instrumentation and electrical engineering, Changchun, 130012)

**Abstract**—The project is to design a kind of streetlight management system based on the technology of ZigBee, to implement management and information collection of the main control unit from the streetlight unit, and monitoring the environment conditions of each terminal in real time, by using the method of current detection to judge whether the fault detection of streetlight status, and according to the light condition to turn on or off the streetlight automatically.

**keywords**—ZigBee technology, streetlight control, fault detection

## I. INTRODUCTION

WITH the development of urbanization, the streetlight as an important part of city-lighting designs, is more and more taken attention by government which invested a lot of manpower and capital to build and manage it, but a lot of questions come out.[1] The existing streetlight management systems is hard to feed back the fault information. We can only patrol and monitor it through manpower, therefore the fault maintenance is not timely. Some road lighting failure could lead to much inconvenience, even cause traffic accidents. In addition, the existing system can't realize the remote management, and mostly is controlled by time. Because of the immobility of set, it can't light in some emergency condition like that the light is too low in cloudy days. This design is based on the ZigBee wireless communication technology to realize automatic remote monitoring, fault detection, and other functions. And it has characteristics of low cost, high reliability, high transmission speed.

## II. THE WHOLE SCHEME DESIGN

ZigBee technology is applied to the design of streetlight management system, that is to realize long-distance wireless data transmission and control[2]. The system includes the total control module and streetlight monitoring module. Total control module includes a single chip microcomputer system, a control module, a display module, a ZigBee general

node module;The streetlight monitoring module includes the single-chip microcomputer subsystem, a current detection module, a sensor module, a switch control module and a ZigBee child node module.

The system uses the method of current detection to judge the streetlight condition and use the sensor module to detect the degree of present light. Then it transmit the information to the single-chip microcomputer system. It transmits to the ZigBee general node via ZigBee child node. The single-chip microcomputer total system summarizes these information to determine whether streetlight is in the fault state and whether it's need to open it. Then the LED display module will show the information. We can also use the buttons on the master control board to control the streetlight. The control signal is transmitted to the single-chip microcomputer subsystem via ZigBee module. The streetlight switch control module in the streetlight board controls the streetlight. It still needs the communications between the ZigBee child node modules to realize long-distance communication. The total system structure diagram is shown in figure 1.

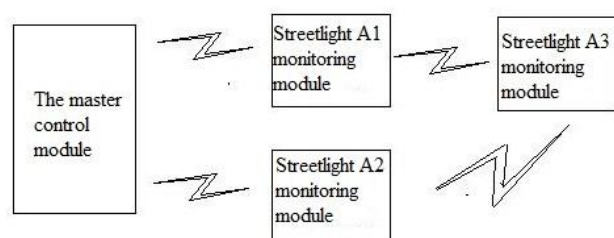


Fig.1 The whole system structure diagram

### III. HARDWARE DESIGN

#### A. The Design of Master Control Module

The master control module mainly includes the single-chip microcomputer total system, the button control module, the ZigBee general node module, the display module and so on. The MCU is using STC89C52 which has the advantages of high performance and low power consumption.

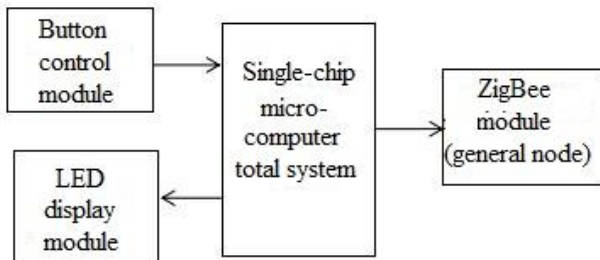


Fig.2 The master control module structure diagram

#### 1. The ZigBee Module

ZigBee is a kind of short-distance transmission of wireless network protocol at a low speed. The present ZigBee module is composed specifically of RF communication module, micro processing module(MCU) and ZigBee wireless communication protocol. It's generally used for small amount of data for wireless transmission of data and ZigBee communication protocol is free, the cost is low. The streetlight current data and local light data is for remote transmission through ZigBee wireless communication protocol. The receiver is also using ZigBee protocol to collect and analyze the data, then transmit it to the single-chip microcomputer total system. The design adopts the CC2530 ZigBee serial transmission chip which could achieve 250 meters of data transmission between nodes and the bit error rate is 0.5%.

#### 2.The Button Control Module

The module is linked beside the total system which could be used to control the streetlight for all kinds of emergency artificially. We could control every streetlight of different areas wireless in long distance by using in a single key scans or combination scanning through the single chip microcomputer system and ZigBee module.

#### 3.The Display Module

The design choose the OLED12864 screen which is only 0.96 inch in size, 128\*64 in resolution and a total of seven pins. It only has five pins which is need to connect to the MCU except the VCC and GND pins. It automatically displays the humiture information and weather the streetlight is fault from the collection of each child module.

#### B. The Streetlight Monitoring Module Design

There are three streetlight monitoring module in total to simulate the streetlight in three areas, each of which includes a current detection module, a sensor module and a switch control module.

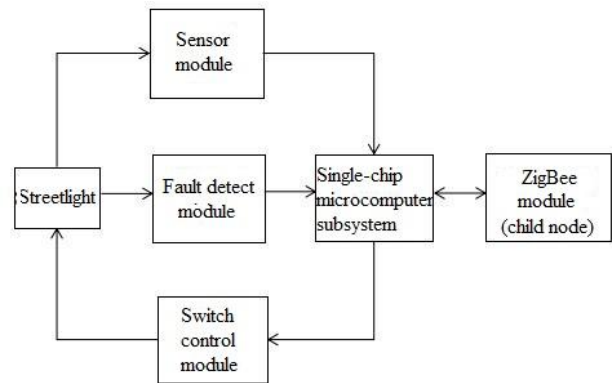


Fig.3 Streetlight monitoring module structure diagram

#### 1.The Current Detection Module

The module judges the fault condition by the method of detecting current. The fault condition includes that the streetlight is off or too dark at night, abnormally on during the day, and so on. The condition of which the streetlight is off or too dark can be detected that the light current is zero or too small. The condition of which the light is on during the day can be detected that the current is normal but the light is bright. The current detection module is connected between the streetlight and the single-chip microcomputer subsystem, which determine whether the streetlight is in fault condition through simple data processing, then transmits the fault information to the total system via ZigBee module to display which light is in fault condition. The design uses the small resistance and light bulb in series, then detects the voltage of the resistance through ADC0804 which is the single channel AD conversion chip. It could not only calculate the light current but protect the circuit as well[3].

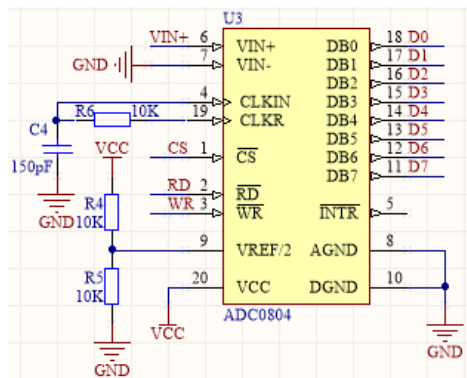


Fig.4 Current detection AD conversion circuit diagram.

### 2.The Sensor Module

It uses the photosensitive sensor to detect local illumination intensity then output high or low level. The MCU judges whether it's need to turn on or off the light and provides data for automatic control. It uses the humiture sensor DHT11 to feed back the environment in different regions to general control board and display.

### 3.The Relay Control Module

It's connected between the single-chip microcomputer subsystem and the streetlight. Due to the current of single-chip microcomputer is too small, the MCU can not control the light bulbs directly by high or low level. So it uses the relay to control the lights which is more convenient to protect the circuit and more effectively to control the circuit. It can also simulate the condition that the small current control 220V AC light bulbs.

## IV. SOFTWARE DESIGN

### A.The Total Control System Program Design

The total control circuit board is set to node 1 and the other streetlight control circuit boards are set to node 2,3,4. The data transmission path is 1-2-4 and 1-3-4 in a mesh transmission way[5]. It can not only stretch the distance of data transmission, but also transmit the data of node 4 when the node 2 is in failure, that can avoid a massive loss of data[6]. The total control circuit can control the corresponding streetlight on or off through the buttons and display the humiture and failure information gathered from the streetlight board. If it's not in fault condition, it will show "normal", fault is displayed "failure". The total control board circuit program flow chat of one cycle is as follows:

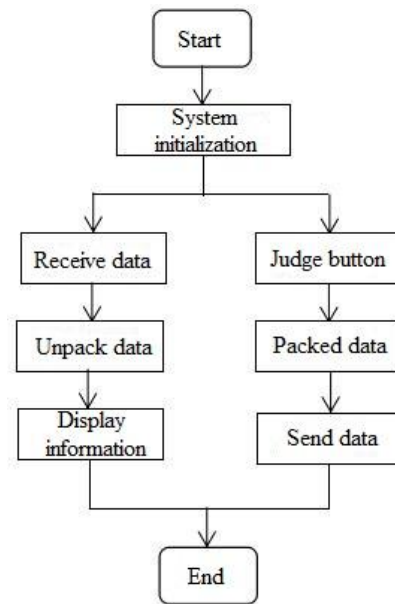


Fig.5 Total control module program flow chart in one cycle

### B.The Streetlight Control Program Design

The streetlight control circuit boards have humiture sensors to collect the humiture information, photosensitive sensors to collect brightness information, then it packs the information and send it to the master control board and receive the control information from the master board to control the streetlights[6]. The node 2 and 3 also need to pass the packaged information from node 4 to the master control board. The program flow chat of the streetlight control is based on the master control program, that just change display information to streetlight on or off, judge button to collect humiture, current, brightness information and judge failure. The flow chat in one cycle is basically in the same process.

## V. OVERALL TEST

### A. Function Test

The hardware circuit products are four circuit boards in total which include a master control board (number board 1) and three streetlight board(number board 2,3,4). Through testing the products basically complete the following functions[4]:

(1)It can transmit information through the circuit boards and the two information transmission ways are 1↔2↔4 and 1↔3↔4. The humiture and streetlight failure information collected from board 2,3,4 will be transmitted to board 1 and displayed. The control information from the master control board will



control the lights in board 2,3,4 on or off. The distance of the information transmission between two board can reach 12 meters in lab.

(2)The board 2,3,4 can control the lights off during the day, on at night according to the signal of the photosensitive sensor and control the lights on or off during the day through board 1.

(3)The board 2,3,4 calculate the light current on the basis of the resistance in series with the light and its voltage collected by AD chip, then transmit the failure information to board 1 judged by the current and the present light state.

### B.Data Test

Transmission distance test: We supplied power to the boards in an open filed and collected data after testing. The furthest distance between each board is 20.5 meters and the test effect will be better in a more open place.

Current collection test: We welded a screen strip at a side of the streetlight board and display the light current when the light is normal or current through programming. The fault current range of the three streetlight boards is 0~20mA and normal current range is 80~113mA.

Humiture collection: Through the screen on the master control board it shows temperature difference of three streetlights is  $\pm 3^{\circ}\text{C}$ , humidity difference is  $\pm 5\%$ .

## VI.SUMMARY

Through the study of the streetlight management system based on ZigBee technology, we analyze the advantages of ZigBee technology in the streetlight management system and give the specific implement plan of the system which can realize the functions of automatic fault detection, remote control and so on[7]. And we can decide the scale of every streetlight management system according to actual needs and add functions appropriately if there are other needs.

## References

- [1] Güttler F V, Rump J, Seebauer C et al.. [A wireless communication system for interventional MRI].[J]. *RoeFo. Fortschritte auf dem Gebiet der Roentgenstrahlen und der bildgebenden Verfahren*, 2010, 183(1).
- [2] Kang Kyungtae, Park Kyung-Joon, Song Jae-Jin et al.. A medical-grade wireless architecture for remote electrocardiography.[J]. *IEEE transactions on information technology in biomedicine : a publication of the IEEE Engineering in Medicine and Biology Society*, 2011, 15(2).
- [3] Guraliuc Anda R, Barsocchi Paolo, Potortì Francesco et al.. Limb movements classification using wearable wireless transceivers.[J]. *IEEE transactions on information technology in biomedicine : a publication of the IEEE Engineering in Medicine and Biology Society*, 2011, 15(3).
- [4] Guarascio-Howard Linda. Examination of wireless technology to improve nurse communication, response time to bed alarms, and patient safety.[J]. *HERD*, 2011, 4(2).
- [5] Fang Qiang, Lee Shuenn-Yuh, Permana Hans et al.. Developing a wireless implantable body sensor network in MICS band.[J]. *IEEE transactions on information technology in biomedicine : a publication of the IEEE Engineering in Medicine and Biology Society*, 2011, 15(4).
- [6] Woo Hyunsik, Lee Hak Jong, Kim Hyun-Chul et al.. Hospital wireless local area network-based tracking system.[J]. *Healthcare Informatics Research*, 2011, 17(1).

# Research and design on improving the operation efficiency of elevator

Zhang Si-yu; Zhou Yang; Ren Gui-ying

(College of Instrumentation and Electrical Engineering, Jilin University, Changchun 130012)

**Abstract**--The first-come first service algorithm of traditional elevator is poor real-time performance. The average waiting time of the user is too long. In order to reduce the energy consumption of elevator and improve the operation efficiency of the elevator, the model based on Bayesian algorithm is proposed in this paper, according to the prior probability and conditional probability Classification, the idea of probability parking at different periods is put forward, and combined with the infrared detection technology to avoid the empty stop of the elevator. In order to verify the actual operation efficiency of the algorithm, the simulation test is carried out on the elevator model, Based on Bayesian algorithm the average waiting time is about 47.8s. The time compared with the traditional algorithm is improved by about 28%. The model will treat peak and valley period of using elevator differently, improving the real-time efficiency of the system.

**Key words**--Bayesian algorithm; Probability statistics; Operating efficiency; Posterior probability

## I. INTRODUCTION

IN the rapid development of modern society, the elevator plays an indispensable role in the high-rise buildings. The elevator control algorithm has gradually become a hot research topic. At present, the elevator control system uses the 'First Come First Served' (FCFS) algorithm[1] and this kind of random service algorithm does not have the real-time characteristic, affecting the user's efficiency.

This paper puts forward the probability and statistics[2-3] of the number of elevator used in each floor, with statistical learning ability and intelligent Bayesian algorithm[4] based on in-depth analysis of traffic in the building and extracting the features of the information system. Generate forecast according to the principle of expected utility maximization. Control the elevator when the floor with the highest probability of use in the forecast[5-7]. According to the different operating conditions, use different scheduling schemes[8] and more and more people ride the elevator in the shortest time to the maximum extent. On one hand, it improves the operation efficiency of the elevator. On the other hand it can save most time people waiting for the lift, improving the overall efficiency[9]. At the same time, the infrared detection technology is integrated into the design and control of the elevator[10] to avoid the phenomenon that nobody outside after the elevator stopped when

elevator runs in the actual operation, improving the efficiency of the elevator operation.

## II. ESTABLISHMENT OF PROBABILITY STATISTIC MODEL

### OF ELEVATOR

#### A. Modeling basis

A number of factors affecting the flow of passengers in the elevator:(1) hospitals, office buildings, residential quarters, such as the use of different nature;(2) the distribution of different floors of different;(3) the use of time period of the peak hours;(4) the flow of passengers caused by unexpected events, etc. Among the above mentioned factors, the first three are the laws of the factors and the latter is a random factor. For the analysis of the influencing factors of the law, the method of the average value of the random factors is treated in the same way[11]. At the same time for the unified evaluation criteria, the time of waiting for the passengers to wait for each floor of the elevator needs to be modeled.

#### B. Modeling process

Take the N layer elevator model as an example. Assume that after the elevator single operation is completed it will stay in the floor waiting for the next call. Mark the floor number to stay down as x and the calling floor as m and the time required to reach the call floor from the stop floor as t.

Mark the number of calls on each floor of the elevator as  $N_x$ . According to empirical formula calculates  $N_x$ :

$$N_x = \frac{x\{1 - [(x-1)/x]^r\} - 1}{n} \quad (1)$$

'r' is the effective number of passengers for the  $r=0.8\mu rc$ , which rc is the actual call number,  $\mu$  is for the correction factor.

Assuming the elevator runs several cycles, the total time required for all floors to be recorded is  $T_n$ , and the retention time of each floor is recorded as  $\Delta T$  [12]:

$$\Delta T = 0.8 + K(f + 1)^{1/3} \quad (2)$$

Where 'k' is the coefficient of carriage entrance open width, 'f' is the integral values of  $N_x$ ;

Using the traditional FCFS program, the elevator stops at the fixed floor (in fact, more than 1 floors), passengers in different states need to lift the elevator from the floor to reach the total time required to reach the floor, the total time required to write the following:

$$T_n = \sum_{m=1}^n (|1 - m| \Delta T) N_x + (n-1)\Delta T \quad (3)$$

If the idle stop position based on probability determined in this research program, so that the elevator stays in the highest frequency of use floor, building K, using the assumption here is that the highest frequency, lift idle stop at k layer ( $n=k$ ), namely, all the floors need total time waiting for T 'down;

$$T_n' = \sum_{m=1}^n (|n - m| \Delta T) N_x \quad (4)$$

The ratio of saving time to total waiting time :

$$\beta = \frac{T_n - T_n'}{T_n} 100\% \quad (5)$$

The proportion coefficient reflects the efficiency to a certain extent, by the formula (5) shows that the K floor elevator frequency is high, the value of  $N_k$  compared to other floors of the greater proportion coefficient is higher, from a certain extent to improve the efficiency of the more obvious.

According to the theory of probability, a single variable in the same position in stochastic models, in this case, if the other floors of the highest efficiency,

the new algorithm can get the same results.

### C. Model conclusion

The model is based on the statistics of the number of users in each floor of the elevator. According to the empirical formula, the time of the elevator stay in each floor is obtained. Combined with the call number of each floor and the elevator operation scheduling scheme to calculate the proportion coefficient  $\beta$ . To a certain extent,  $\beta$  reflects the proportion of the overall efficiency of elevator operation with the new scheme compared to the traditional elevator dispatching scheme. It is in a certain period of time if there is a floor to use the elevator frequency compared to other floors using the high frequency of the elevator. When the elevator is idle, the new scheduling scheme will be used to reduce the average waiting time and improve the overall operation efficiency of the elevator.

## III. BIAS ALGORITHM FOR PREDICTION OF ELEVATOR

### CALL FLOOR

#### A. Algorithm application design

According to the above modeling results, it can be concluded that when the elevator is idle it stays on the floor with the largest frequency, which is beneficial to improve the overall efficiency of the elevator. So in the actual elevator system according to the probability distribution of existing data obtained using the frequency of each floor elevator, and a more accurate prediction of a certain period of time the next use lift the maximum probability of several layers of floor is particularly important. On the one hand, Bias algorithm can according to some of the existing elevator information to predict the user call event, on the other hand can call events as new users update the next sample prediction results. And this prediction results just can elevator control reference information for efficient scheduling of the elevator.

The analysis shows that the feature vector of the elevator can use  $X=\{X1, X2, X3, \dots, Xn\}$  to express. The characteristic property 'Xn' indicates whether the call is measured in different floors. From the overall point of view of the elevator, the characteristic property [13] has two categories. 'Y=0' shows no call request and 'Y=1' shows call request. Maximum a posteriori

probability[14] can be obtained according to Bias's theorem:

$$P(Y | X_n) = \frac{P(X_n | Y)P(Y)}{P(X_n)} \quad (6)$$

By comparing  $P(Y_n / X)$ , select the items and can get the elevator to use the frequency of the largest floor 'n'.

*B. Algorithm application design*

The characteristic function of elevator system is  $\psi(x)$ , Sample values are derived from a fixed interval T in a period of time t to obtain the sample data.

$$\varphi(k) = \begin{cases} I, & \text{Expression 'k' is true} \\ O, & \text{Expression 'k' is wrong} \end{cases} \quad (7)$$

Through the elevator statistics in the past the number of calls to obtain a priori probability, that is, the elevator in the state of the call, the corresponding floor of the call probability such as type (8), the elevator at a certain time is called the probability of such as type(9)

$$P(X_n = h | Y = 1) = \frac{\sum_{m=1}^n \varphi(X_n = h \cap Y = 1)}{\sum_{m=1}^n \varphi(Y = 1)} \quad (8)$$

$$P(Y = 1) = \frac{1}{n} \sum_{m=1}^n \varphi(Y = 1) \quad (9)$$

The probability of staying at different floors in a fixed time T as type (10)

$$P(X) = \prod_{m=1}^n P(X_n | Y = 1)P(Y = 1) + \prod_{m=1}^n P(X_n | Y = 0)P(Y = 0) \quad (10)$$

When the elevator operation to change new access

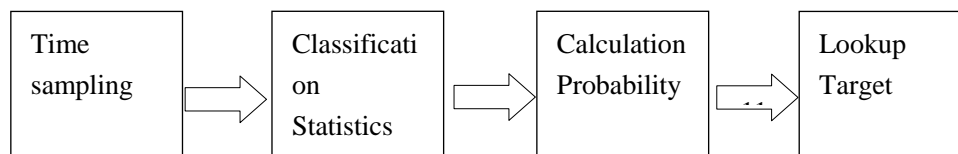


Fig.1 Data processing procedure chart

As shown in Figure 1, sampling was carried out in a fixed time interval, according to the sampling results to determine whether there is a call request, and according to a call request classification statistics, and calculate each floor there is a call request of the posterior probability recorded in Table 1 using Bayesian algorithm, the posterior probability of the number of floors are sorted to find the maximal the frequency of use, with search target.

According to the statistics of the elevator in the table 1, the probability of different floors, combined with the

to statistical data, the Bayesian posterior probability formula for [15], namely the elevator next call request in the probability that a floor value such as type (11)

$$P(Y = 1 | X) = \frac{\prod_{m=1}^n P(X_n | Y = 1)P(Y = 1)}{\sum_{i=0}^1 \prod_{m=1}^n P(X_n | Y = i)P(Y = m)}$$

( 11)

*C. analysis of data*

Get a key hospital stay in 8:00--11:00 morning lift times on different floors through investigation and statistical processing. The process is shown in Figure 1, to obtain the relevant probability data as shown in table 1:

Table 1. The probability statistics of the elevator stays in different floors

| state<br>floor | Statistic value |         | Probability |
|----------------|-----------------|---------|-------------|
|                | call            | no call | P(Y=1 X)    |
| 1              | 0.10            | 0.15    | 0.15        |
| 2              | 0.16            | 0.04    | 0.24        |
| 3              | 0.07            | 0.03    | 0.11        |
| 4              | 0.08            | 0.04    | 0.12        |
| 5              | 0.12            | 0.03    | 0.18        |
| 6              | 0.05            | 0.02    | 0.08        |
| 7              | 0.06            | 0.02    | 0.09        |
| 8              | 0.02            | 0.01    | 0.03        |
| total          | 0.66            | 0.34    | 1           |

The data processing process is shown in figure 1:

Bayesian formula to calculate the posterior probability, and draw a posterior probability distribution map as shown in figure 2:

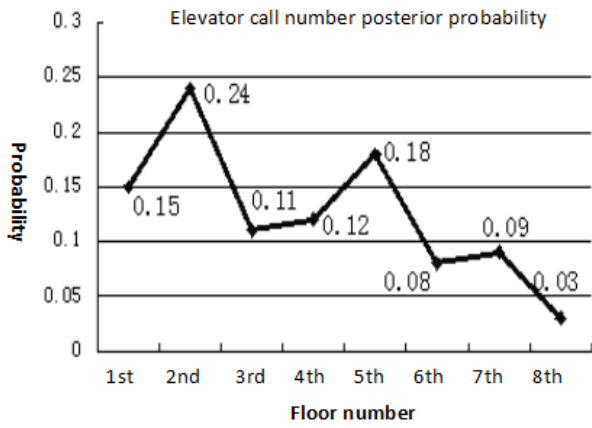


Fig. 2 posterior probability distribution

According to the probability distribution map, in the elevator call request and call the maximum probability in floor 2 floor, 2 floor with the actual research found that the outpatient department, and frequent personnel exchanges, therefore, if the elevator control in the period of idle stop automatically to the 2 floor, then on the one hand, improve the efficiency of the elevator itself, on the other hand, the majority of people waiting for the elevator to save time, improve the overall efficiency.

IV. THE DESIGN AND IMPLEMENTATION OF ELEVATOR

DISPATCHING ALGORITHM

A. Algorithm flow design

Based on the above mathematical model of the elevator, and the application of detection technology, simulate the operation mode without changing the vertical lift hardware structure on the basis of existing, and the traditional elevator operation mode to optimize the transformation, changing its algorithm structure, design more intelligent and efficient operation mode, Which is based on the probability of idle stop position. Through the infrared detection technology to determine whether the elevator, the car stopped outside the elevator to prevent one, avoid unnecessary retention phenomenon. Thus greatly improving the efficiency of the elevator operation, saving more time for the user. Fig. 3 flow chart of probabilistic algorithm for single elevator operation:

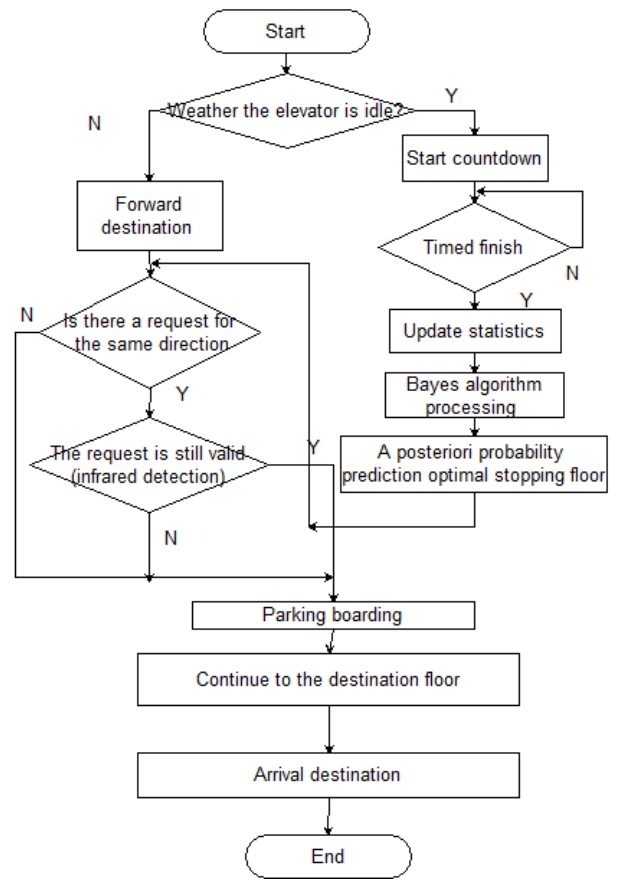


Fig.3 Algorithm flow chart

According to the model analysis, in the elevator control algorithm can be treated as a state machine, according to the different status of the elevator system to different control commands, to achieve efficient and orderly system. The elevator operation procedure is as follows:

- 1) The elevator system to detect the current state, whether in the idle state to decide whether to start a Bayesian algorithm to determine the best parking floors, the use of the probability of parking in the car technology;
- 2) System also added infrared detection technology, to prevent the emergence of the elevator after the user presses the call button, but for some reason not to ride the elevator, the elevator has arrived at the floor door open, the door was empty phenomenon (investigation of this phenomenon is particularly common in hospitals and other places);
- 3) The elevator call request the interrupt mechanism, an arbitrary process could interrupt, to perform a higher level program, or to start a new cycle, the premise does not affect the normal operation of logic.

*B. Algorithm implementation and integrated system*

Figure 4 shows the model diagram of the controller, through a variety of sensors, obtain lift the running status, combined with the actual operation logic of

elevator, and according to the scheduling algorithm into the car stop probability and infrared detection of elevator control system scheduling algorithm, achieving the function.

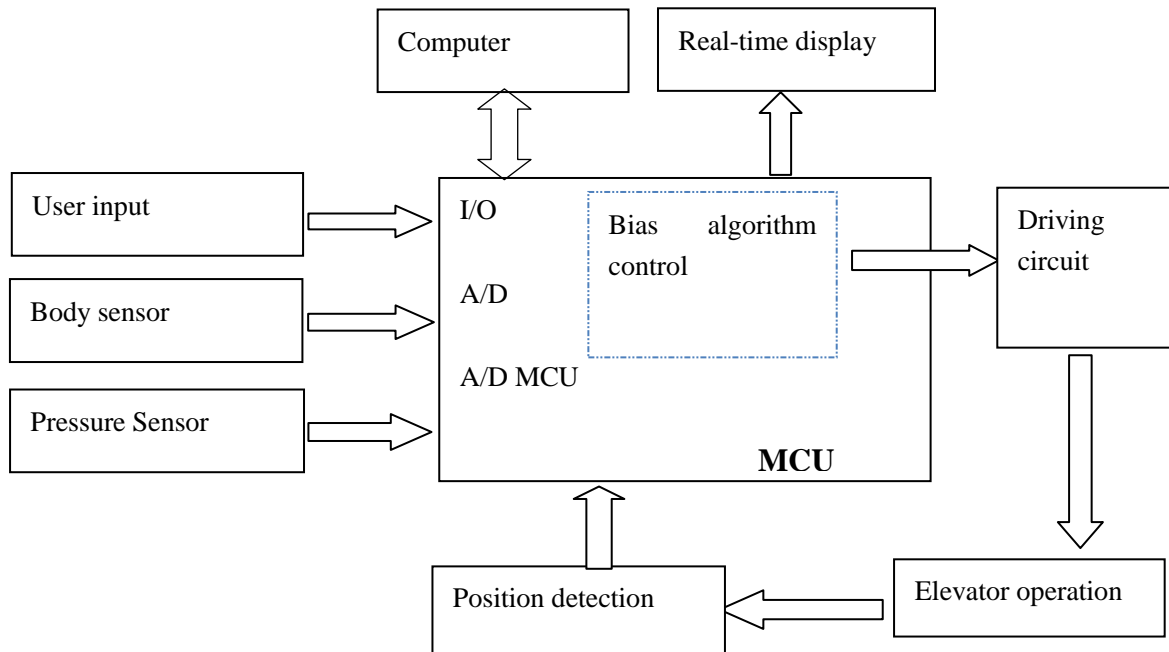


Fig.4 System diagram

V. COMPARATIVE ANALYSIS OF SIMULATION RESULTS

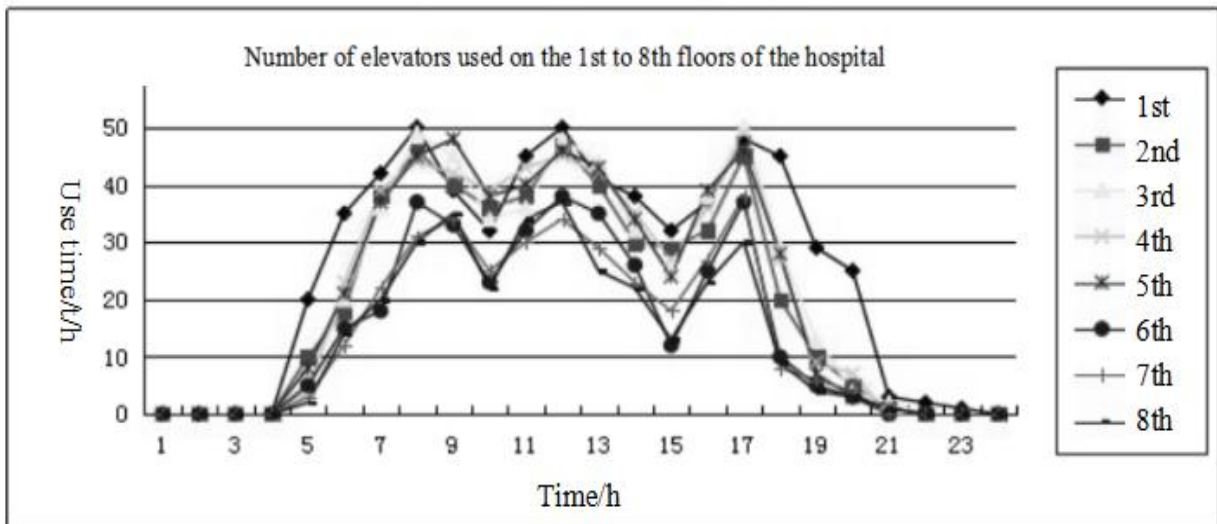


Fig.5 The model test data sheet

Figure 5 is the use of 1 to 8 floor elevator in key hospital number of dynamic map, can be seen from the elevator at 8 in the morning, 12 noon, 17 PM respectively, the passenger flow peak, and different floors in different periods each call times have all the same, the distribution of differences, these data are

calculated from formula (3) and type (4) is determined in the traditional elevator operation and Bayesian algorithm in probability at the car users average waiting time algorithm based on simulation according to equation (2) is =20s, the actual simulation model based on the data of the chart at 8 in the morning, the

test results are as follows:

The simulation data of 1 to 8 floors : 20, 39, 36, 30, 25, 23, 22, 20

The average waiting time in traditional operation mode

$$t_n = \frac{\sum_{m=1}^8 (|1 - m| \Delta T) N_x + (m - 1) \Delta T}{\sum_{x=1}^8 N_x} = 66.7s \quad (12)$$

Bayesian algorithm based on n=2 average waiting time

$$t_n' = \frac{\sum_{m=1}^8 (|n - m| \Delta T) N_x}{\sum_{x=1}^8 N_x} = 47.8s \quad (13)$$

Equivalent operating efficiency increase

$$\beta = \frac{t_n - t_n'}{t_n} \approx 28\%$$

From the above analysis of simulation data contrast, using Bayesian algorithm in probability at the car lift technology overall operating efficiency is improved by about 28%, saving the user waiting time to a certain extent, increase the efficiency of the whole system in real time.

## VI. CONCLUSION AND ANALYSIS

This time on each floor elevator using the number of probability statistics, processing and analysis, according to some estimates of a posteriori prediction information of the elevator user call after the incident, the prediction results for the implementation of the elevator control strategy to provide reference information for efficient scheduling of elevator.

The system uses infrared detection technology, is to determine whether the elevator, the way to prevent users to abandon the use of the elevator, elevator outside no one phenomenon where the elevator stops the car, to avoid unnecessary stay to further save the user travel time.

In order to verify the feasibility and practicability of scheduling algorithm based on Bayesian algorithm, elevator operation simulation model established by the model, the simulation results and data shows that the algorithm can predict in advance and weaken the peak passenger flow, reduce the waiting time of users,

improve overall operating efficiency of the elevator system.

## References

- [1] CHEN Yu-xian. Research on the Scheduling Algorithm of the New Generation Elevator[D].Changsha: Central South University,2010.
- [2] LIANG Hao,XU Chang-geng, LIN He-ping. Practical and Efficient Spam Filtering Algorithm[J].Journal of Jilin University: Information Science Edition,2010,28(03):298.
- [3] AN Peng. Optimization of PSO Algorithm Based on Chaos Theory and Adaptive Inertia Weight[J].Journal of Jilin University: Science Edition, 2015,53(06):1223-1228.
- [4] ZHANG Lun,YANG Wen-chen, LIU Tuo,SHI Yi-cheng. Freeway Traffic Incident Detection Based on Naive Bias Classification[J].Natural Science Edition,2014,42(4):2-6.
- [5] HUANG Shang-jun. Talking about the Elevator Design of Super High Rise Building[J].Science and Technology Innovation Herald, 2009(19):1.
- [6] LI Zhang-lv. Research on Bias Decision Theory[D].Tianjin: Nankai University,2012.
- [7] QING Xiao-xia, WANG Bo,DUAN Jun. Simulation Test and Energy Saving Analysis of Elevator Operation Considering Waiting Time[J].Computer Engineering and Applications,2012,48(31):232-235.
- [8] LIU Yao-wu, NIE Feng-hua,SU Qiang,HUO Jia-zhen. Elevator Energy Saving Scheduling Algorithm with Time Constraint[J].System Engineering Theory and Practice,2013,33(9):3-6.
- [9] FAN Ci-meng. Research on Elevator Model System for Teaching[J].Mechanical and Electrical Engineering Technology,2009, 38(12):52-54.
- [10] LIU Shu-qi, SHI Guo-liang. Alarm System Based on Pyroelectric Infrared Sensor[J].Foreign Electronic Components, 2005(3):5-8.
- [11] XIAO Hai-rong, LI Hui-xian. Grid Task Scheduling Optimization Based on Adaptive Genetic Algorithm.

Journal of Jilin University: Science Edition ,  
2015,53(02):297-301.

- [12] Siikonen M L. Customer Service in an Elevator System During Up-peak. *Transpn Res*, 2001,25(02):27-36.
- [13] BISHOP C H, SHANLEY K T. Bayesian model averaging problematic treatment of extreme weather and a paradigm shift that fixes it[J]. *Monthly Weather Review*, 2008,136(12) :4641-4652.
- [14] Raftery A E. Using Bayesian model averaging to calibrate forecast ensembles[D]. Washington: University of Washington, 2005.
- [15] OZBAY K, NOYAN N. Estimation of incident clearance times using Bayesian networks approach[J]. *Accident Analysis & Prevention*, 2006(38):542-555.



# The design and implementation of a portable alcohol detector based on GPS & GPRS

Wen Xue-jun; Cai Yao; Liu Xiao-han

(College of Instrumentation & Electrical Engineering Jilin University, Changchun, 130021, China)

**Abstract**—The world health organization in the traffic accident investigation pointed out that more than half of the car accidents are related to drunk driving, which has become the main cause of traffic accident. With ‘Drunk driving’ officially in the sentence, the design and application of alcohol concentration detector to detect whether the driver is drunk driving are become very important. This project designs a portable alcohol detector based on GPS and GPRS to reduce traffic accidents more effectively and to overcome the shortcomings in traditional supervision and law enforcement. The detector uses single chip microcomputer, controlling the gas sensor to monitor the concentration of alcohol in people's breathing, and implements LCD display, threshold setting, sound-light alarm functions. The designed detector is a portable gas alcohol concentration detection tool with strong practicability and safety. It can also send detectors' information of location and alcohol detection results to PC, plays a role in the supervision of law enforcement to a certain extent.

**Keywords**—Drunk driving, Alcohol concentration detector, GPS, GPRS, Alcohol gas concentration

## I. FOREWORD

IN recent years, China's economy develop rapidly, people's living standards continue to improve, China has gradually entered the "automobile society", the accident caused by the drunk driving behavior is also more and more, and the impact on society is also growing. According to statistics, the probability of drunk driving traffic accidents is 16 times the non-drunk driving[1]. Visibly, alcohol become increasingly fierce "the road killer", and the detection and prevention of it attracts more and more attention from countries around the world[2]. Therefore, it is particularly important to determine whether the driver is drunk driving, accurate and effective detection of alcohol content is particularly important, and therefore alcohol concentration detector has a very broad market and important significance.

At present, the method of detecting alcohol at home and abroad is a more mature method, which is a breath alcohol detection method and a blood sampling method[3]. Blood tests often can't do that, and after the blood test would increase law enforcement time, and it is a invasive detection, the process is complex, high cost. Which simple and feasible is to detect the alcohol concentration in the breath of the driver[4].

This project is designed based on STC12C5A16AD

MCU, using MQ-3 gas sensitive sensor to detect and realize the LCD display of the breath alcohol concentration, drunken threshold setting, audible and visual alarm, portable gas alcohol concentration detector with GPS positioning and GPRS data transmission function.

## II. THEORY FOUNDATION OF PROJECT DESIGN

### A. Breath Alcohol Detection Technology

Breath alcohol detection technology is a non-invasive, a technique for detecting the gas exhaled breath of the human body. The current testing technology used mainly consists of colorimetric technology, Semiconductor testing technology, electrochemical detection technology and infrared detection technology[5]. Because there is a certain proportion of the concentration of alcohol in the lung and blood alcohol concentration, therefore, the accuracy of the test results of the breath alcohol detector which conforms to the national standard is still relatively high[6]. This project is the use of breath alcohol detection technology to carry out the design.

### B. GPS Positioning Technology

Global Positioning System is a new generation of satellite navigation and positioning system with sea, land and air navigation and positioning capabilities[7].

The basic principle of the GPS system is to measure the distance between the satellite to the user's receiver, and then the data of the satellite can be known[8]. This project selects the GPS module directly connected with the main control chip through the fixed program to know the location information of the sensor.

### C. GPRS Network Communication Technology

GPRS (Packet Radio Service General) is a general packet radio service technology for short, GSM mobile phone users can use it's mobile data service, which belongs to the second generation mobile communication data transmission technology. This technology is located between the second generation (2G) and the third generation (3G) mobile communication technology[9]. This project is the position signal numerical and GPS module to collect the alcohol content obtained, are input to the main control chip for storage, the main control chip process the information , then input into the SIM900A, the SIM900A of the signal sent to the target machine, to receive information.

### III. SYSTEM OVERALL DESIGN

The whole system includes MCU control module, alcohol detection module, GPS positioning module, threshold setting module, EEPROM memory module, LCD display module, GPRS communication module, alarm module and power supply module. The system module is shown in Figure 1.

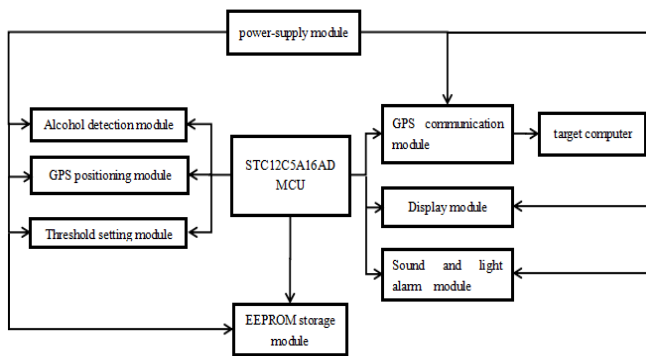


Fig. 1. System diagram.

The main control module uses STC12C5A16AD microcontroller, alcohol detection module with MQ-3 gas sensitive sensor.MQ-3 will collect the alcohol signal and send them into the microcontroller to carry out analog digital conversion. Single chip microcomputer for digital signal analysis and

processing, and the results are displayed on the LCD. You can set the button with different alcohol concentration threshold of EEPROM storage, once the alcohol concentration detected exceeds the preset threshold, the microcontroller will control the buzzer alarm and the diode. GPS positioning module to obtain the measured position information to the microcontroller, monolithic machine of alcohol and position information is stored and entered into the SIM900A of GPRS, packaged and sent to the target machine in the way of information, and play the role of supervision and law enforcement. Power supply module for the entire system.

### IV. SYSTEM HARDWARE DESIGN

#### A. Single Chip Microcomputer System

This system includes a main control module, threshold setting module, sound and light alarm module. Main control chip using STC12C5A16AD microcontroller, the chip is 8 bit microcontroller core 52,and it's memory is 4 times larger than the 51 single chip microcomputer, with 8 bit high speed A/D converter, and writing program is convenient and rapid, with exactly the same program structure the other 51. The main control module also comprises a clock circuit and reset circuit. When the alcohol concentration over threshold, the buzzer will ring and the diode will be lighted. Threshold settings using the button to add and subtract, using program to control (shown in Figure 2).

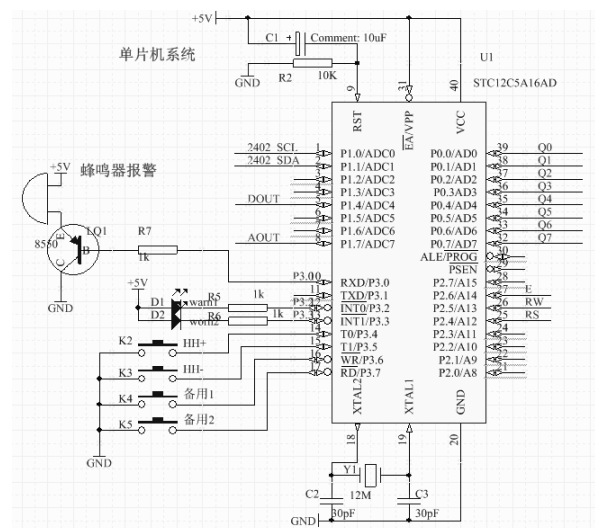


Fig. 2. Schematic diagram of MCU system.

### B. Alcohol Detection Module

The alcohol detection module comprises a gas sensor unit and a signal conditioning unit, and a MQ-3 is used for the gas sensor with the following reasons:

- ◆ High sensitivity and good selectivity to ethanol vapor;
- ◆ Quick recovery characteristics;
- ◆ Long life and reliable stability;
- ◆ Simple driving circuit;

MQ-3 gas sensor can be seen as a gas sensitive resistor which resistance varies with the concentration of ethanol. The concentration of ethanol gas can be judged by the size of the output resistance.

We use MQ-3 module to collect gas ethanol signal, which contains the alcohol sensor and the detection signal from the resistance value into the voltage value of the signal conditioning circuit. Schematic diagram shown in figure 3:

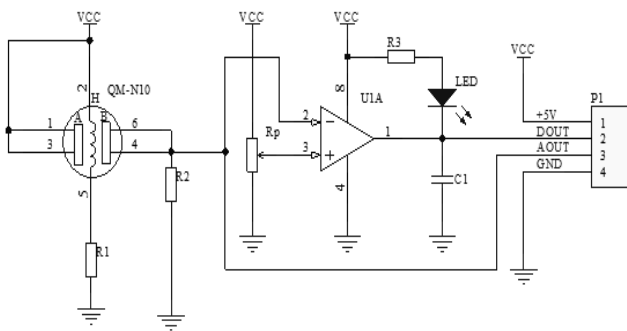


Fig. 3. Schematic diagram of MQ-3 module.

The four pins of module respectively corresponding to power supply terminal (+5V), TTL level output terminal (DOUT), analog voltage output (AOUT) and end (GND). AOUT output voltage detection signal transmitted to the microcontroller ADC7 port for processing, according to the concentration of alcohol in the air, the digital signal can be DOUT direct output alarm signal.

### C. LCD Display Module

The display part uses LCD1602 LCD data display, and the microcontroller interface circuit shown in Figure 4. The VO is for the backlight pins, we can adjust backlight brightness with potentiometer. RS, E/W and E are control pins for liquid crystal, the rest are for the data pins and power pins.

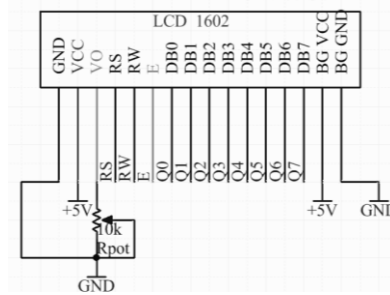


Fig. 4. Circuit of LCD and MCU.

### D. EEPROM Storage Module

The EEPROM memory module uses AT24C04 chip with I2C interface, using the advantage of the power down without loss of data to realize the storage of the threshold of alcohol. You can use the increase, reduction key to set the threshold and save. Its principle is shown in Figure 5. A0, A1 and A2 are address pins of the chip, generally lined with ground. SCL and SDA are clock and data lines used for communication between AT24C04 and I2C.

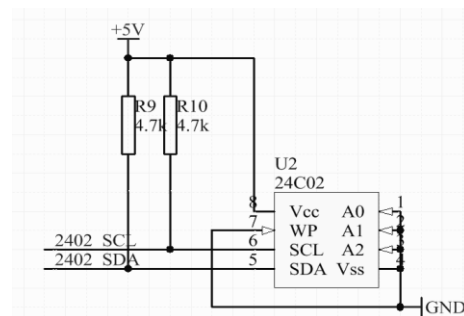


Fig. 5. Schematic diagram of EEPROM storage circuit.

### E. GPS Positioning Module

This project uses the integrated GPS module, the antenna make it more easy to receive location information. The information GPS microcontroller received sent to the computer through the USB-TTL tool, we can receive the time, latitude and longitude information on the serial port assistant. The module lights lit which means module has been started, but not yet implemented location; lights flashing means positioning module has been successful. The connection is shown in figure 6:

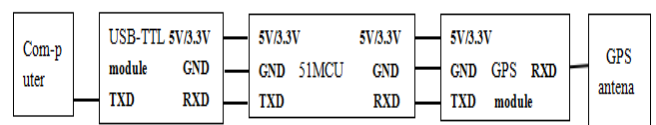


Fig. 6. GPS, MCU and PC connection diagram.

### F. GPRS Communication Module

This project uses the integrated GPRS module, this

module is based on SIM900A. With the mobile phone SIM card insert into the slot, you can put the module as a mobile phone to realize telephone voice, SMS, MMS, GPRS data transmission and other functions. We mainly realize send information by text messages to the target machine through the GPRS module. MCU control SIM900A to receive message sent by computer serial assistant and then send to the target machine. SIM900A and computer also need serial converter. The connection diagram is shown in figure 7:

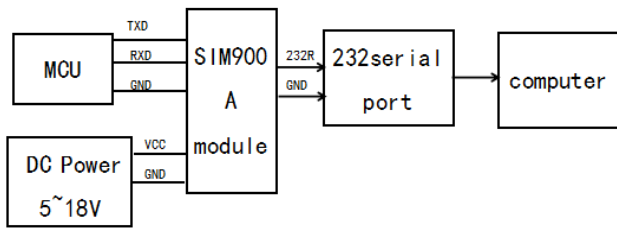


Fig. 7. GPRS, MCU and PC connection diagram.

### V. SOFTWARE PROGRAMMING

Download the C code to the STC12C5A16AD microcontroller which control alcohol collection, data processing, display, threshold setting storage, alarm, GPS positioning, GPRS data transmission. Start power and operate GPS positioning, signal acquisition and processing of alcohol display, and scan button, set the threshold, open the GPRS data transmission. Once exceeding the threshold, start the alarm the function of control. The program flow chart is shown in Figure 8.

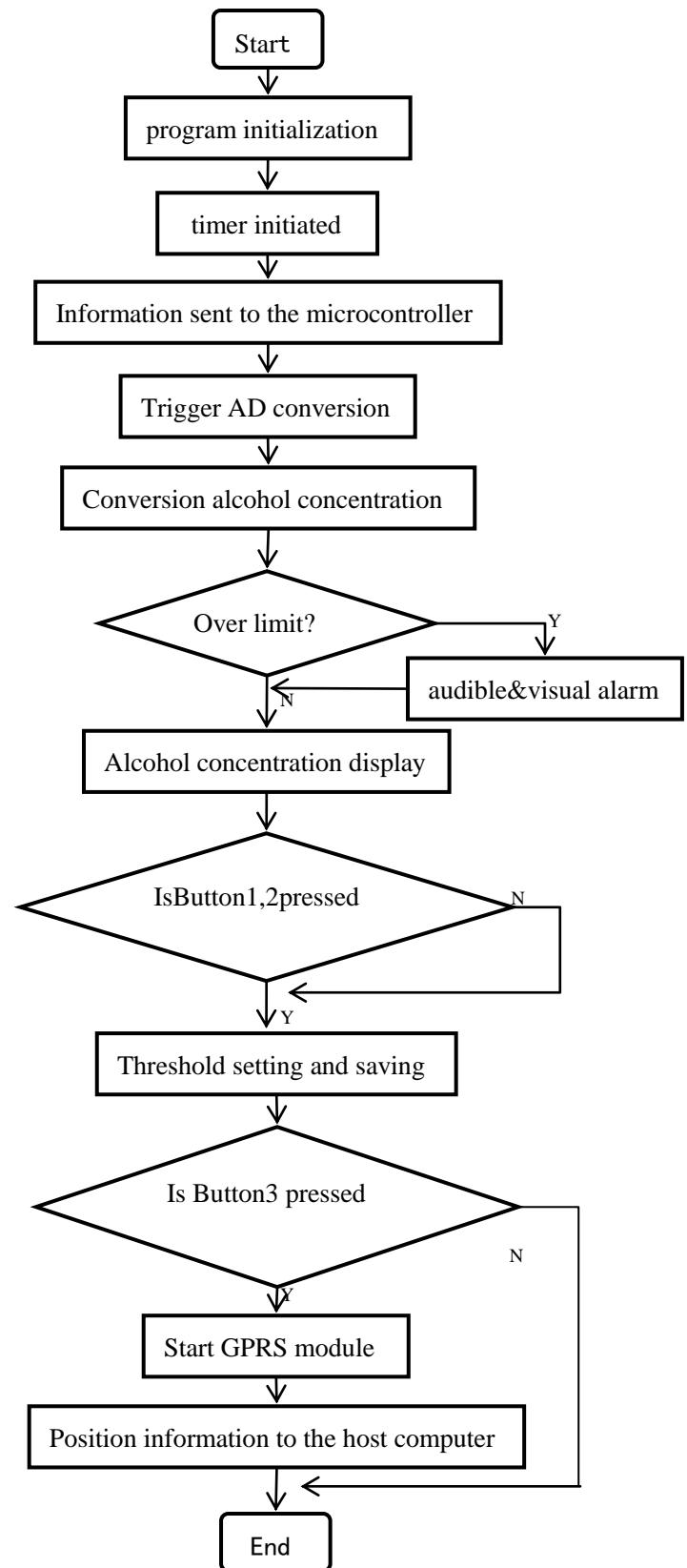


Fig. 8. Flow chart of control program.

### VI. TEST AND ANALYSIS

According to the method above-mentioned of the hardware and software to debug every module. First teste and debug the GPS module. Use the RXD and

GPS module TXD port docking of a USB-TTL line , the other end connected to the PC machine, install USB driver of the GPS module , the position information received by the serial port as shown below:

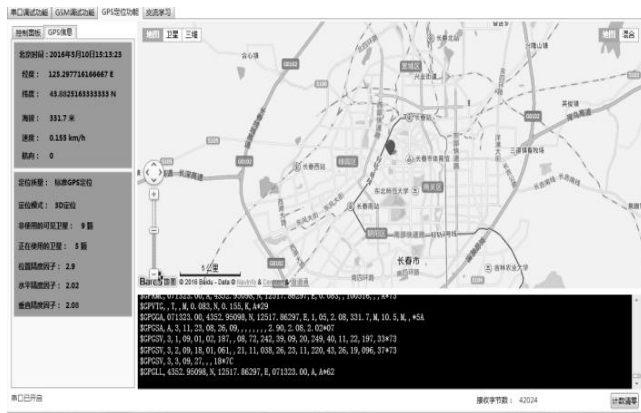


Fig. 9. Results of GPS debug.

GPRS also use serial converter. First we need to insert the SIM card, start module, waiting for module to register successfully we can see the green light slowly flash, cycle 3S, indicates that the system has registered to the 2G network. Then set the short message form, recipient cell phone number and SMS content, eventually received the message and debug process picture as shown in figure.

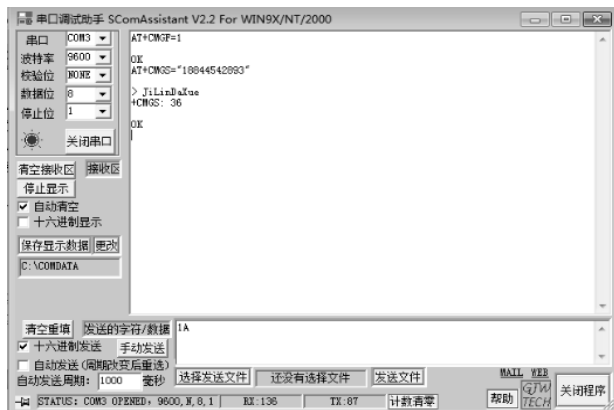


Fig. 10. Initialization settings of GPRS in serial interface.



Fig. 11. Message received of the target machine.

Finally, the above two modules and alcohol detection and other modules are combined to observe the phenomenon as shown in figure 12:

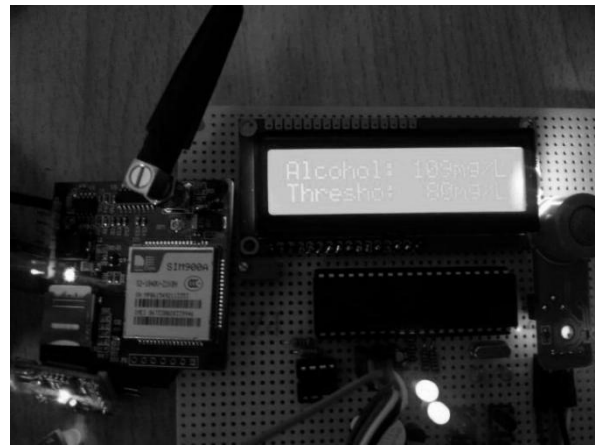


Fig. 12. Prototype of the alcohol detector.



Fig. 13. The final message received by the target machine.

Therefore, the system can display the measured alcohol content, the alcohol content in the image above is 109mg/100mL, exceed the threshold of 80mg/100mL, so we can see the diode light. And GPS, GPRS data transmission will ultimately send the location (longitude 125.29, latitude 43.88, altitude 265.8m) and alcohol content the in the form of text messages to the target machine. The message received by the target machine is shown in Figure 13.

In addition, we do the contrast experiment with the alcohol detector, the alcohol content (%): 4.3 wort concentration: 11 (%) of Tsingtao Brewery. Participants (weight difference is not large) drink different amounts of alcohol, measured after drinking alcohol content of 30min value to conduct comparative experiments. The experimental data are shown in Table 1

Table1

EXPERIMENTAL DATA RECORD OF ALCOHOL DETECTOR

| Measured person                  | 300mL |    |    | 600mL |    |    | 900mL |     |     |
|----------------------------------|-------|----|----|-------|----|----|-------|-----|-----|
|                                  | A     | B  | C  | A     | B  | C  | A     | B   | C   |
| alcohol concentration (mg/100mL) | 36    | 44 | 42 | 71    | 78 | 75 | 103   | 109 | 112 |
| average value                    | 40.67 |    |    | 74.67 |    |    | 108   |     |     |
| Ideal predictive value in blood  | 32.25 |    |    | 64.50 |    |    | 96.75 |     |     |

We can see that the true value is generally lower than the breath alcohol from the experimental data, and the difference increased with alcohol consumption increases, so we need to use a number of experimental comparison curve for curve correction. The above chart can also reflect: GPS based on the design of this project, GPRS portable alcohol detection method is feasible in theory and in practice, the traffic police check drunk driving can be used as a good tool to provide a good guarantee for road safety.

## VII. CONCLUDING REMARKS

Drunk driving is a major social ills currently endangering public safety, is an important cause of traffic accidents. The project detect alcohol concentration by breath test, on this basis add localization of GPS and GPRS network data transmission module, according to the different environment set the different drunken threshold, make the instrument using more convenient; and during the traffic police in the inspection of drunk driving, automatically send drinkers position and alcohol content information. real-time, safe and reliable, to play the role of supervision and law enforcement. In the next step of work, we'll optimize the project, make up some shortcomings of this project. As many people were tested many times, strengthen and improve the sensor. We'll make the measurement more accurate, measurement methods more health, more humane.

## References

- [1] Deng Jin, Li Kun, Luo Kai-jian et al. Investigation of road traffic accidents in Guizhou Province in 2002[J]. Chinese Journal of Traumatology, 2004,20 (10): 620-621
- [2] Chen Guo-qiang. Noninvasive Analysis of Blood Alcohol in DriversBased on Near-infrared Spectros- copy[D]. Shandong University, 2012.
- [3] Lu Li-qian. A Blood Alcohol Content Nondestructive Detecting System Based on Near-infrared Spectrum[D]. Shandong University, 2014.
- [4] Lin Fang, Zhou Li-ping. Talking about the Electronic Alcohol Detector[J].SCI-TECH INFORMATION DEVELOPMENT & ECONOMY, 2011 (2);214.
- [5] Lu Li-qiang, Fang Xue-xin. Application Research in Traffic Enforcement of Breath Alcohol Testing[J]. China Public Security (Academy Edition), 2011, No.2504:116-119.
- [6] Yu Chun-jun, Lu Li-qiang.The legality study ofBreath alcohol concentration detection[J].Journalof Road Traffic Management,2012,05:36-37.
- [7] Duan Jun-yu. Analysis on common navigation technology [J]. China Electric Power Education, 2010, S1:794-795.
- [8] Zhou Zheng-xing. Analysis of the composition and principle of GPS global satellite positioning system[J]. Appliance Maintenance:The Public Version, 2012,01:51-57.
- [9] Zhao Guo-qing, Remote Monitoring System of Train' s Electricity Based on GSM-R/GPRS. Taiyuan University of Technology master's thesis: 43-44.

# Design and application of multi direction wind energy collection device based on PZT

ZHOU Xiao-hua; GOU Xin; Chen Yu-da; Liu Li-jia

(College of Instrumentation & Electrical Engineering, Jilin University, Changchun 130021, China)

**Abstract**--In order to solve the power supply problem of the micro power equipment which needs long time working in the outdoor, this paper presents a multi direction wind energy collection device based on PZT. Based on the piezoelectric effect, the design of the piezoelectric cantilever beam array is used to convert wind energy into mechanical energy, and mechanical energy can be converted into alternating current energy under the action of piezoelectric effect. Through the rational design of the conversion circuit, the wind-induced vibration produced by the electrical energy stored in the lithium polymer batteries. In addition, wireless data transmission system based on MSP430F149 microprocessor is designed in this paper. The experimental test, the device in the 6-9m/s wind speed environment to achieve the best working state, continuous work 40min can be a 25mAh of lithium polymer battery full. The device has the advantages of simple structure, no pollution, etc, and can be widely used in field data monitoring, wireless data transmission and other fields.

**Key words**-- piezoelectric effect; cantilever beam array; energy conversion; wireless data transmission

## I. INTRODUCTION

WITH the development of networking technology, micro power devices of all kinds gradually into our lives, they are more and more widely used, but the problem is that the long-term power supply, especially for long-term work in the field of data acquisition and monitoring equipment, the collocation of the limited battery capacity, and it is not convenient for timely replacement the rational allocation of the power supply system. For the power supply of micro power equipment, researchers at home and abroad have favored the solar energy[1],thermal energy[2]and vibration energy [3-4]in the natural environment. Wind energy, as a common form of energy in the environment, can be a good combination of energy and other forms of complementary. The design idea of the micro wind energy collecting device is to convert the wind energy into mechanical energy, and then convert the mechanical energy into electrical energy by electrostatic, electromagnetic and piezoelectric devices [5].Piezoelectric ceramic is a kind of electronic ceramic material with piezoelectric properties, which can convert mechanical energy and electrical energy to each other, and has been widely used in medical imaging, acoustic transducer, acoustic transducer, ultrasonic motor, etc [6].The wind collecting device of

the proposed transducer element selection of lead zirconate titanate piezoelectric ceramics (abbreviated as PZT) [7],it is able to achieve the effective collection of it from different directions in the wind energy, in order to achieve the self powered micro power equipment.

## II. MECHANICAL SYSTEM DESIGN

Mechanical system is an important part of the whole device, it is directly coupled with the wind to carry out energy conversion, its structure design directly affects the energy conversion efficiency of the whole device. The mechanical system is mainly composed of a shell and a piezoelectric cantilever beam, the core of which is the piezoelectric cantilever, and the mechanical system is shown in Figure 1.

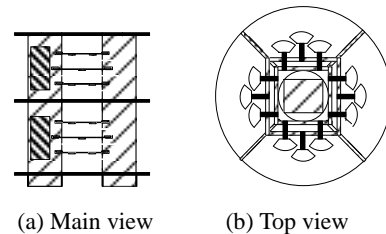


Fig. 1 Structure of mechanical system

### A. Housing

The shell thickness of 3.0mm by organic glass cutting, assembly, except for the connection, support, fixing and protection, but also play the role of the shell

fluid constraint; cylindrical shape, divided into horizontal clapboard and longitudinal clapboard, longitudinal clapboard and the horizontal clapboard is provided with a small groove, mutually embedded between the groove and the groove a shell. A transverse partition ring sheet structure 30.0cm outer diameter, 13.0cm, longitudinal baffle for rectangular sheet structure, the height of each layer is 10.0cm, three and four across the longitudinal transverse clapboard vertically staggered arrangement, the cylindrical space into the horn mouth unit eight angle is 90 degrees.

### B. Piezoelectric cantilever beam array

The piezoelectric cantilever beam array is distributed around the eight elements of the whole cylindrical device, and the piezoelectric cantilever array in each unit is arranged in the same arrangement mode. Only from a unit, a piezoelectric cantilever beam array consists of 5 piezoelectric cantilever beam, divided into three layers, the upper and lower layers are arranged in parallel two piezoelectric cantilever beam, the middle layer is only a place, but the distance from the center line of the upper and lower than the cylindrical laminated cantilever the beam from the circle centre line of the columns and the far distance, five piezoelectric cantilever top form a positive four pyramid structure, as shown in Figure 1 (b).

The piezoelectric cantilever beam is composed of an electrode, a piezoelectric ceramic sheet and a sector flexible beam. Two long strip electrode made of single-sided copper-clad plate by screw clamping and clamping, with fixed piezoelectric ceramics and the effect of the current leads. The generation principle of piezoelectric ceramic chip is based on the first kind of piezoelectric equation:

$$D = dT + \varepsilon^T E$$

$$S = S^E T + d' E$$

Where  $D$  is the displacement vector,  $d$  piezoelectric strain constant,  $d'$  is the transpose of  $d$  and  $S$  as the dependent variable,  $S^E$  as the elastic compliance coefficient,  $T$  stress,  $E$  field strength vector,  $\varepsilon^T$  dielectric constant[8].

The fan-shaped flexible beam selection of polyethylene terephthalate film (PET), the aluminum plate and screw clamp, which is tightly connected with the front end of the piezoelectric bimorph. Finite element analysis and optimization design of the use of

ANSYS model as shown in Figure 2, the effective size of the piezoelectric bimorph is 30.0mm long, 10.0mm wide and 0.7mm thick, fan-shaped flexible beam angle of 90 degrees, the radius is 25.0mm, thickness 0.1mm.

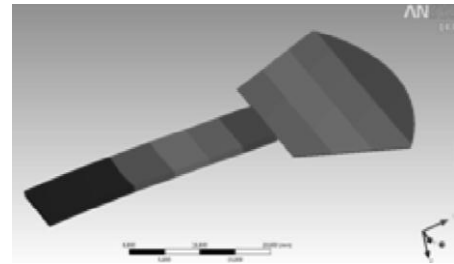


Fig. 2 Simulation model of piezoelectric cantilever beam

## III. CIRCUIT SYSTEM DESIGN

The circuit system is the function of each piezoelectric cantilever beam array to produce irregular AC power into DC power by various low-power devices can use, contains rectifier, DC-DC converter, parallel buffer and storage areas, its structure as shown in figure 3.

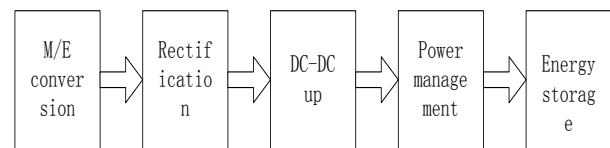


Fig. 3 Circuit system structure

### A. Voltage doubling rectifier and polymer flow buffer

The commonly used rectifier scheme has four kinds: half wave, Quan Bo, bridge and double pressure. Because the output voltage of the piezoelectric cantilever is small, the output voltage of the piezoelectric cantilever is effectively utilized, and the voltage rectification circuit is adopted in the two times [9], as shown in Figure 4. Compared with the bridge rectifier circuit, voltage drop smaller, two voltage doubler rectifier circuit and circuit for diode type SD103AWS Schottky diode forward voltage drop of VF is only 0.4V, can effectively reduce the loss of the rectifier circuit. Each piezoelectric cantilever beam is connected with a two voltage doubling rectifier circuit, and the irregular alternating current voltage is converted into a less pulsating DC voltage for subsequent circuit processing.

Considering the single piezoelectric cantilever beam current output capacity is limited, not up to the minimum requirements for the subsequent processing circuit, it will be all a bellmouthing unit of piezoelectric cantilever beam array output current



converged to the super capacitor, when starting voltage capacitor of the power accumulated to the subsequent circuit, and driving circuit operation. The output of a single two times voltage rectification circuit is connected with a super capacitor through the diode, and the charge flow in the super capacitor can be avoided effectively.

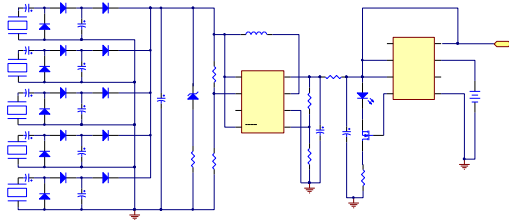


Fig. 4 System circuit diagram

### B. DC-DC boost and power management

When the circuit works, the voltage of the super capacitor at both ends of the lower reach 5V supply voltage of electronic system, so it needs to boost DC-DC circuit low voltage super capacitor at both ends of the pump up to constant DC high voltage. MAX1678 chip is a high efficiency, low noise boost type DC-DC converter, starting voltage as low as 0.87V, quiescent operating current is only 37uA [10], to meet the requirements of the proposed circuit power loss low. In addition, the MAX1678 has a fixed 3.3V with adjustable 2V-5.5V two output modes, can greatly meet the needs of the circuit. The DC-DC circuit with MAX1678 chip as the core, by adjusting the sampling resistance R4 and the resistance R5, the output voltage is 5.5V, at the same time, by adjusting the sampling resistance R2 and the resistance R3, the effective input voltage boost circuit for 2V.

Due to the limit of the input voltage of the MAX1678 value of +6.0V, in order to ensure the safe and reliable circuit, in between the super capacitor with DC-DC circuit parallel zener diode 1N4734, to prevent the super capacitor voltage continuous charging in long time under the condition of over voltage.

In order to collect the electric energy which is collected by the 8 units of the whole device, the electric energy can be stored in the lithium polymer battery effectively, and at the same time, it is necessary to introduce the power management link to avoid the battery charging and discharging. LTC4071 chip can be intermittent or continuous charging battery, charging current range of 550 nA ~50 mA, to provide

4.0V, 4.1V, 4.2V three kinds of floating voltage selection [11]. In addition, the chip has a low battery power loss function which is close to the zero current, and can effectively prevent the lithium battery from being damaged due to over discharge. As shown in Figure 4, connected with the LTC4071 chip ADJ terminal and VCC, programming BAT suspension output voltage is 4.2V; LBSEL is connected with GND, when the battery voltage is lower than 3.2V and VCC disconnect the battery; when the battery voltage reaches 4.2V, HBO output high level, the N channel MOSFET conduction the LED lights, alarm, and the formation of discharge channel, avoid overcharge phenomenon. The lithium polymer battery capacity of the device is 25mAh, which can meet the requirements of general application system.

## IV. APPLICATION SYSTEM DESIGN

By using the multi direction wind power collection device can supply power to the wireless data transmission system, to realize the data acquisition node energy. The wireless data transmission system comprises a plurality of data acquisition nodes and a base station, and the communication network is composed of a network [12]. For the convenience of the description, the system is composed of a single data acquisition node and a base station, as shown in figure 5.

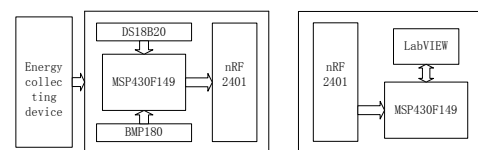


Fig. 5 Structure of application system

### A. Data acquisition node

The data acquisition node is composed of MSP430F149 microcontroller, DS18B20 temperature sensor, BMP180 pressure sensor and nRF24L01 [13]. MSP430F149 microcontroller will continue to pressure and temperature sensor real-time data readout, internally calibrated processing to meet the communication requirements after sent to nRF24L01, the data collected by the wireless data transmission module nRF24L01 to send to the surrounding space, for base station access.

### B. Data receiving node

The base station data receiving node is responsible for collecting the whole application system, under the

information data acquisition node and transmitted to the switchboard. The base station also uses the MSP430F149 microcontroller as the main control chip, which uses the interrupt working mode to read the data obtained from the nRF24L01 receiver in real time. The microcontroller will collect data through the UART serial number, and the computer using the LabVIEW development of PC communication [14], The whole system of data packets transmitted to the host computer display and storage, for the subsequent data analysis and research to prepare.

## V. DEVICE INTEGRATED TEST

In order to prove the practical application level of the device, the related test should be carried out. The design of the multi direction wind energy collection device is in kind as shown in figure 6. In laboratory conditions, the use of four simultaneous work of AFB0612EHE type axial flow fan, AS836 digital wind speed measuring instrument and GDS-2202A digital oscilloscope and other test equipment to build the system test environment.

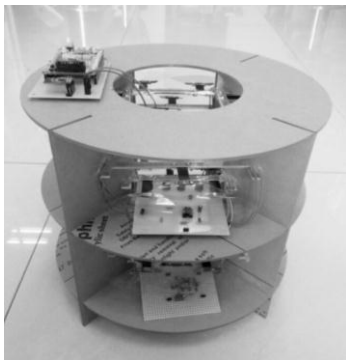


Figure 6 the real system

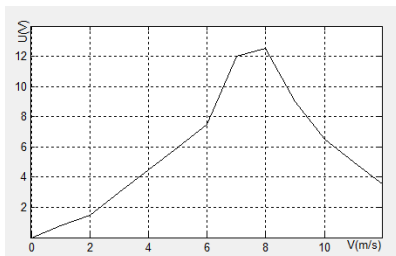


Fig. 7 Voltage peak change with wind speed

From zero to gradually increase the output power of the axial flow fan, the measurement of the AC voltage peak of the output of the single piezoelectric cantilever, and draw the corresponding change curve as shown in figure 7. According to the curve of the curve, it can be known that when the wind speed is

8m/s, the output voltage of the piezoelectric cantilever beam is the largest; when the wind speed is 6-9m/s, the piezoelectric cantilever beam is in an efficient working state. To reflect the current output capacity of one unit of piezoelectric cantilever beam array, to the piezoelectric cantilever beam array with 8m/s wind speed. Measured LTC4071 output voltage is 4.16V, slightly lower than the ideal value of 4.2V. The device works continuously 40min, can be filled with 25mAh battery. At the same time, the lithium battery is connected with the data collecting node, and the data acquisition node can work normally, and the temperature and the pressure value of the laboratory can be sent to the upper computer.

## VI. SUMMARY AND PROSPECT

Multi direction wind energy collection device is designed in this paper to simulate the natural environment in the laboratory, can effectively collect wind from different directions, meet the requirements and can be applied in the field of data acquisition system. In the near future, with the in-depth research of piezoelectric materials and piezoelectric cantilever beam and gradually improve the preparation technology, energy recovery efficiency will be multi direction wind energy collection device is designed in this paper to get a huge boost, thus pushing animal networking project to a new height, make people's life more intelligent and digital.

## References

- [1] Dittrich T, Belaidi A, Ennaoui A. Concepts of Inorganic Solid-state Nanostructured Solar Cells[J]. *Solar Energy Materials and Solar Cells*, 2011, 95(6): 1527-1536.
- [2] Wang Z Y, Leonov V, Fiorini P, et al. Realization of a Wearable Miniaturized Thermoelectric Generator For Human Body Applications[J]. *Sensors and Actuators A: Physical*, 2009, 156(1): 95-102.
- [3] Aladwani A, Arafa M, Aldraihem O, et al. Cantilevered Piezoelectric Energy Harvester With a Dynamic Magnifier[J]. *Journal of Vibration and*

- Acoustics, Transactions of the ASME, 2012, 134(3): 1-10.
- [4] DAI Xian-zhi, ZHANG Zhang. Study on Ambient Energy Sources For Self-powering Sensors[J]. Chinese Journal of Power Sources. 2012(03): 440-443.
- [5] XU Zhuo, YANG Jie, YAN Le, et al. Research Progress on Micro Vibration Energy Harvesters[J]. Transducer and Microsystem Technologies. 2015(02): 9-12.
- [6] LI Xiao-juan, LI Quan-lu, XIE Miao-xia, et al. New Headways and New Applications of Piezoceramics at Home and Abroad[J]. Bulletin of The Chinese Ceramic Society. 2006(04): 101-107.
- [7] LI Tao, PENG Tong-jiang. Research Progress and Development Trend of Lead Titanate Piezoelectric Ceramic[J]. Journal of Xiangnan University. 2004(02): 54-57.
- [8] MENG Qing-chun, CHEN Guang-zhu. Design of Self-Powered Wireless Sensor Network Node[J]. Instrument Technique and Sensor. 2012(07): 102-104.
- [9] DANG Zi-heng. Analysis of Charging and Discharging Process of Two Times of Voltage Rectification Circuit[J]. China Market Marketing. 2013(22): 30-31.
- [10] LIU Jun, TAO Jianping, LV Xiaolan .Key Environmental Factors Monitoring System of Low-power Greenhouse Based on WSN Technology[J]. Agricultural Science & Technology, 2016, 17(2): 449-452.
- [11] Rong Xun, Chen Zhi-min, Cao Guang-zhong. The Design of a Low-Power Circuit For Ultra-Low Energy Harvest[J]. Application of Electronic Technique. 2016(07): 42-49.
- [12] LI Yan, LUO Xu-ye. Research on Systems and Application Technology of Wireless Sensor Networks for Ocean Monitoring[J]. Ocean Technology. 2009(01): 8-11.
- [13] QIAN Cheng-hui, YANG Hui-ting, REN Tong-yang, et al. Real-Time Aerial Photography and Global Positioning System for A Quadrotor Design[J]. Journal of Jilin University: Information Sci Ed. 2015(04): 454-462.
- [14] SHEN Wen-yi, QIN Ning-ning, SUN Shun-yuan, et al. Gas Monitoring System Based on the MSP 430 and LabVIEW[J]. Journal of Jiangnan University: Natural Science Edition. 2012(02): 142-148.

# Design of intelligent refrigerator food management system based on QR code scanning

Zhang Bilan; Du Junqi; Zhao Zuo

(The College of Instrument Science & Electrical Engineering, Jilin University, ChangChun, 130022, China)

**Abstract**--At present, intelligentize become the trend of the development of household appliances. Home life can not be separated from the refrigerator, so smart refrigerator has good innovation, convenience and practicality. This project is based on the Android system, with SQLite database, 51 microcontroller, Bluetooth and other knowledge, to design and implement smart refrigerator food management system based on QR code scanning. It can not only scan QR code to record food information, generate food list, but also have the function of reminding expired items, producing a shopping list and menu. In addition to combining with STC89C52 and HC-05 Bluetooth module to realize Bluetooth communication, temperature and humidity data can be transferred. The system is simple, low-cost, feature-rich, and has a certain market development potential.

**Key words**--Android SQLite database STC89C52 Bluetooth communication

## I. INTRODUCTION

WITH the rapid development of people's living standards, the pace of life continues to accelerate. The refrigerator is more and more important for our lives. Large quantities of food placed into the refrigerator, to a large extent, brings convenience to people's lives. However, along with the increase of stored food in the refrigerator, it is very likely that food stored for a long time is ignored, which can bring about the following two aspects: first, eating expired food could pose a threat to our health; second, facing disordered food in the fridge, we can't accurately know all the food needed to purchase.

To solve these problems, after the study, we developed an intelligent refrigerator food management system based on the QR code scanning, aiming at making refrigerator become manager rather than container. This application will provide convenience for the people who are busy working and studying.

The overall operation of the system is as follows: first, by scanning the QR code, food information can be inputted into the system, which is convenient, quick, simple and feasible. Secondly, establishing a SQLite database, add information to the database. Finally, through operating database, generate food list.

In addition, there are statistical information of expired food, including the name and days overdue, which will be clearly presented to the user. The system

will deal with the expired food or non-existent food. They will be removed from the "food list" then join the "shopping list" in order to remind users with tips in shopping. With the development of science and technology, the first way people get information has already become the network rather than the paper books. In order to adapt to this transformation, help more and more people more efficiently use the refrigerator, digital products gradually replaced a variety of paper-based materials. The system collects lots of electronic menus, including four major cuisines, Home Dishes, cold dish and so on. In addition, DHT11 sensor is used to simulate to collect the refrigerator's temperature and humidity data. Through Bluetooth communication between the HC - 05 Bluetooth module and APP, the APP can receive and display the temperature and humidity data.

Home life can't be separated from the use of refrigerators, and intelligent home appliances are also the trend of the development of electrical appliances. From scanning code, checking the storage situation, reminding expired food, recommending recipes to generating food list, these functions are necessary in daily life. These little bits of functions are an important step towards our ideal life.

## II. OVERALL DESIGN

Replying on Android Studio development software, we build the food management system based on

scanning QR code. First of all, using ZXing open source project to achieve scanning and parsing two-dimensional code, get food information; through the operation of the SQLite database, generate a list of food and remind expired food; reading and writing files based on the the SD card make implementation of the recommended recipes possible; using STC89C52 as the core, combined with the HC - 05 Bluetooth module, transfer refrigerator' temperature and humidity data that sensor DHT11 collect to tablet through Bluetooth communication. The function module of the whole APP is shown in Figure1:

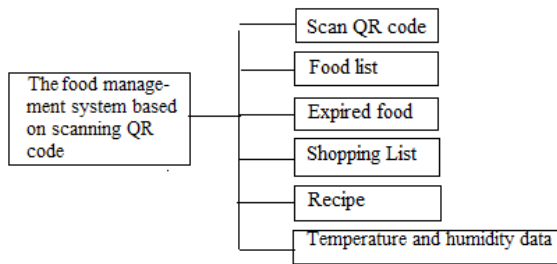


Fig.1: Structure of system function

III. MAIN INTERFACE DESIGN

The main interface consists of 4 regions. Three regions on the left side of the interface from top to bottom in turn are as follows: receiving a two-dimensional code scan results, user operation function button area, temperature and humidity data display area. The right interface region is a FrameLayout, according to the 4 function buttons to display the relative contents. UI interface is as shown in figure 2:

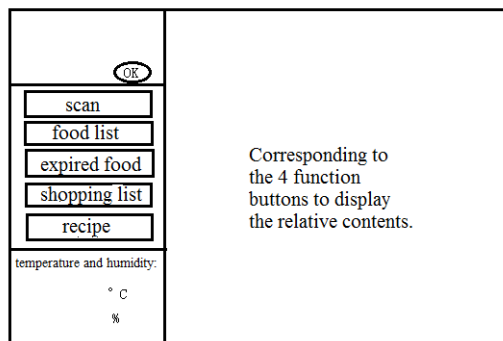


Fig2: APP main UI

Food list interface is as shown in figure 3:

|                                       |   |
|---------------------------------------|---|
| QR                                    | Food category: Seafood<br>Food name: prawn<br>Production date: September 10, 2016<br>Shelf life: 7 days<br>Due date: September 17, 2016           |
| scan                                  | Food category: meat<br>Name of food: the bacon<br>Production date: on September 10, 2016<br>Shelf life: 60 days<br>Due time: on November 10, 2016 |
| food list                             |   |
| expired food                          |   |
| shopping list                         | Food category: Vegetables<br>Name: winter melon<br>Production date: September 10, 2016<br>Shelf life: 5 days<br>Due date: September 15, 2016      |
| recipe                                |   |
| temperature and humidity:<br>° C<br>% | Food category: Milk<br>Food name: shi tian yogurt<br>Production date: September 10, 2016<br>Shelf life: 10 day<br>Due date: September 20, 2016    |

Fig3: Food list

Other interface to which other functions button corresponding is similar, no longer displaying.

To realize the interface, first, build resource file under the res directory in a layout of the Android studio, second, register the listener in MainActivity, and then add a click event. Through these steps, UI interface can be realized.

IV. DESIGN AND TEST OF EACH FUNCTION MODULE.

A. Get information by scanning QR code

QR code, the two-dimensional code, according to the concept of computer internal logic "0", "1" bit stream, use a plurality of geometric shapes corresponding binary to represent the text value of information.[7] Compared to the bar code that can only store number, its application is more extensive. Food' two-dimensional code cards include food category, name, production date, shelf life, expiration date and other information.

Scanning code, decoding and other work is tedious. This project, directly download the ZXing open source project on the Github open source website. In the application, citing it as the third party libraries, then the QR code scanning can be realized in this project.

B. The establishment of SQLite database

The Android system integrates a lightweight database SQLite, which is an embedded database engine, specifically applicable to the limited resources of the equipment to read moderate data.[1] Android provide SQLite Database object represents a database. Once the application accessing to the SQLite Database object, you can manage the database. The database structure is shown in Table 1 :

Table1: Structure of database

| _id | Food category | Food name    | Production date    | Shelf life | Due date           |
|-----|---------------|--------------|--------------------|------------|--------------------|
| 1   | Sea-food      | prawn        | September 10, 2016 | 7 days     | September 17, 2016 |
| 2   | Vegetables    | winter melon | September 10, 2016 | 5 days     | September 15, 2016 |
| 3   | meat          | bacon        | September 10, 2016 | 60 days    | November 10, 2016  |

### C. Add food information

The input of food information is to add food information to the database. To do this, first you need to extract text with a newline branch, in turn inserting into the database. How to selectively extracted data, there are two solutions:

The first is to manually enter the required information, selectively copying needed items, and then adding to the database;

The second way is through `split()` method, giving a separator, taking out the required information, storing in the `ContentValues` variable in the form of the key-value; Binding listener for the button, setting the click event, insert the information in the database, to complete the entry of food information.

Two methods have their own advantages and disadvantages: although plan one relatively tedious, goes against the wish of freeing hands. But you can easily manage the food without two-dimensional code. Plan two is simple and convenient, only need to click the OK button, the background dealing with data, it can automatically add the necessary information to the database. But for food without a two-dimensional code, the management system won't have any records.

Although the two-dimensional code label is not yet universal, but we can't deny that it is the future trend of development, which will play an increasingly important role in life. For this reason, the research of plan two is full of necessity.

### D. Generate food list

`ListView` is a UI component that is best suited to present a food list. The messenger connecting database with `ListView` is the `SimpleCursorAdapter`. `Adapter` is the interface connected to the back-end data and

front-end display. It is an important link between the data and UI (View). In the common View (`ListView`, `GridView`) and other places it is necessary to use `Adapter`[5].

`SimpleCursorAdapter` can be applied to `ListView` containing simple text. It needs UI field and match them with the id of the UI. When the program continues to insert data, `ListView` can real-time present information of the underlying database. Through the database query operation, we can get food information. Food list can be generated when combining `ListView` with `SimpleCursorAdapter`.

### E. Expired food statistic

For expired food' statistic, keeping the current time and due time for subtraction, you can real-time judge situation about food expiration.

By the method of `format.format()` get the current time. By querying database, take out of the due time. The problem is that two `String` type data can't compare the size. To this end, we propose the following solutions: first convert `String` type into `Date` type, and then through the `getTime()` getting the `int` type data.

`getTime()` returns the current `Date` object time values used to use local time. The time values mean the number of milliseconds since midnight on January 1, 1970 to the current `Date` object, subject to Greenwich time [2].

### F. Generate shopping list

For expired food, or already eaten food, it will be deleted in the food list, at the same time, automatically added to the purchase list.

In view of this requirement, we first made the following attempt:

Data transfer is performed while the system responses to the delete operation. Two fragment transfer data through by the bundle. However, there is a problem in the process of execution: whenever click on the purchase list button, the running program will stop running. APP flash back. The question is: in addition to the bluetooth module, the other part is equivalent to on the working mode of a single thread. Two different buttons on the different layout operating the same fragment at the same time, is bound to be a problem.

As a result, we have adopted the following methods: after deleting food in the list, don't transfer data between fragments, but write files using the data in the

form of the input stream. Main interface' purchase list button open the fragments, reading the file content at the same time.

There are problems when testing the second programs: the contents of the file can only be added but can't be cleared. Even if you delete the EditText' content, you can't save the file. Therefore, when you open the application again, there will still be the last record. To solve this problem, when the main interface button open the fragment. it should open the file input stream with `MODE_WORLD_WRITEABLE` mode. In this way, the empty shopping list button, can play a role of clearing the document.

#### G. *The realization of the recipe*

Java provides a complete set of IO flow, including `FileInputStream`, `FileOutputStream`, etc. Through these IO streams, it can be very convenient to access the contents of files on the disk, Android also supports in this way to access files on phone memory. Set up electronic recipes in SD card. These recipes contain four major cuisines, homely cold dishes, seafood and so on. It can satisfy people's needs to a certain extent. The system also provides the user with personalized extension function. If the user wants to add other recipes, he just need to add files to the menu folder.

Another advantage is that the system has good man-machine interactive. Users can according to their needs, personalized modify parts of the system function, make it more adapted to the different family.

If an application need to read and write files on the SD card, it must add the application permissions of reading and writing SD card on the manifest file.

Referring to mobile phones file manager, the file can be presented in the form of `ListView`. First create a List collection, whose element is `Map`. Then create a `SimpleAdapter` and configure `Adapter` for the `ListView`. In this way, the recipe will visually be presented on the UI in the form of `ListView`. By this way, the classification is more clear and the operation is more convenient

#### H. *Acquisition, transmission and reception of the temperature and humidity data.*

The project using `DHT11` and `STC89C52` MCU to simulate to collect the temperature and humidity data of the refrigerator, through the `HC-05` Bluetooth module, communicate with tablet. APP open Bluetooth, and open a new thread, to receive the temperature and

humidity data. The principle of the method is clear, and can reflect the internal temperature and humidity data of the refrigerator in real time.

The Android platform provides the Bluetooth API to realize communication between Bluetooth devices. Communication between Bluetooth devices including four main steps: setting up Bluetooth device, finding the local area network possible or matched equipment, connecting device, transferring data between devices. Connecting equipment needs `UUID`. So-called `UUID`, is used to match, whose full name is Universally Unique Identifier, is a 128-bit string ID, for a Unique Identifier. `BluetoothSocket` class: representing a Bluetooth socket interface (similar to the socket in TCP), it is the the connection point of communication between the application' input or output stream and other Bluetooth devices.[1]

When carrying out initial tests, APP can't receive the transmission data of Bluetooth module. Through the analysis there are two possible errors: first, bluetooth source part is wrong. When this APP is connected to the computer serial port assistant, it could receive transmission data, therefore, excluding this possibility. Second, Bluetooth module is set wrong. `HC-05` is master-slave one bluetooth module. Here it is used to receive the data sent by the microcontroller, playing the role of the slave. Therefore, it should be set to the slave' state. It turns out to be the case that it can be normal to send and receive data. After modification , problem is solved.

## V. CONCLUSION

The project is based on the Android system development. Combined with `51 MCU` and Bluetooth communication, we designed an intelligent refrigerator food management system based on the QR code scanning. We provide the functions such as scanning QR code to record food information, generating food list, reminding expired food, automatically generating purchase list, displaying temperature and humidity data. At the same time, there are electronic recipes. After testing, it can be used fluently and response quickly. Besides, it has a great convenience and practicability.

## References

- [1] Li gang. Crazy Android notes [M]. Beijing: Electronic Industry Press, 2015:1-412
- [2] Kathy Sierra & Bert Bates. Head First Java [M]. O`Reilly TaiWan company, eds. Beijing: China Power Press, 2015:27-165
- [3] Song Changlong. Fundamentals of Computer [M].Beijing: Higher Education Press, 2011:142-166
- [4] Li Xinghua. Java classical development (teacher Forum) [M].Beijing: Tsinghua University press, 2009
- [5] Wu Yafeng, Suo Yina. Android core technology and examples' explain [M]. Beijing: University of Electronic Industry Press, 2010
- [6] Yang Yunjun. Design and implementation of Android [M].Beijing: Mechanical Industry Press, 2013
- [7] Lan LongHui, Qiu Rongzu. Application of two dimensional code technology in agricultural products logistics tracing system [[J/OL]].Logistics engineering and management, 2013
- [8] Jiang Shen. Design of intelligent refrigerator informatization based on Internet [[J/OL]].Internet Of Things Technology, 2011
- [9] Tan Zhen. Intelligent control technology and development trend of domestic refrigerator[[J/OL]]. Home Appliances Science And Technology, 2000
- [10]Cai Juntao. Intelligent refrigerator embedded food management system [[D/OL]]. Master's Thesis, 2008
- [11]Zhao Zixian. Design and implementation of intelligent refrigerator food management system[[D/OL]]. Master's Thesis, 2015



# Research of intelligent vehicle lock based on RFID

ZHANG Ruo-xi; SHI Jia-qing; ZHU Wu-fang

(College of Instrument Science and Electrical Engineering, JiLin University, Changchun, 130012, China)

**Abstract**--Now the use of bicycle lock is complex, as for short distance journey ,it can not be a smart choose. The paper proposes a smart car lock based on SCM, which locks users through the card identification, to determine whether the cardholder is the true owner, so as to make the corresponding instructions. Solar power is used for the lock energy. The experimental results show that the vehicle lock can identify the identity of the cardholder by the IC card, and realize the automatic opening and closing of the vehicle lock, and the realization of the intelligent vehicle lock. Apart from these, the lock also has an important function, if someone else amid to move the bicycle deliberately, the lock will be issued a sharp warning sound. Compared with the traditional bike lock, the use of the lock is more convenient, and it can achieve the goal facilitating the travel.

**Key words**--RFID Bicycle lock Automation Intelligent

## I. INTRODUCTION

THE form of lock is soft and U type lock chain, the use of universal chain is complex, users will spend a lot of time to roll the lock the around on the bike,as for short distance travel is very inconvenient. Apart from this ,they do not have anti-theft alarm function, so the bicycle will lost . After investigation and research, at present, the research on the intelligent bicycle lock is in the front of the technology is lock8, but because of the high cost of lock8, it is not widely used at present. IC card is mainly used in microelectronics technology, the large scale integrated circuit chip embedded in a plastic card, mainly used in the field of identity cards, banking, transportation and other fields, the use of simple and convenient [1-3].

In order to solve the above problems and change the traditional car lock is used, this paper designs a kind of intelligent car based on SCM lock, the user receiving device and IC card carrying integration, without the need to manually lock to lock and unlock the lock, card users open automatically stop after the credit card closed [5]. Considering the long period of bicycles in the outdoor, by the characteristics of the sun exposure, the use of solar batteries for car lock power supply. In order to realize the intelligence of the bicycle, the bicycle lock is more convenient to use.

## II. INTELLIGENT VEHICLE LOCK BASED ON MCU

The project design of the smart car lock based on single chip control module, mainly through the identification of IC card UID on the user to determine the identity of the user is correct or not, at the same time according to different users to identity execute different instructions, so as to realize the intelligent lock and improve the safety and reliability of the lock. Then according to the use of the car lock and the use of the environment to carry out other functional components of the design, the use of clean energy vehicles lock, so that the whole car lock more environmentally friendly.

## III.SYSTEM DESIGN

The system takes the ARM chip as the main body, and realizes the automatic recognition function of the vehicle lock by combining with the radio frequency card module. This design mainly includes the main control module, the card module, the display module, the power module, the mechanical structure module. Figure 1 for the overall block diagram of the vehicle lock.

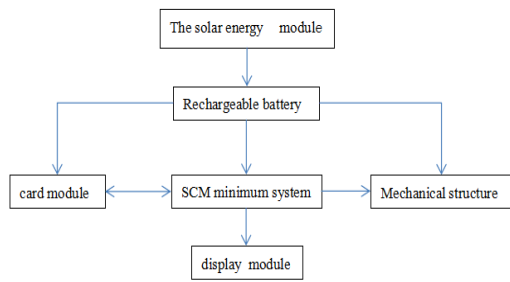


Fig.1 System structure diagram

The main control part controls the whole bike lock to work, according to the cardholder by IC card to determine the identity of users, according to different user identity, judge whether the lock unlock instruction execution, while UID display on the display screen, in addition to the buzzer and LED have corresponding reaction. The entire system is required to work in the 12V voltage, taking into account the environmental issues of the bicycle, choose clean and environmentally friendly solar panels as a power source, but the solar panel by the weather and light intensity influence, so choose the rechargeable battery charging by solar panels, and the rechargeable battery of the system to provide a stable voltage plan. For the alarm part, the acceleration sensor is used to judge whether the bicycle is moved or not, so as to realize the alarm.

#### IV. THE DESIGN OF HARDWARE CIRCUIT

##### A. Master control module

This design is based on the enhanced STM32F103C8T6 as the main chip [13] STM32 comes with a 72M clock, 20KRAM, 64KB storage space of the program, with a 12 bit A/D converter, timer, I/O port and communication port, strong practicability, can work normally in the range of 2-3.6V, and the lowest power consumption in the current market, so STM32 is a very good choice for the design.

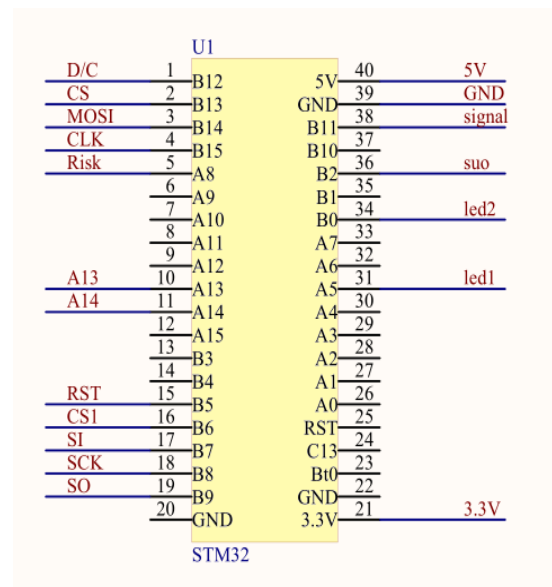


Fig.2 Main control module circuit

##### B. Power module

The whole car lock system needs to be stable 12V power supply, so the use of rechargeable 12V polymer lithium battery, with a higher safety performance, more stable chemical properties. Considering the long-term lock outside, thus it can use the solar cell batteries, lithium batteries due to high requirements on charging power supply, so the LM358 and XL4005E1 chip module for voltage regulation, so as to realize charging function, make the design more environmentally friendly [4].

##### C. RF card reading module

The RF card module adopts non-contact card reader FM1702SL[7]. FM1702SL high degree of integration, for the external wiring requirements of small, wide operating range, maximum up to 10cm, internal encryption, including a programmable timer, an interrupt processor, EEPROM 512byte and 64 bit FIFO[8-10]. FM1702SL hardware connection circuit is simple, compared to other RF communication module, and easy to use [6]. Figure 3 for the card module interface.

The IC card in the form of cards, with micro chip embedded in a certain standard of kika. Combined with IC and RFID technology RF card, can achieve non-contact credit card work [11]. The electromagnetic wave emitted by the radio frequency reader through the LC oscillation circuit and charge accumulation, as a power supply to other parts of the power supply, so as to achieve the RF card read and write operation [12].

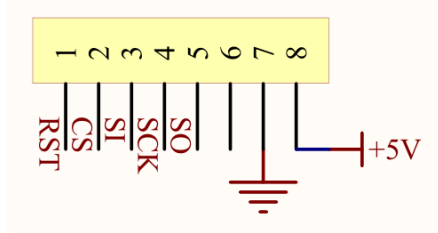


Fig.3 Card module circuit connection diagram

*D.Mechanical structure module*

The mechanical structure adopts electromagnetic lock, the voltage is 12V, and the working voltage of the system is in line with the working voltage of the system, and the power supply module is not used. In order to reduce the power consumption of the whole system, the choice of the car lock power is only 5.2W, telescopic range 20mm.

*E.Display module*

Display module using OLED12864 module, the OLED12864 does not require a backlight, low power consumption, saving IO, built-in driver chip, which can realize Chinese man-machine interface and communication with the 3 line SPI, compared with the LCD module, in a fixed small volume can be realized under the condition of high resolution

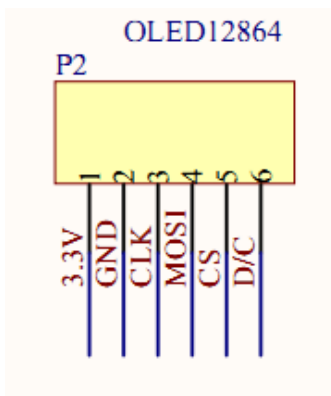


Fig.4 LCD module circuit diagram

*F.Anti-theft alarm module*

Ordinary bike lock does not have alarm function, can not guarantee the safety of car lock. In this regard, the car lock using acceleration sensor ADXL202[13]. By the acceleration sensor to detect the peak acceleration, the output duty ratio is proportional to the speed and, analyze the main control logic, judgment is stolen bicycles, if identified as stolen, the alarm will make a sharp sound detonation.

V .SOFTWARE DESIGN

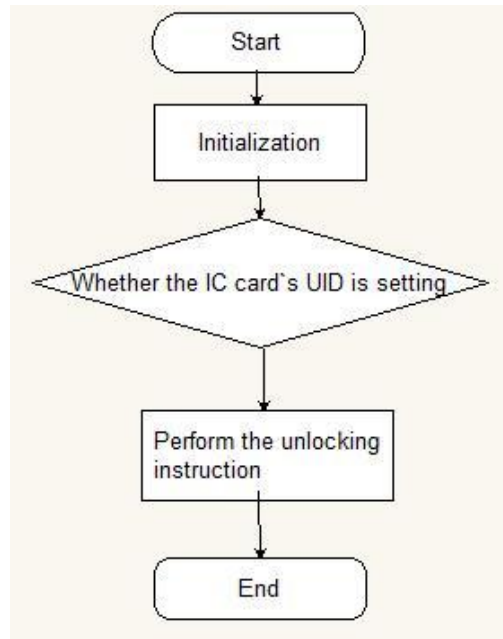
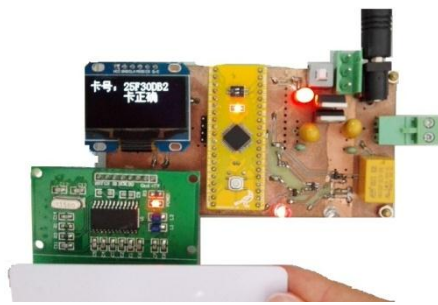


Fig.5 Card module program flow chart

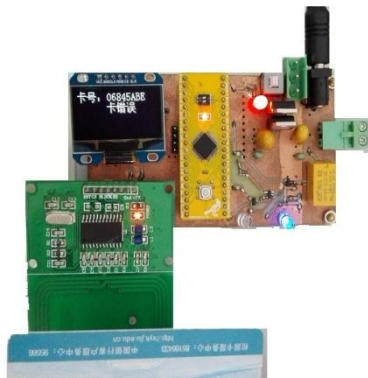
The first initialize registers and OLED of the system, so that each part can work normally when the car corresponds to the UID for the recognition of single phase to determine whether the correct UID, if the right to lock out will unlock instruction. Display indicator lights flashing, buzzer issued a regular sound, display the card number and card correctly. Otherwise, the wrong display lights, buzzer alarm sound, the display screen also shows the card number, but at the same time display card error.

VI.EXPERIMENTAL RESULTS AND ANALYSIS

The results show that, according to the different settings of the program, the car lock can identify different IC cards, but also can identify more than one IC card, display the corresponding card number. If the identity of the user to correctly display lights alternating red and green flashes, buzzer regular sound drops, show the cardholder identity right, display card number and card right; on the other hand, the blue light display display, buzzer sharp noise, can realize alarm function, the user ID is not correct, the display still shows the corresponding number, but that card error.



(a)The correct effect of IC card



(b) The wrong effect of IC card

Fig.6 Credit card effect under different circumstances

#### The main experimental parameters

##### 1).Working power

Maximum output voltage of solar panel: 15V  
 Polymer lithium battery output voltage: 12V  
 Polymer lithium battery charging voltage: 12.6V  
 Rechargeable battery capacity: 5500mAh

##### 2).Appearance size

Bike lock: 140X30mm  
 Key length: 20mm  
 Solar panel: 240X160mm  
 Credit card area: 14X12.5mm

##### 3).Card reading distance

Credit card sensing distance is 7.0~7.5cm

##### 4).Power consumption

Bike lock power: 5.2W  
 Total power of the system: <5.4W

## VII.THE DISCUSSION OF RESULTS

The design will be carried by the client receiving device and card integration, users without any operation, the lock according to the set procedures according to the different situation to achieve open and close the lock of the car, while the identity of different users with the corresponding reaction. Taking into account the use of car lock environment, the use of

solar cells and rechargeable batteries for the car lock power supply, not only to solve the problem of car locks, but also to make the whole car lock more clean and environmentally friendly. The method is simple and the cost is low, and it provides a feasible and easy operation scheme for the intelligent bicycle lock. So for the daily needs of the use of the card is very convenient for college students, and we believe that the future will be suitable for many occasions, can be extended to the masses.

To change the way of traditional bike lock, solve common bicycle lock complex, is not conducive to a short trip, anti-theft function is poor, problems can not be timely alarm, this paper presents a new type of car lock, intelligent embedded system and non-contact RF communication technology to realize the whole car lock, car lock more intelligent, more convenient, more security in a timely manner, so as to ensure the safety of property owners, has very high practicability, is suitable for the majority of the crowd.

## Reference

- [1] XU Xia-li. Wireless communication principle[M].Beijing: The Peking University Publishing House.2014
- [2] WANG Wen, Design of A New Type of Vehicle Anti — theft Alarm Positioning System[D].North University Of China. Control Theory and Control Engineering.2013
- [3] FAN Yao. The practice of campus card system[M].Beijing: The Chinese People's Public Security University press.2007
- [4] YANG Su-xing. Analog electronic technology based on simple tutorial[M].Beijing: Higher Education Press.2008.4
- [5] Hussain Almassawi & Marin Myftiu;Hussain Almassawi. E-bike ncycle.[U] 2014.P2
- [6] JIA Jiang-ye.Design and implementatio of the experiment platform iot. Beijing University of Posts and Telecommunications. 2013
- [7] PAN Shao-ming, LUO Gong-kun, LAO You-lan.

- Design of RFID System Based on WSN[J].  
 Electric Information and Control Engineer,  
 2012(06):86-87.
- [8] Qi W K, Yu W D. A novel operation mode for  
 spaceborne polarimetric SAR[J]. Science China  
 Information Sciences, 2011, 54(4):884-897.
- [9] LU An-xing. Analysis and Design of Campus  
 Mobile One-Card System[D]. Xiamen  
 University,2014.
- [10]ZHENG Chuan-tao, MA Chun-sheng, YAN xin et  
 al. Manufacture tolerance analysis and control for  
 a polymeron-silicon  
 Mach-Zehnder-interferometer-based electro-optic  
 switch[J]. [11] Editor.The Differences and  
 Application Fields of RF Card, IC Card and  
 Magnetic Card[J]. Interactive  
 Space.,2008(6):67-69.
- [11]LING Zhen-bao,LI-Jiaoyang,PIAO-Guanyu,et  
 al.The Design ang Implementation of Attendance  
 System Used in Classroom Based on Radio  
 Frequency Identification Technology[J].Journal of  
 Jilin University:Information Science Edition,  
 2013, 31(05):470-476.
- [12]PAN Rui-yun,NIU Guo-zhu.Design of embedded  
 vehicle-mounted pre-warning system[J].Modern  
 Electronics Technique.2013

# Research of Wireless Remote Video Surveillance System Based on FPGA

Wang Ning; Fan Meng-xuan; Wang En-hui

(College of Instrumentation & Electrical Engineering Jilin University, Chang chun, 130022, China)

**Abstract**--In view of the long distance radio video monitoring system has dependence on the internet so far, therefore, using environment limited. This project has developed a kind of radio video monitoring system which is in car and can working in the environment without network, in order to solve the problem. This system controls the car and camera's movement and position through the microcontroller by radio so that we can get the maximum visual angle, at the same time, the system collects image information in the surroundings use the camera OV7670 driven by FPGA, transfer the video signal to receiver in the 1.2GHz band in order to display the video on the host computer. Test shows the car runs stably, can monitor surroundings in narrow space, transfer video data by radio successfully, with a clear and stable picture, and a long distance. This system's transfer distance is up to 25M indoors and 80M outdoors.

**Key words**--radio video monitoring car; FPGA; 1.2GHz; microwave communication

## I. INTRODUCTION

WITH the development of modern technology and progress, the observation and detection of hazardous environment is no longer directly involved in personnel, but by controlling the mobile wireless video monitoring system[1] to realize the observation. This system can not only detect in hazardous environments, but also observe the environment of limited space. It reduces the damage caused by the direct observation of the hazardous environment, and to carry out effective real-time video image transmission in harsh environments[2-4].

Traditional video surveillance systems need complex connection lines, resulted in waste of resource[5]. It also has certain requirements to the installation environment, and monitoring range will be subject to the camera installation location restrictions, existence blind area, there is no way to carry out a comprehensive monitoring of multiple perspectives[6-7] the mobile wireless video monitoring system solve the above problems, by controlling the movement of the moving carrier and the rotation of the camera, it realizes a full range of monitoring[8], and the control signal and video data in the system are transmitted in a wireless manner, expand the scope of application, widely used in all walks of life[9].

At present home and abroad, there are mainly two kinds of moving carriers, which are remote control car and airplane. The use of wireless way is also divided into two kinds, one kind is the wireless transmission mode of connection network, one of the most common is WIFI[10], the other is wireless transmission mode of

non connection network, it includes Bluetooth Technology[11], ZigBee Technology[12], various frequency band wireless transmission technology, etc. The rapid development of wireless network technology[13] leads to the low utilization rate of the second methods, but in a non network environment, this method shows its necessity. This design is aimed at no network environment of video surveillance, choose a caterpillar vehicle to carry, control algorithm is simple and can be stable control, small size of the CMOS camera used, mobile flexible, wireless transmission of signals using 1.2GHz band, transfer farther than Bluetooth and ZigBee mode, greater amount of data, Penetration stronger.

## II. SYSTEM DESIGN

The system is divided into three parts in the physical space: Vehicle, wireless remote control and receiving display part, each part of the power supply for its. The system block diagram is shown in Fig. 1.

The vehicle part mainly includes the FPGA master module, the car driving module, the wireless remote control receiving module and the wireless video transmitting module. The wireless remote control part mainly includes the key control and the wireless remote control transmitting module. The display part of the host computer mainly comprises a wireless video receiving and display module.

Within visual range, According to the observation of the human eye to the environment, through the wireless remote control of the car movement, including left, right, forward and backward. When the human eye is unable to observe the position of the car, we control

camera capture image signal, through wireless transmission to the receiving end, according to the received image to control the movement of the car, we can according to the actual needs of the location in the right location, and then control the steering gear. adjust the camera angle, in order to carry on the detailed observation to the specific position.

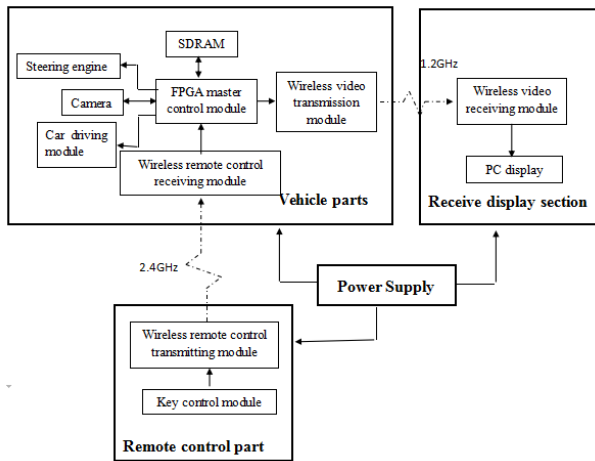


Fig. 1 System chart

### III. SYSTEM HARDW DESIGN

#### A. FPGA Master Control Module

FPGA main control module has three main functions, the first is to control the tracked vehicle, the second is the localization of the steering gear, third is driving head, and image acquisition of camera. In order to ensure the running stability of the vehicle, the track vehicle is selected as the vehicle body, and the L298N module is used to drive two DC motors to control the movement of the vehicle. For the observation of large scope, this system uses the steering platform to adjust the orientation of the camera, the size of the camera is small, weight is very light, required torque is relatively small, the power of steering gear is low, which is easy to reduce the overall power consumption. The system uses the CMOS digital camera OV7670, simulation volume is much smaller than the analog camera. Installation is convenient as to achieve multi angle rotation, the collection of video quality can meet the needs of the use, excellent cost performance, suitable for the system to use the environment.

#### B. Wireless Video Transmission Module

The wireless video transmission module includes a transmitter and a receiver. Transmit analog video signal to avoid the quantization error in the transmission of digital signals. Compared to the digital signal transmission, analog signal has a high fidelity, the received signal with respect to the acquisition signal distortion is less, at the same time, the transmission rate

requirements are higher. The system uses the 1.2GHz band, to avoid the congestion of the 2.4GHz band, the use of the bandwidth is relatively wide, the transmitter has a large power 5W, can be carried out at a higher rate of data transmission. At the same time, compared to the 2.4GHz frequency band, the low frequency band has stronger diffraction phenomenon, so it has stronger penetration. The module has the advantages of small size, high power, and the use of shielded enclosure package, greatly enhance the anti interference performance.

#### C. Wireless Remote Control Sect

Wireless remote control mainly has two parts, one part is the key control circuit, and the other part is the wireless remote control transmitter module. The control circuit uses 51 single chip microcomputer, through judging the input key value to produce the different eight position signals, carries on the transmission through the wireless transmission module. Its circuit diagram is shown in Fig. 2.

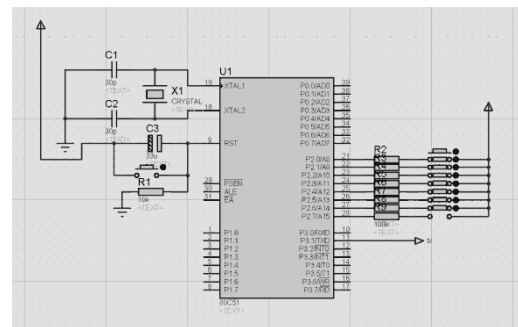


Fig. 2 Schematic diagram of remote-control circuit

The output in Figure 2 is the serial port TXD, which is used to connect the receiver pin of the wireless transmit module RXD. Eight buttons to control the car forward, backward, turn left and turn right and control the camera up, down, turn left and turn right.

The wireless remote control transmitting and receiving module of the system uses the wireless module based on the NRF24L01 chip, which is the same, and is used for the wireless transmission of the serial control signal.

NRF24L01 is a kind of radio frequency chip which works in the 2.4GHz frequency band. The serial communication interface of the wireless module with the TTL level, and support a variety of baud rate. When the SET pin is low level, users can set ID, baud rate, channel module and space velocity parameters. Before use, the corresponding modules should be matched to the same value as the ID and the channel, after the completion of the SET pin to maintain a high level, in order to carry out the signal transmission.

### IV. THE DESIGNING OF CONTROL PROGRAM

The control procedure is mainly divided into two parts, the first is the wireless remote control program, which is used to generate the control signal of the track vehicle and steering gear;the second is the FPGA main control program, its function is: (1) according to the received signal generation control track vehicle operation and steering gear rotation of PWM wave, (2) real-time acquisition of image data and the cache and output.

*A. Wireless Remote Control Program*

The wireless remote control program generates 25 control signals, each of which is composed of eight bits of data. The eight bit output and its corresponding event of the most basic 9 states as shown in Figure 1.

The states shown in Table 1 can only control the car or steering gear,in order to realize the control of both.We can match the status of car and the status of steering gear,"Or" operation of the corresponding data to get a new eight bit data, and then the serial output.

TABLE I

EIGHT BIT CODES AND ITS CORRESPONDING EVENTS

| the eight bit data of Serial transmission | Corresponding event        |
|---|----------------------------|
| 0000 0000                                 | No operation               |
| 0000 0001                                 | Car forward                |
| 0000 0010                                 | Car backward               |
| 0000 0100                                 | turn left.                 |
| 0000 1000                                 | turn right                 |
| 0001 0000                                 | Horizontal rudder Upward   |
| 0010 0000                                 | Horizontal rudder Downward |
| 0100 0000                                 | Vertical rudder turn left  |
| 1000 0000                                 | Vertical rudder turn right |

By getting the key information,Through the serial output corresponding to the eight bit data,and using wireless remote control transmitter module to launch.

Its program flow chart is shown in Fig. 3.

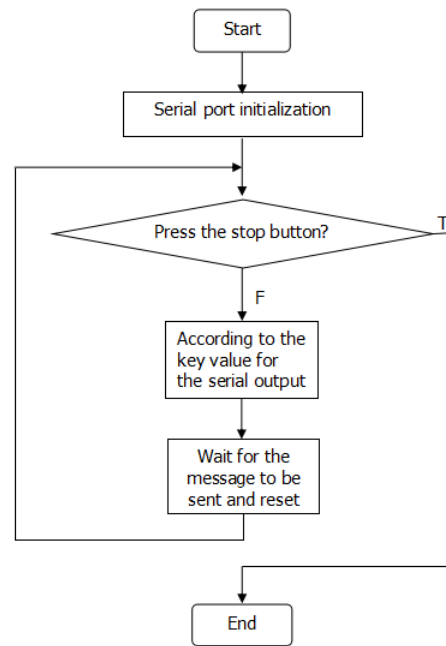


Fig. 3 Program flow chart of wireless remote control

*B. FPGA Master Control Program*

FPGA master program includes the drive of the car, the steering platform and the camera ,buffer and output of video data.Through the wireless remote control receiving module, receiving the remote part of the transmission of the eight bits data, according to the eight bits data obtained to judge the event which is should be performed, to control of the car and steering gear.The flow chart of the control car and steering gear is shown in Fig. 4.

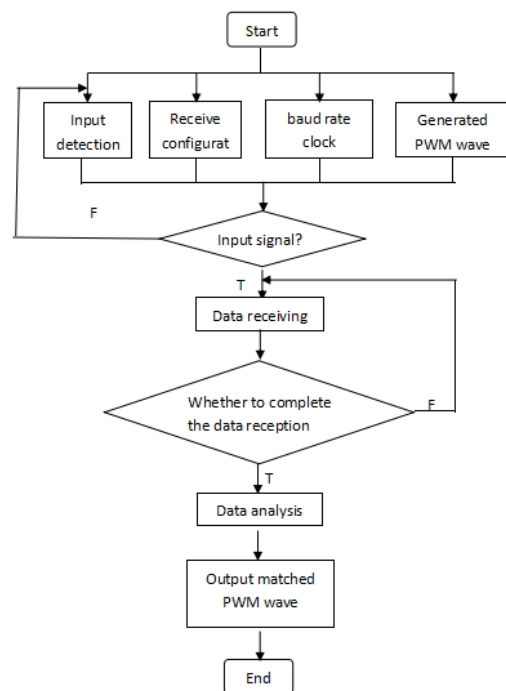


Fig. 4 Program flow chart of FPGA control

*C. Camera Driver And Image Acquisition Program*



Camera driver is for the initialization, the concrete content includes three parts: (1) implementation of the clock control module of the system, the configuration of the FPGA system clock. 25MHz clock is generated by the clock frequency of 50MHz, and it is used as a working clock as a camera; (2) According to the Data Sheet of OV7670, the camera working mode and the output form of the various registers can be set; (3) According to the agreement to set the I2C controller work time sequence, and use the I2C controller to configure the camera parameters.

The image acquisition program includes two parts: data acquisition and caching, and the process is as follows: Performing the camera image acquisition module, under the camera clock to carry out the field synchronization, generating the signal which means that synchronization is done, so that the camera can be used for image acquisition. The camera module used in this project is only 8 data output ports. Each pixel in the image is made up of 8 bit luminance data and 8 bit color data, so the camera's data output mode is brightness and color alternately, so after the line synchronization and field synchronization, we will be the two adjacent group of 8 data to be combined, we can get the data that represents the full information of a pixel point. According to Data Sheet of OV7670, when the camera in the color video capture, at the beginning of the time there are at least 10 data is not stable. The program needs to shield the invalid frame, the acquisition time that the initial 12 frame cost is set to the invalid time of the data output, shielding the data that may not be valid. When the data output is valid, the data cache is carried out, set the read-write of the SDRAM, write the collected video data to the output buffer, and through the VGA interface to the output.

Camera driver, image capture and data cache program flow chart as shown in Fig. 5.

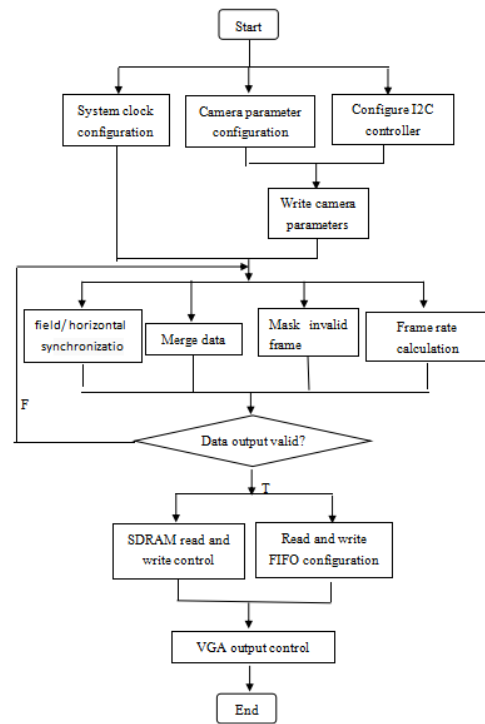


Fig. 5 Program flow chart of FPGA driver and image acquisition

## V. HOST COMPUTER

Using USB video capture card matching software as the host computer, we receive the video signal and process it, save it can also grab the image and do other operations.

The software of the host computer can adjust the brightness, contrast, color and saturation of the video image. When the video image is preserved, the different parameters of the video can be set, including the format of the video, the size of the screen, and the quality of the video. Reduced the strict requirements of the set of parameters of the camera, shorten the development time, at the same time, after the video is saved, the format conversion process is omitted.

The format converter is used in the input port, which can adjust the size of the video. Before running, you should to test the adjustment, the screen will be adjusted to the appropriate size, and then to use, so flexible and convenient. It can meet the needs of different environments.

## VI. TEST AND ANALYSIS

The main content of the test are the speed of the car, the range of the camera can observe, the effective transmission distance, as well as the quality and jitter of the video, and other issues. Table 2 lists the values of various parameters of the system obtained after the test.

TABLE II  
SYSTEM PARAMETER TABLE

| Test parameter   | Test result |
|--|-------------|
| Speed of the car   | 9m/min      |
| Camera in the horizontal direction of the monitoring range | 0-180 °     |
| Camera in the vertical direction of the monitoring range   | 0-180 °     |
| Effective transmission distance (indoor)                   | About 25m   |
| Effective transmission distance (outdoor)                  | About 80m   |
| Picture size pixel   | 640X480 30W |

From table 2, we can see that when the speed of the car is 9m/min, it can make the system meet a stable state, which can not only ensure the quality of video, but also enable the car to run in a stable state.

According to the actual test results, we can know that the system can realize multi angle and full range video surveillance.

Adjust the color video image through the PC brightness, contrast and saturation of the image reaches its best effect, the image is shown in Fig. 7, the image is clear, give full play to the pixel camera itself.

According to the effective transmission distance in Table 2, we can know that the system has good transmission performance both in indoor and outdoor, and the transmission distance can meet the practical application requirements.

By testing the wireless remote control and wireless video transmission without interference problems, Can be relatively independent of their own data transmission, The mobile platform can be controlled and at the same time return video image.

The overall appearance and structure of the car is shown in Fig. 6.

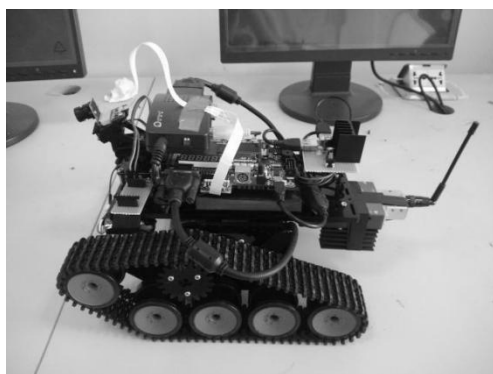


Fig. 6 Prototype of the car

In order to understand the difference of the image quality between wireless transmission and the wire transmission, the comparison test is carried out by using the wireless transmission mode and the wired transmission mode. The results obtained by using the wired method are shown in figure 8. Comparing Fig. 7 and Fig. 8 of the results, we can conclude that wireless transmission video quality and cable transmission video quality in the effective transmission distance is not obvious gap. We can know that wire transmission mode can be replaced by wireless transmission mode to achieve the same effect of video transmission.

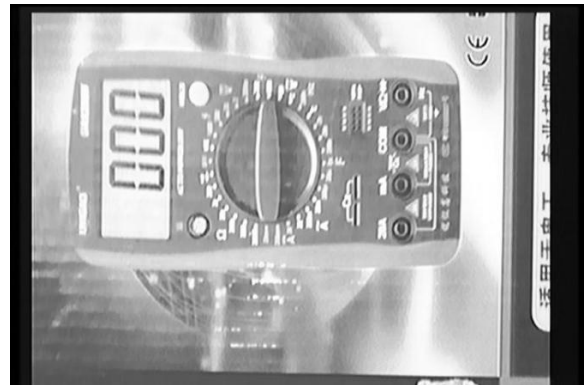


Fig. 7 Wireless video return results

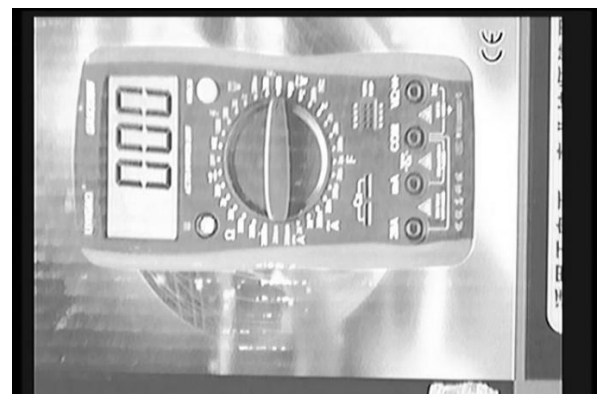


Fig. 8 Cable video return results

## VII. CONCLUSION

This system uses 2.4GHz frequency band wireless microwave to remote control car and steering gear, can remotely control the movable carrier into the observation area, and carries on the omni-directional multi angle observation; Using the 1.2GHz band wireless microwave to realize the video transmission, and use the analog transmission, to ensure the quality of the video. The whole system realizes the wireless video surveillance which can be moved in the non network environment. Solve the problem of video surveillance without network and some bad environment. But there are some deficiencies in the system. we need to carry out adequate experiments in

different environments, adjust its parameters. In order to realize more functions, different sensors can be added in the actual situation to measure the environment and realize the real-time detection of environmental parameters, which is conducive to the further analysis of the actual environment.

## References

- [1] Li Hao. Research and design of mobile wireless video surveillance system[J]. Bei Jing: College of Information and Communication Engineering, Beijing University of Posts and Telecommunications, 2012.
- [2] Yang Shnag-gang. Design on Real-Time video monitor & control system based on DSP[D]. Chong Qing: College of Automation, Chongqing University, 2006.
- [3] Ma Lin. The Development of Long-distance Video Transmission Software System Based on H.264[D]. Ji Lin: Ji Lin University[D]. Ji Lin: College of computer science and technology, Jilin University, 2014.
- [4] Liu Yan-bing. Design and realization of surveillance and navigation systems in digital mine[D]. Bei Jing: College of electronic information engineering, Beijing Jiaotong University, 2009.
- [5] Yu Rong-Fa. Design and implementation of mobile video surveillance system on Android-based[D]. Guang Zhou: College of computer science and engineering, South China University of Technology, 2011.
- [6] Dong Yong-Bo. Research on the H.264-Based Remote Video[D]. Wu Han: College of logistics engineering, Wuhan University of Technology, 2014.
- [7] Zhang Di. The design and implementation of police video-surveillance preparedness system based on GIS[D]. He Nan: He Nan University, 2011.
- [8] Li Tao. Implementation for Mobile Surveillance Based on Omni-directional Vision[D]. Tian Jin, Tianjin University of Technology, 2011.
- [9] Wang Fang. Microwave broadband transmission of video monitoring system based on embedded design and research[D]. Shan Dong: College of information science and engineering, Shandong University, 2013.
- [10] Zeng Lei, Zhang Hai-Feng, Hou Wei-Yan. Design and Implement of Wi Fi Wireless Measurement and Control Network[J]. Electrical Measurement & Instrumentation. 2011, 48(547): 81-83.
- [11] Zhang Qun, Yang Xu, Zhang Zheng-Yan, et al. Design and Realization of Serial Communication in Bluetooth Module[J]. Research and Exploration in Laboratory. 2012, 31(3): 79-82.
- [12] Zhang Men, Fang Jun-Long, Han Yu. Design on remote monitoring and control system for greenhouse group based on Zig Bee and internet[J]. Transactions of the CSAE. 2013, 29(1): 171-176.
- [13] Yu Yi-Ping, Zhou Man-Li. Application of wireless network in intelligent building[J]. Computer Engineering and Design. 2006, 27(22): 4264-4267.

# The Design and Implementation of an intelligent lighting System of energy-saving

ZHANG Jie; ZHAO Liang; ZHANG Sheng-yu

(College of Instrumentation & Electrical Engineering, Jilin University, Changchun 130026, China)

**Abstract**--Aiming at the huge energy consumption in street lighting in our country, the article proposes the design of an intelligent lighting system of energy-saving which combines the power conversion unit and intelligent control system based on the fuzzy control algorithm. Via the processes of gathering optical signal and sounds around the lamp by the sensor and transforming control signal into the power conversion unit after the A/D conversion and the procedure of the fuzzy intelligent controller and then to adjust voltage of the lighting lamp, the street lamp lighting system can change the brightness of the lighting according to the environmental conditions. The experimental results indicate that the system by the means of intelligent control achieves the goal of improve the efficiency of lighting and save energy in the case of not affecting the normal lighting. At the same time, the system can realize soft-start of lighting lamps and reduce the impact of the lamps through the power conversion unit thus prolong the service life of a street lamp.

**Keywords**--intelligent fuzzy control; energy saving; power conversion; soft-start

## 0 INTRODUCTION

WITH the rapid development of the Chinese economy, the street lamp lighting system power consumption accounts for a large proportion in China's overall electricity consumption, the proportion is also increasing. At the same time, traditional backward timing switch, manual care and other control methods are still used in most areas which not only caused the waste of electricity, but also greatly reduced the power supply equipment and lighting efficiency[1]. In recent years, some improvements have emerged which can not be popularized because of poor real-time performance or high cost of shortcomings [2].

Based on the current situation of street lighting system, the system can realize the real time control of the street lamp by sensing the actual situation around the street lamp under the premise of satisfying the requirement of lighting, the street lamp realizes energy saving, and improves the efficiency of the lighting system, and reduces the cost of maintenance and the control of the system. The dynamic energy saving of the street lamp illumination system is realized, and the purpose of the green environment protection is achieved.

## 1 BASIC PRINCIPLE

### 1.1 Principle of variable reactor

The variable reactor is composed of two parts, the variable reactance converter and the power conversion unit. The structure of the block diagram is shown in figure 1.

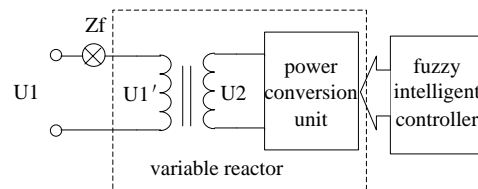


Fig.1 The structure diagram of variable reactor

The variable reactance converter is divided into a primary coil and a two secondary coil, a primary coil and an external load street lamp are connected in series to form an impedance circuit, and the two secondary coil and the power converter are connected to form a two impedance circuit[3]. Obtained by impedance transformation:

$$\frac{U_1'}{I_1} = \frac{N_1}{N_2} U_2 / \left( \frac{N_2}{N_1} \right) = \left( \frac{N_1}{N_2} \right)^2 \frac{U_2}{I_2}$$

Assuming an equivalent impedance of the coil is  $Z_1'$ , the power conversion unit impedance is  $Z_2$ , the current in the primary coil and the two coil is  $I_1$  and  $I_2$  respectively and the coil turns ratio is  $K$

$$Z_1' = K^2 |Z_2|$$

The variable reactance converter circuit can be

equivalent to a model circuit as shown in Figure 2.

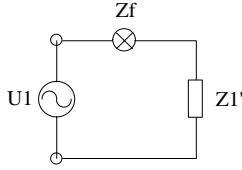
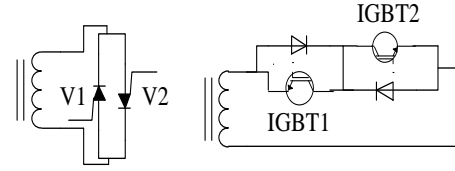


Fig.2 The equivalent circuit of variable reactor

Therefore, the power conversion unit receives the control signal of the intelligent controller, by changing the reactance value to adjust current value of the two secondary impedance circuit, thereby changing an impedance circuit current, when the input voltage is constant, the purpose of changing the primary coil reactance is achieved[4]. At this point, the impedance proportion between the primary coil and the street lamp is changed, and the voltage at both ends of the street lamp is also changed, thus the change of the power of the street lamp is realized. The system can change the terminal voltage of the street lamp through the variable reactor, so as to realize the real-time control of the soft start and the brightness of the street lamp, reducing the impact of the lamp and saving the energy consumption.

### 1.2 Principle of power conversion unit

The traditional power conversion unit is composed of thyristor reverse parallel, thyristor power conversion unit as shown in figure 3a. By adjusting the thyristor control angle, the equivalent impedance of the thyristor is changed, and the current value of the two impedance circuit is changed, and the thyristor is equivalent to a variable reactance[5]. However, due to the thyristor phase control method contains a large number of harmonics, so consider using a pair of IGBT tube in series. Its structure is shown in figure 3b. IGBT tube is a self turn off full control device, which can achieve high frequency switch off under the control of high frequency switch signal. Meanwhile, in order to greatly reduce the harmonic content, Using high frequency PWM wave duty cycle D control IGBT pipe[6], by changing the Z2, and then change the equivalent impedance of a coil, and ultimately control the load voltage [7].



(a) The SCR power conversion unit (b) The IGBT power conversion unit

Fig.3 structural comparison between SCR and IGBT power conversion unit

Assuming a variable reactor coil input for the  $U1$ , the two coil voltage is  $U2$ , the maximum value is  $U2m$ , the cycle is  $T$ , for the control of the PWM wave period is  $T_w$ , IGBT conduction time is  $\tau$ , the duty cycle is  $D$ . The transform  $U2$  into  $U_w$ , set switch function  $f$ , and hypothesis:

$$f = \begin{cases} 0. \text{ IGBT1 turn - on forward or} \\ \text{ IGBT2 turn - on reverse.} \\ 1. \text{ IGBT1 cut - off forward or} \\ \text{ IGBT2 cut - off reverse.} \end{cases}$$

$f$  with Fourier series expansion

$$f = D + \frac{2}{\pi} \sum_{n=1}^{\infty} \frac{F(D,k)}{n} \cos(n\omega t)$$

In the formula  $D = \frac{\tau}{T_w}$ ;  $\omega = \frac{2\pi}{T}$ ;  $k = \frac{T}{T_w}$

$$F(D,k) = \sin(n\omega t) + \sin(n\omega(T_w + \tau)) - \sin(n\omega T_w) + \dots + \sin\left(\frac{k-2}{2} \frac{2n\pi}{k} + \frac{2n\pi}{k} D\right) - \sin\left(\frac{k-2}{2} n\omega T_w\right)$$

o secondary voltage

$$U_w = f U_{2m} \sin \omega t$$

Two formulas are integrated

$$U_w = U_{2m} \sin \omega t \left[ D + \frac{2}{\pi} \sum_{n=1}^{\infty} \frac{F(D,k)}{n} \cos(n\omega t) \right]$$

Variable reactor using IGBT tube, the high order harmonic is suppressed, and the two secondary voltage

$U_w = f U_{2m} \sin(\omega t) * D$ , thus there is a two coil current

$$I_2 = U_{2m} \sin(\omega t - \varphi_1) * \frac{D}{Z_2}$$

$Z_2$  is the two fundamental impedance value, which is the fundamental impedance angle. The turn number

ratio of the first and two sides of the variable reactance converter is  $K$ ,

thus primary coil current

$$I_1 = U_{2m} \sin(\omega t - \varphi_1) * \frac{D}{K * Z_2}$$

and

$$U_{1m} = K * U_{2m}$$

So

$$Z_1 = \frac{U_{1m}}{I_1} = \frac{K^2 * Z_2}{D}$$

From the above formula we can know that the first equivalent impedance of the variable reactor decreases with the increase of the PWM wave duty cycle  $D$ [8-10]. Its change curve is shown in figure 4.

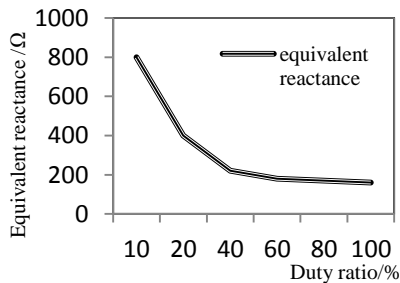


Fig.4 The influence between duty ratio and impedance module

Therefore, by changing the duty cycle of the PWM wave, the adjustment of the first order equivalent reactance of the variable reactance can be realized, and then the power conversion of the lighting system can be realized.

## 2. THE HARDWARE DESIGN OF INTELLIGENT CONTROL SYSTEM

### 2.1 System composition block diagram

The system is composed of optical and sound signal acquisition circuit, signal conditioning circuit, main

controller, power conversion unit and lighting system. Block diagram of the system is shown in figure 5.

The intensity and sound signal are processed in real time by the main controller, so as to produce the control signal, the control signal after D/A conversion into duty cycle changes of PWM wave, and PWM wave control the power conversion unit to realize the real-time control of lighting system power.

### 2.2 Signal acquisition circuit design

The sound signal is selected by the sound sensor module, which can detect the sound intensity of the surrounding environment. The sound sensor module outputs a high level, and vice versa, when the sound intensity of the environment reaches a threshold value. Detection of high and low level through the microcontroller, which to achieve the detection of the sound intensity of the environment changes. Circuit diagram is shown in figure 6.

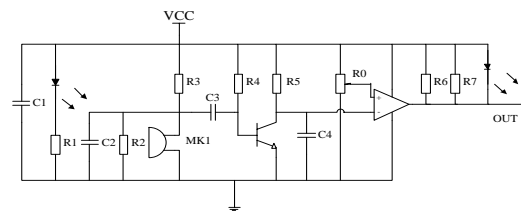


Fig.6 The acquisition circuit of sounds

The opening and closing of the street lamp is controlled by the environment illumination which is detected by the system. The optical signal acquisition circuit uses photosensitive resistance ordinary, the principle is that the photosensitive element induced by the optical signal change as the output signal, when there is no light, the photosensitive resistor is great, and current is very small; On the contrary the resistance will rapidly become smaller, so that the current increases. Its circuit diagram is shown in figure 7.

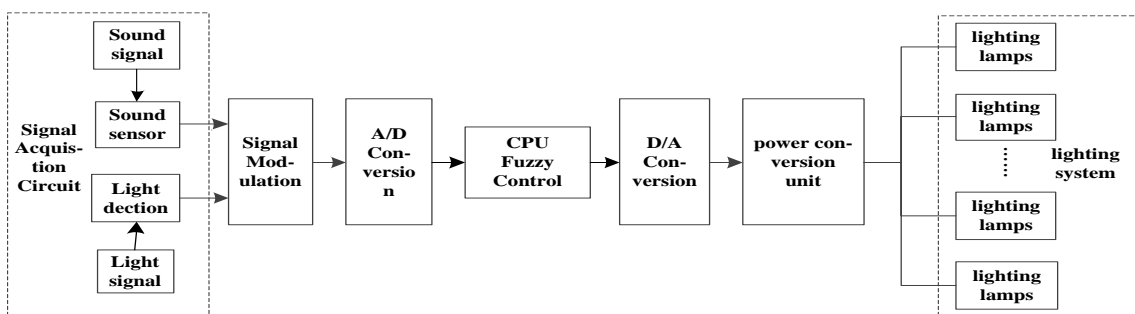


Fig.5 The schematic diagram of system composition

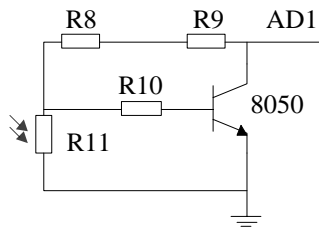


Fig.7 The acquisition circuit of optical signal

The opening and closing of the street lamp is controlled by the environment illumination which is detected by the system. The optical signal acquisition circuit uses photosensitive resistance ordinary, the principle is that the photosensitive element induced by the optical signal change as the output signal, when there is no light, the photosensitive resistor is great, and current is very small; On the contrary the resistance will rapidly become smaller, so that the current increases. Its circuit diagram is shown in figure 7.

By detecting the light in the circuit, The photosensitive resistor changes, The base voltage of the transistor is also changed, thus transistor is turned on or off. Single chip then detect the level of output to determine whether the street lights is going to switch control or not.

### 2.3 Design of power conversion unit

The power conversion unit of the system is controlled by PWM wave. PWM wave using ARM internal DAC output function, and then the two order RC filter, the filter circuit as shown in figure 8. And through the IGBT driver chip EXB841 to drive IGBT, achieving the purpose of voltage regulation by changing the pulse duty cycle then changing the output voltage fundamental wave amplitude,

At the same time, the design of the power conversion unit select high speed IGBT power tube whose voltage change rate is too large between the collector and emitter, so the phenomenon of breakdown and mis-conductions is possible emerged, therefore ,the need for overvoltage protection of the IGBT is highly necessary The parameters of IGBT, such as voltage drop, switching time, fast switching loss and short circuit current capacity, are influenced by the gate driver circuit of IGBT, and the static and dynamic characteristics of IGBT are determined. In order to realize the IGBT short circuit protection, over current detection must be performed. When the short circuit current appears, in order to avoid the excessive

formation of the current, the IGBT lock is invalid and damaged, and reduce the electromagnetic interference, the soft reduction gate voltage and soft shutdown integrated protection technology is usually adopted.

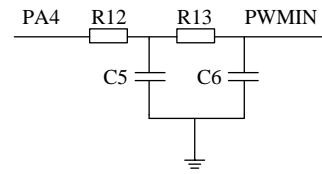


Fig.8 The filter circuit

As shown in figure 9 is the circuit for protecting the IGBT from the increase of  $V_{ce}$ , If there is a current flow around 10mA between 14 pin and 15 pin of the EXB841, then  $V_{ce}$  decreased to about 3V, while the 6 pin voltage is clamped at about 8V, the gate emitter voltage is about 20V, at this time the IGBT is conducted.

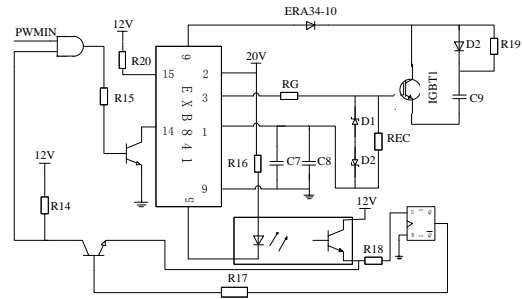


Fig.9 Overcurrent and overvoltage protection circuits

As shown in figure 9 is the circuit for protecting the IGBT from the increase of  $V_{ce}$ , If there is a current flow around 10mA between 14 pin and 15 pin of the EXB841, then  $V_{ce}$  decreased to about 3V, while the 6 pin voltage is clamped at about 8V, the gate emitter voltage is about 20V, at this time the IGBT is conducted;

On the contrary, if no current flows through the gate, IGBT gate charge rapid discharge, then 3 pin voltage down to 0V, the voltage between the gate emitter becomes negative 5V, finally, At this point IGBT shutdown reliably.

If overcurrent of the IGBT occurred, 5 pin of the EXB841 changes from high to low, S terminal of RS trigger is driven to high level, and the output terminal of the Q export high level which make the transistor conduction and level on the and gate is low, as a result, the input signal of EXB841 is blocked and the purpose of withdrawing gate signal and protecting IGBT is achieved .

### 3. SYSTEM ALGORITHM AND SOFTWARE DESIGN

Fuzzy system identification is an identification technique that does not depend on the mathematical model of the identified object. Fuzzy controller algorithm will first enter the exact amount into the fuzzy input based on information according to the known language control rules for proper reasoning, so output decision, and then converted to the exact amount of system to achieve the required control. It reflects that fuzzy decision was made by thinking and logical reasoning in the control process and then into a precise amount of control to achieve the whole process[11].The system needs to collect the sound signal of the surrounding environment of the street lamp in real time, it is difficult to get a specific mathematical model since the sound signal has a very strong time lag and nonlinearity and the interference is too large at the same time, therefore, it adopts fuzzy control algorithm which not only omits the process of establishing a mathematical model, and achieve high precision, small fluctuations in the control effect simultaneously[12]. The schematic diagram of the system control is shown in figure 10.

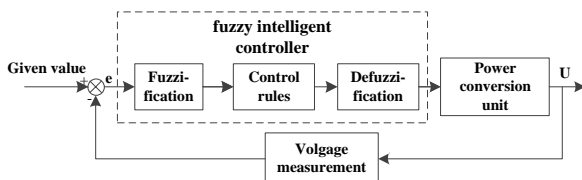


Fig.10 The principle diagram of the fuzzy controller

The system fuzzy control assumes that the noise input variable is  $E$ , noise input deviation change rate is  $EC$  and output control is  $U$ , Noise input variables are divided into 5 grades which are small (NB), partial small (NS), medium (Z), partial large (PS), large (PB) that represent noise status of the lighting system, Noise input bias change rate  $EC$  is also divided into 5 cases which are weak (NB), slightly weak (NS), medium (Z), slightly strong (PS), strong (PB), respectively.

And to assume that the domain is  $\{-2, -1, 0, 1, 2\}$ . Output control is similarly divided into small (VL), small (RL), medium (ZO), partial large (VB), large (EB) 5 grades ,and Set the domain to  $\{-2, -1, 0, 1, 2\}$ , According to the relationship between input and output:

$$U=[\beta E+(1-\beta)*EC]$$

the  $\beta$  is correction factor which is found by considering the actual factors . Therefore, the integrated control rule table is shown in table 1.

TABLE. 1  
THE FUZZY CONTROL RULES

| $EC$ | $E$ |    |    |    |    |
|------|-----|----|----|----|----|
|      | NB  | NS | Z  | PS | PB |
| NB   | VL  | RI | RL | ZO | VB |
| NS   | VL  | RL | ZO | ZO | VB |
| Z    | RL  | ZO | ZO | ZO | VB |
| PS   | RL  | ZO | ZO | VB | EB |
| PB   | RL  | ZO | VB | VB | EB |

The system fuzzy process the sound signal collected by fuzzy control firstly, then make the fuzzy rule judgement which determine the output change control quantity by judging the sound signal at this time is larger than that of the previous state, so as to change the power of the lighting system and the brightness of lighting lamp .The flow chart of the system is shown in figure 11.

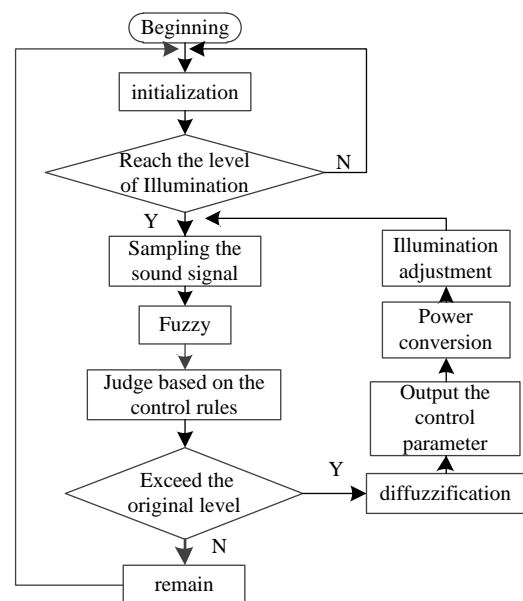


Fig.11 System program flow chart

### 4. TEST RESULTS AND ANALYSIS

By using the pulse width modulation (frequency invariant) trigger IGBT, the voltage and current value of the street lamp can be obtained when the duty cycle is different than that of the  $D$ . To access the street lamp of the control system as the test object, the working voltage, current and power of the street lamp are shown in table 2 under the control of PWM wave with



different duty cycle:

TABLE 2

STREET LAMP OPERATING POWER TEST

| Serial number | Duty ratio D/% | voltage U/V | Current I/A | Power P/W |
|---------------|----------------|-------------|-------------|-----------|
| 1             | 0              | 200         | 0           | 0         |
| 2             | 20             | 109         | 0.33        | 36        |
| 3             | 40             | 118         | 0.35        | 41        |
| 4             | 60             | 179         | 0.54        | 96        |
| 5             | 80             | 190         | 0.57        | 108       |
| 6             | 90             | 200         | 0.6         | 120*      |
| 7             | 100            | 200         | 0.6         | 120       |

Notes: The IGBT already turned on, the power reached the maximum.

At the same time, for ten hours real-time contrast test under the same environment between method of the system and that of the traditional control .the comparison curves are obtained as follows:

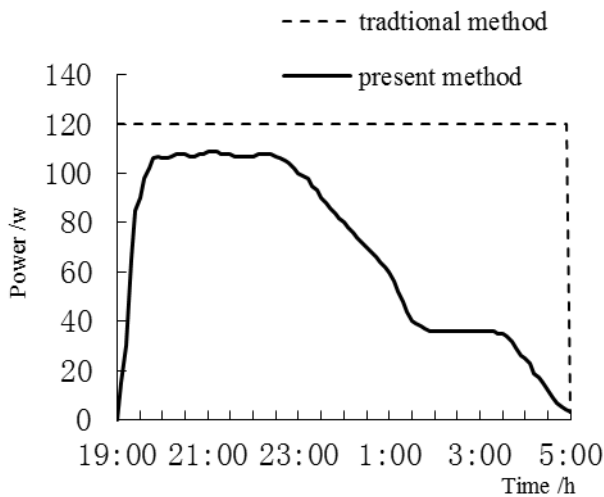


Fig.12 The power comparison between algorithms before and after being improved

The experimental data showed that using variable reactor power converter, can achieve real-time control of power system lighting lamps, and lighting at the maximum power can only reach the rated power of 80%, It not only meets the demand of illumination, but also uses the soft starting mode to avoid the damage of the street lamp when the current is too large, as a result the service life of the lamp is prolonged, and the energy is saved as well.

5.CONCLUSION

In regard to the energy saving of the lighting system, it is necessary to improve the control mode of the street lamp lighting system while vigorously promoting the new energy-saving lighting lamps and lanterns. In this system, the intelligent controller based on fuzzy control algorithm is combined with the power electronic power converter unit, the change of the end voltage of the street lamp and the function of real-time control of street lamp illumination can be achieved through impedance transformation of the primary coil and the two coil

The illumination efficiency of the street lamp system is improved, and the cost of the illumination is reduced, and the remarkable energy saving effect is achieved. At the same time, with the development of communication, energy saving and control technology, the lighting system is bound to be more efficient, economical and intelligent.[13-14].

References

- [1] HE Yi-ming, WANG Chong-gui, LIU Jin-yu. Design and Application of Street Lamp Intelligent Control System[J]. Modern Electronics Technique, 2010, 33 (1): 207-210.
- [2] QIU Fa-chao, CHEN Xian-ping, CHEN Wei-bin, et al. Energy-saving Street Lighting System Based on Internet of Things[J]. Mechanical Engineering & Automation, 2016, 0(2): 201-202.
- [3] YUAN You-xin, ZHAO Yan-wei, DING Yi ,et al. fuzzy control arithmetic variable reactor soft starter[J]. Electric Drive, 2006, 36 (5): 13-15.
- [4] WANG Ya-lan. The Research on the Saving Energy Controller of the Intelligence Lamp[D]. Wuhan, Wuhan University of Technology,2008.
- [5] XIAO Yi-ping, YUAN You-xin. Research on Discrete Variable Frequency Heavy-load Soft Start Based on Variable Reactance Technique [J]. Power Electronics ,2006, 36(5): 13-15. 2011, 45(3): 106-108.
- [6] A. Mirvakili. High efficiency LED driver design for concurrent data transmission and PWM dimming control for indoor visible light communication[J] . Photonics

- Society Summer Topical Meeting Series, 2012IEEE. 9:  
132—133.
- [7] XIAO Yi-ping. Research on Variable Reactor Based on Power Conversion[D]. Wuhan, Wuhan University of Technology,2008.
- [8] LIN Wei-xun. Modern Power Electronics Circuit[M].Hangzhou: Zhejiang University Press , 2002:200-240.
- [9] YANG Zhi-tai, SHI Xiang, MA Lei, et al. Research on variable reactance motor soft starter[J]. Journal of Shandong University of Technology: Natural Science Edition, 2012, 26(5): 84-87.
- [10] CHEN Jian. Power electronics-power electronic conversion and control technology [M]. Beijing: Higher Education Press, 2011:200-220.
- [11] QIU Chun-ling, BAI Yu-xin, WANG Kai, GU Jia-yue. Study on Automatic Berthing Model Based on Fuzzy Control[J]. Journal of Jilin University: Information Science Edition, 2016, 1, 134-139.
- [12] J . J . Buckley. Universal fuzzy controllers [J]. Automatica.1992. 28(6): 1245-1248.
- [13] ZHANG Kun, LUAN Hui, JIANG Ming-jie,et al. The Design of Intelligent Street Lamp Control System with the Function of Environment Monitoring[J]. Research and Exploration in Laboratory, 2015, 34(12): 61-64.
- [14] LING Zhen-bao, ZOU De-bao, XU Min. Design and Realization of Intelligent Lighting System for Classroom[J]. Journal of Jilin University: Information Science Edition, 2009, 27(4):435-440.

# Based on ERT Electromagnetic Simulation and Optimization Design on ANSYS

JI Yanju; WU Yonghong; SONG Shuang

(School of Instrument Science and electrical engineering, Jilin University, Changchun 130000)

**Abstract--Resistance Tomography (Electrical Resistance Tomography, called ERT) is based on electromagnetic theory of process tomography technology, but also electrical impedance tomography (Electrical Impedance Tomography, referred to as the EIT) a simplified form of art, it has a non invasive, low cost, no radiation, fast response and visualization features, and there are broad prospects for industrial measurement and medical testing. The issue of ERT electromagnetic simulation and design optimization.**

**Keywords--Resistance Tomography ERT electromagnetic simulation optimization design**

## I. FOREWORD

IN the department in chemical, petroleum, metallurgy, oil and energy, as well as medical, health, food, the prevalence of multiphase flow flow process. With the industrial automation level of production continues to develop, the demand for two-phase flow parameter measurement is increasingly urgent, process tomography technology at this time came into being. The electrical resistance tomography is one of them, it is suitable for two-phase flow in a continuous liquid phase production process[1].

Resistance Tomography (ERT) technology is based on a different field conductivity sensitive to get step by step information multiphase medium. This paper analyzes the mathematical description of ERT and positive issues, electromagnetic simulation, optimization and other electrodes, and introduces software ANSYS and APDL language.

## II. ERT MATHEMATICAL DESCRIPTION

### A. Mathematical description of ERT sensitive field

ERT basis of electromagnetic theory is based on the theory of 'up the field' on 'up the field' meet the following criteria[2]:

$$\begin{cases} \nabla \times H = J_f = \sigma E \\ \nabla \cdot D = 0 \\ \nabla \cdot B = 0 \\ \nabla \times E = -\frac{\partial B}{\partial t} = -\mu \frac{\partial H}{\partial t} \end{cases} \quad (1)$$

Based on the assumption (ERT sensitivity field to 'up the field') and a constant electric field theory (ERT sensitive field as a constant electric field) and Maxwell's equations, in any field of ERT sensitive point,

$$J = \sigma \cdot E \quad (2)$$

$$\nabla \cdot J = 0 \quad (3)$$

Wherein, for the electrical conductivity, the electric field strength, the current density. also because

$$E = -\nabla \phi \quad (4)$$

Which is sensitive to the potential field distribution, and meet

$$\nabla \cdot (\sigma \cdot \nabla \phi) = 0 \quad (5)$$

$$\nabla \sigma \cdot \nabla \phi + \sigma \cdot \nabla^2 \phi = 0 \quad (6)$$

In uniform, isotropic, linear medium, is constant, then, so that  $\nabla \sigma = 0$ , equation (6) can be simplified into a Laplace equation

$$\nabla^2 \phi = 0 \quad (7)$$

### B. EIT forward problem analysis

The method of calculation of ERT forward problem can be divided into two categories: analytical and numerical calculation. Analytical method requires

detailed theoretical analysis to obtain analytical expressions, and then solve for analytical solution, the derivation of the analytical method is more complex, only for calculating two-dimensional uniform field, it does not apply to the direct problem solving ERT. The numerical method is divided into the finite element method (FEM), boundary element method (BEM) and the finite difference method (FDM), and so on. ERT while solving the direct problem for the finite element method, finite element method is based on the variational principle and the Transformation of partial differential equations for the functional extrema, then the numerical method to solve problems and then give extreme value obtained numerical solution . Its Solving steps include[3]:

- ① set out with Boundary Value Problems to be solved and the corresponding functional equivalent variational problems;
- ② using the finite element method split field, and select the corresponding difference function;
- ③ into discrete extremal problems stand out in parallel export algebraic equations;
- ④ with the method of finite element solution of algebraic equations, numerical approximation obtained solution, post-processing procedures to obtain equations to obtain the final result.

Sources of error:

Discretization error: in essence, the finite element method to the entire field broken down into many small areas to solve the problems caused by continuous into discrete, errors generated during the conversion process is the discretization error, and can not be eliminated, as FEM inherent.

Rounding errors: in the use of computer work, due to the limited word length of the computer itself, the original data will have some errors in the calculation process will produce a new error, the output results are not accurate, such an error is rounding errors can not be eliminated.

### C.ANSYS Introduction

ANSYS software is a set of acoustic, electric, thermal, structural and fluid in one of the large-scale general finite element analysis software, is divided into three main parts: pre-processing module, analysis and post-processing module calculation module. The electric field can be studied three aspects: circuit analysis, static analysis, and current conduction. It can

be used for analysis: static structures, structural dynamics, nonlinear structure, dynamics, thermal analysis, electromagnetic field analysis, fluid dynamics, sound field, piezoelectric analysis.

ANSYS analysis of the main steps of the process:

- (1) create / read geometry;
- (2) the provisions of material properties;
- (3) mesh;
- (4) applied load and solving set load options, setting constraints;
- (5) to view and analyze test results.

### D.APDL language Introduction

ANSYS software is powerful and complex, widespread problem can be solved, the calculation process is quick and easy. The ANSYS parametric design language (ANSYS Parametric Design Language, APDL) is a language of ANSYS batch files, write APDL language is also easy to maintain and modify, it is more than the ability to extend the ANSYS finite element analysis, the provincial convenient.

## III.ERT ELECTROMAGNETIC SIMULATION AND OPTIMIZATION DESIGN

### A.ERT Electromagnetic Simulation

Because the three-dimensional ERT 'soft-field' characteristics (sensitivity field distribution with the change of the measured medium changes), we use large-scale simulation software ANSYS ERT electrode electric field simulation by APDL language.

ERT imaging is a relatively mature one electrical imaging modality, depending on a variety of media conductivity distribution derived sensitive field conductivity[4].

ERT electrodes were measured medium conductivity is much larger than metal, and therefore the actual measurement, the rectangular electrodes are used equipotential body.

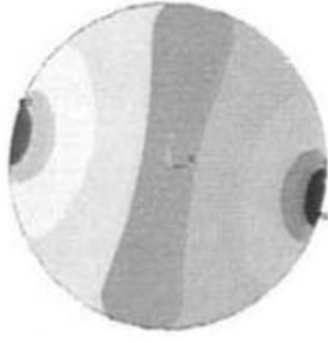


Figure 1 electrode opening angle of 16° and other potential cloud

Figure 1 shows, the equipotential lines of the electric field in the vicinity of the electrode deviations occur, the surface of the electrode body is forced to equipotential, the reaction can not be point information, the width of the electrode, and other more serious potential line offset errors introduced easily.

### B. Selective Electrode

ERT electrodes must be met:

- (1) Good conductive properties;
- (2) chemically stable;
- (3) machining characteristics of a good, easy processing, low thermal stress, low cost;
- (4) having a certain wear.

### C. Optimization goal ERT electrodes

Optimization goal ERT electrodes from the following considerations:

- (1) Spatial resolution: get more than the range of the excitation current range boundary voltage difference between the response of the different conductivity.

$$d(\sigma_1, \sigma_0, I_s) = \left\| \frac{U_1(\sigma_1, I_s) - U_0(\sigma_0, I_s)}{I_s} \right\| \quad (8)$$

Which is the excitation current and voltage measurements boundaries were changed to a point from the conductivity. Spatial resolution should be better. And from the simulation results, to make the greater the resolution, the smaller the electrode coverage should be, namely the electrode opening angle is smaller.

(2) Sensitive field uniformity: uniform change sensitive field, we can not improve the stability of the ERT, therefore the system more uniform the better. The simulation can know, the larger the opening angle of the electrode, the electrode coverage, the more uniform distribution of sensitive field.

- (3) Imaging errors: the reconstructed image fidelity

(SIE). SIE is capable of reacting with the model image difference recombinant human eye can observe between. It is a good evaluation. From simulation image, the larger the size of the electrodes, and seek solutions more close to the real solution, the better.

### D. Point electrode design optimization

Dot electrode diameter is very small circular electrodes capable of measuring 'points' related potential information. In this paper, two different points electrode diameter to compare, find suitable diameter optimization point electrode[5].

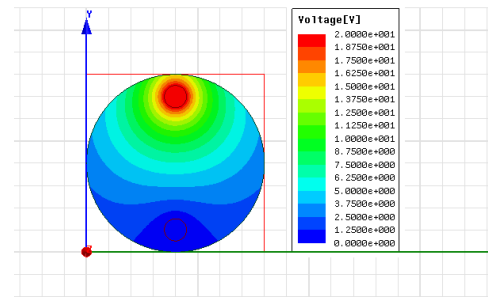


Figure 2 2.5mm radius point electrode potential simulation map

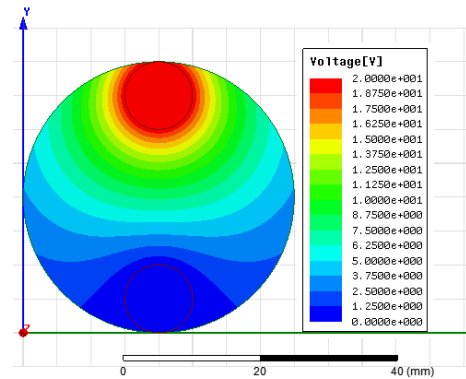


Figure 3 5mm radius point electrode potential simulation map

### E. Electrode height different simulation optimization design

Field high-impact pipe electrode axial space distribution uniformity, but the higher the height of the electrodes, the filtering effect of the sensitive field of space, the stronger, and we are difficult to obtain sensitive information in the field of media on a thin section only region where the average information obtained electrode can cover. Although the precision is difficult to obtain information on the section, but the measurement of the average three-dimensional space in the media within the larger area of the information is feasible. As used herein, it is slightly larger rectangular electrodes, with the increase in the axial dimension,

the better the uniformity of the central field, but the edge effect is still there, the spatial extent of the field increases with increasing size of the sensitive region is increased, it should be Considering[6].

This paper compares the height of two electrodes, to find the right height optimization in the appropriate range[7].

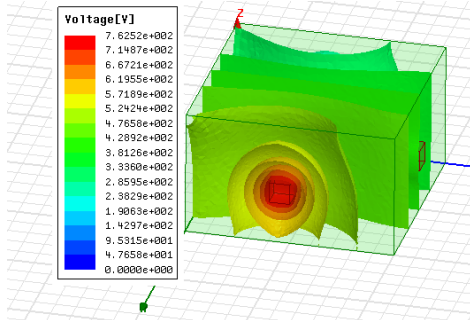


Figure 4 5mm high electrode simulation map

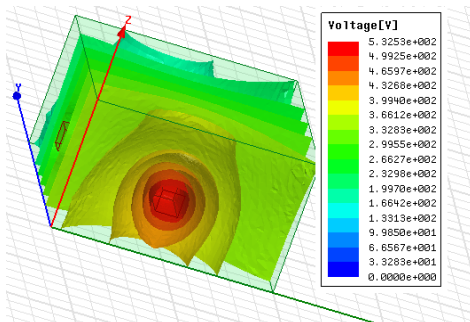


Figure 5 10mm high electrode simulation map

*F. Electrode position different optimization design*

Article 16 and the adjacent electrodes relative positional relationship between the two to compare to see which position the electrodes with better optimization.

Select a relative excitation mode excitation electrode adjacent to the non-excitation electrode as our reference electrode, followed by measuring electrode and the other electrodes is measured; pair of opposing electrodes, repeat the previous steps and then select clockwise[8]. Obtained  $N \times (N-3) / 2$  measurements.

Adjacent excitation mode is also known as four-electrode mode, the establishment of a sensitive field to take on two adjacent electrodes, other adjacent electrodes measured voltage.

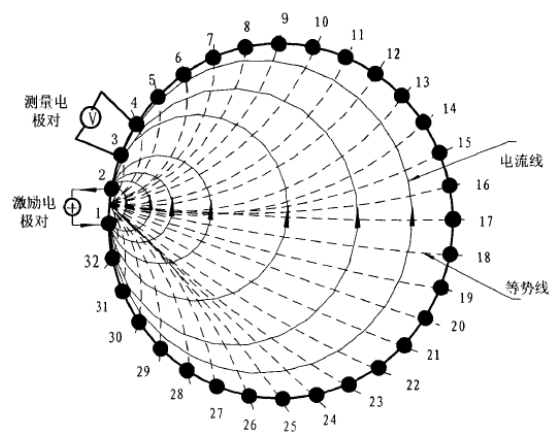


Figure 6 adjacent excitation mode

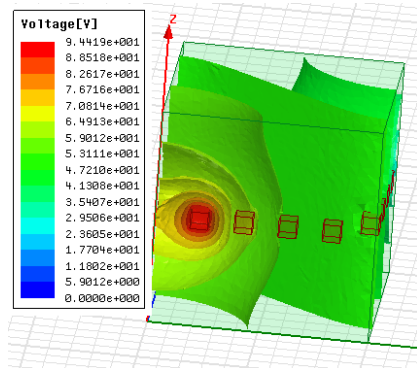


Figure 7 16 Figure electrode relative excitation mode emulation

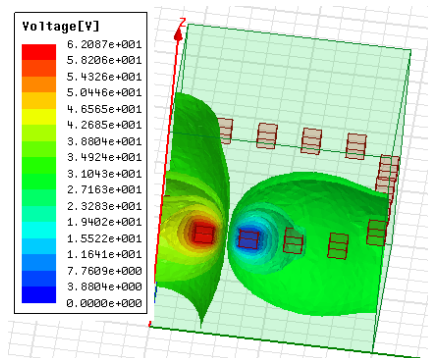


Figure 8 16 emulation mode excitation electrode adjacent diagram

Relative mode and neighboring modes do comparison, a more uniform distribution of the electric field of its sensitive field, center field corresponds to the sensitivity increased, the sensitivity distribution is better[9].

IV.CONCLUSION[10]

(1) ERT electrode optimization Summary:

- ① imaging errors: the size of the electrodes bigger the better;
- ② Coverage field: the size of the electrodes bigger the better;

③ Resolution: the size of the electrodes as small as possible.

(2) calculated using finite element method complex media issues ERT sensitive field, but also for simulation ERT sensitive field, change the number of meshes obtained high precision.

(3) all suitable for three-dimensional field can be deduced.

(4) the establishment of a simulation model of ERT electrode 16, has been relatively adjacent position next two simulation map, analyzes the dot electrode Simulation charts of different diameters under different simulation and height of the rectangular electrodes.

(5) This paper focuses on resistance tomography ERT conducted a mathematical description, and describes the support tools and large-scale simulation software ANSYS auxiliary language APDL, in the understanding of these on the basis of the ERT electromagnetic field simulation and design optimization of the electrode were aspects of shape, size, location and other key analysis also focuses on these aspects in the experiment.

## References

- [1] Q. snow Ning. Electromagnetic Simulation and Electrode Array Optimization Design on ANSYS ECT / ERT based [D] .2007,1,1.
- [2] Jin Jianming finite element method [M] Xi'an University of Electronic Science and Technology Press. 1998; 20-45.
- [3] Wei Ying, XIA Jing-bo, Wang Shi, Luzeng Xi simulation. Resistance Tomography (ERT) Sensitive Field [J]. Journal of Northeastern University .2000,8.
- [4] Xiao Li Qing, Shao Xiao root, WANG Lin-lin, Zhang Liang, Dan Tianming. Resistance Tomography finite element model analysis and design [J]. Journal of Scientific Instrument .2008,2.
- [5] Studies show right .ERT Jia electrode array system design and optimization of single electrode excitation mode [D] .2006,1.
- [6] Ma Xin Yi. Simulation of Resistance Tomography sensitive electrode array [D]. Tianjin University .1996.
- [7] Yanzeng Wei .32 electrode resistance tomography system simulation study [J] .2009,6.
- [8] Chen Licheng digital tomography method and application [M]. Xi'an Jiaotong University Press .1994.
- [9] Zhang Baofen, Peng Lihui, Yao Danya Process Tomography [J] Technical Supervision in Petroleum Industry .2001,17 (6): 12-15.
- [10] Shi Yingjie. Resistance Tomography technology research [D]. Yanshan University .2007.

# Design of Greenhouse's Humiture Measurement and Control System Based on GSM

DUAN Qing-ming; ZHANG Ya-ru; CUI Zhen-shu; ZENG Ling-qi  
(*jilin university instrument science and engineering institute, changchun, 130021*)

**Abstract**--Recently, greenhouse has already been a key factor in agricultural production engineering. Management level of greenhouse humiture impacts (has influence in ) the quality and quantity of agricultural products directly. Therefore, it is important to control the environmental parameter in the production process of greenhouse. The design of used DHT11 digital humiture sensor to gather humiture, signal chip microcomputer was used to deal with the data, keyboard and LCD can implement man-machine conversational function, GSM was used to alarm a message once the humiture was beyond the upper. The users can inquire the current value of humiture, set up the threshold value and control the switch of the fans and pumps by messages. The result shows that the measurement and control system is maintained conveniently with small volume, low power consumption, simple circuit and good expansibility.

**Keywords**--GSM 、 DHT11 digital humiture sensor、 Greenhouse

## 1、 INTRODUCTION

IN our country, there is a large part of the traditional agricultural cultivation depends on the development of greenhouse[1]. Although the scale of greenhouse is very large, it is time-consuming and laborious. In recent years, the Internet of things science and technology and automatic control technology has been used to improve the level of automation of agricultural greenhouses and achieve the goal of increasing crop production and human resources in the greenhouse. Although China's agricultural greenhouses developed rapidly in the respect of automation, it still has some problems such as small monitoring range, unstable remote control signal, low acquisition accuracy and so on. With the continuous innovation of science and technology, we should also improve the large-scale greenhouse technology, so that it can be conducive to scientific and technological control, reduce the operator's requirements of intelligent production technology.

Intelligent greenhouse allows staff to look at the temperature and humidity of the greenhouse at any time, so that it can be adjusted at the fastest speed. Its low price and high reliability has brought a lot of convenience for the transformation of agriculture. The transformation of agricultural production with high and new technology is the fundamental issue of the

sustainable development of agriculture and national economy in China. The aim of this paper is to design the temperature and humidity monitoring system of the greenhouse, and to detect the temperature and humidity in the greenhouse by the high sensitive temperature and humidity sensors, and to regulate the temperature and humidity through the control system[2].

## 2、 REMOTE CONTROL SYSTEM

The structure of the remote monitoring system as is shown in Figure 1 are determined on the basis of its designed capabilities. This system is mainly controlled by the microcontroller module, temperature and humidity acquisition module, keyboard input module, LCD module, GSM communication module, temperature and humidity regulation module.

The device used DHT11 digital humiture sensor to gather humiture, signal chip microcomputer was used to deal with the data, keyboard and LCD can implement man-machine conversational function. When the greenhouse temperature and humidity exceeds the set upper limit, the microcontroller via GSM communication module sends SMS alarm to the user, while driving the fan and water pump to adjust temperature and humidity. Users can also send SMS to inquire current value of the temperature and humidity inside the greenhouse, set the upper limit of



temperature and humidity, the switches to control the fan and pump.

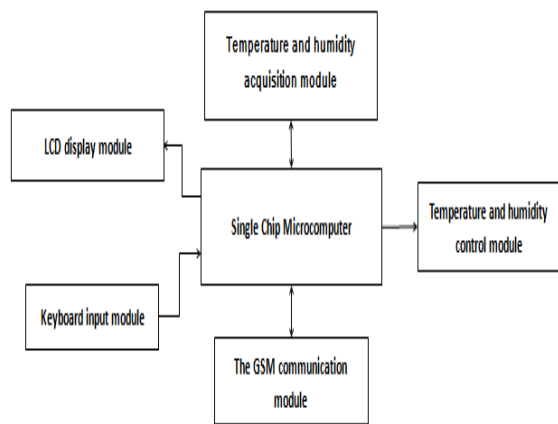


Figure I System Chart

### 3、HARDWARE DESIGN

#### 3.1、Temperature and humidity acquisition circuit design

The system uses DHT11 temperature and humidity sensor to make data acquisition. The sensor which includes a resistive element and a sense of wet NTC temperature measurement devices, is a complex temperature and humidity sensor containing a calibrated digital signal output. The sensor has many advantages such as fast response, anti-interference ability and high property price ratio. It uses a single-wire serial interface, which can be connected directly to the microcontroller pin, it requires only one I / O port. Because of its ultra-small size and low power consumption, its signal transmission distance up to 20 meters[3-4]. DHT11 temperature measuring range: 0~50°C; Temperature measurement accuracy:  $\pm 1^{\circ}\text{C} \sim \pm 2^{\circ}\text{C}$ ; Relative humidity measuring range: 20%~90%RH; Relative humidity measurement accuracy:  $\pm 4\% \sim \pm 5\% \text{RH}$ .

#### 3.2、GSM communication circuit design

GSM communication module uses SIM900A module which is produced by SIMCOM company. It is a dual-band GSM / GPRS module, the working frequency band: EGSM 900MHz and DCS 1800MHz. It supports GPRS multi-slot class 10 / class 8 encoding format and GPRS CS-1, CS-2, CS-3 and CS-4. SIM900A use VBRT of 3.4V to 4.5V single power supply, since the module will transmit sudden voltage drop, then the peak current reaches 2A, the power supply must therefore be able to provide enough

current to 2A. In order to ensure the GSM module starting normally, the system takes the method for its power alone[5-10]. The microcontroller sends AT commands to SIM900A through the serial port to control the sending and receiving of SMS messages. So we can connect microcontroller's serial ports pins with GSM's directly.

### 4、SYSTEM SOFTWARE DESIGN

#### 4.1、The main program design

Modular software design. All program consists of the main program, DHT11 temperature and humidity measurement subroutine, serial communication routines, subroutines LCD, keyboard scan subprograms. The main process: When DHT11 temperature and humidity values is detected by the SCM system, the data will be processed by the microcontroller and then be sent to the LCD display module for display and compared with the set temperature and humidity values which is set by the keyboard to determine whether or exceeds the set value, if exceeded, the microcontroller sends AT commands through the serial port to the GSM module to control the alarm out of SMS. In addition, the microcontroller can also read SMS received by the GSM module through AT commands to perform the corresponding functions, such as query the current temperature and humidity values, set the upper limit of temperature and humidity, control the switch of pumps and fans. The flow chart is shown in Figure II.

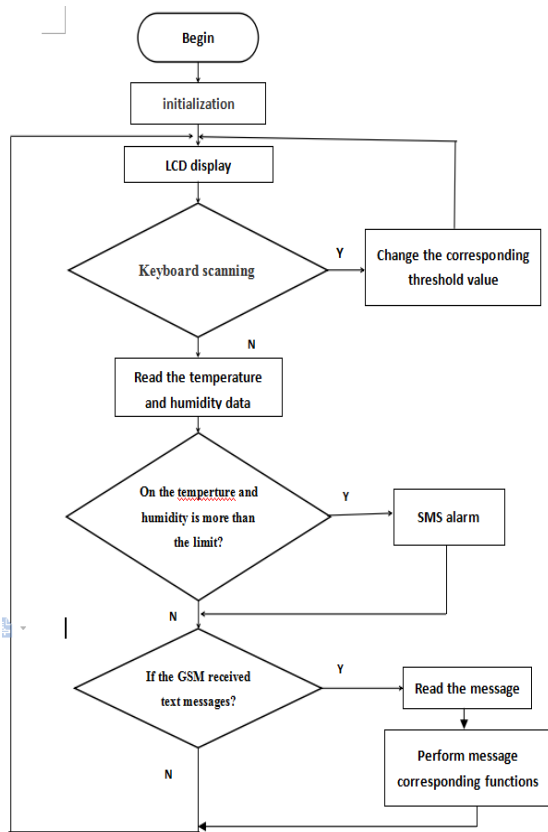


Figure II Main flow chart

4.2、DHT11 temperature and humidity acquisition module

DHT11 using a single data bus mode to communicate with the microcontroller , each communication are 4 ms or so. Procedure is as follows:

Complete data transfer is 40-bit, high-first-out. Data format: Temperature integer data (8bit) + temperature fractional part(8bit) + humidity integer data(8bit) + humidity decimal data(8bit) + Checksum (8bit). If the transmission data is correct, the checksum is equal to "Temperature integer data+ temperature fractional part + humidity integer data + humidity decimal data".The system take the last eight of the results calculated. DHT11 communication process with the microprocessor is shown in Figure III:

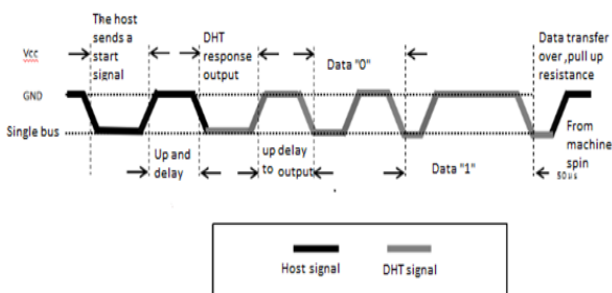


Figure III Communication sequence chart

The communication timing DHT11 and a microprocessor, its data acquisition flow chart shown

in Figure IV.

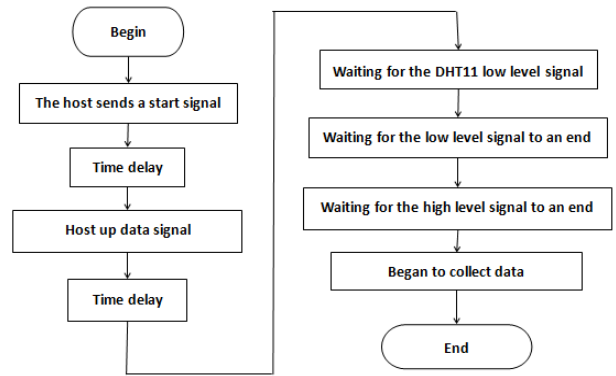


Figure IV DHT11 data acquisition flow chart

5、ANALYSIS OF THE RESULTS

We use DHT11 temperature and humidity sensor to test the indoor environment in a time period, the temperature and humidity of the collected data is shown in table 1. The paper use humidity measured by hygrometer with precision of 2% RH as humidity, compared with the humidity value of DHT11 sensor measured as shown in Figure V. Mercury thermometer with precision of 0.1 measuring temperature as the temperature of the actual value, compared with DHT11 sensor measured temperature value as shown in Figure VI.

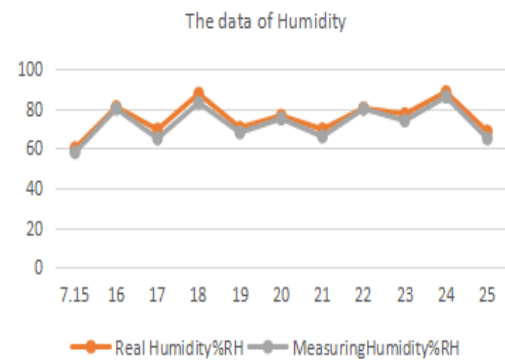


Figure V Humidity contrast diagram

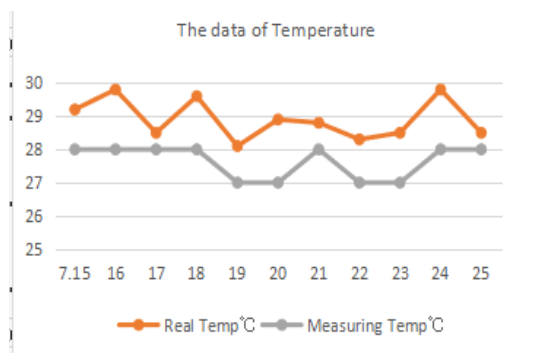


Figure VI Temperature contrast diagram

TABLE 1  
Temperature and Humidity Data Acquisition

| Date | Real Temp℃ | Measuring Temp℃ | Temp Error $\delta_i$ | Real Humidity RH% | Measuring Humidity % RH | Humidity Error $\delta_i'$ |
|------|------------|-----------------|-----------------------|-------------------|-------------------------|----------------------------|
| 7.15 | 29.2       | 28              | -1.2                  | 60.1              | 58                      | -2.1                       |
| 7.16 | 29.8       | 28              | -1.8                  | 80.8              | 80                      | -0.8                       |
| 7.17 | 28.5       | 28              | -0.5                  | 69.5              | 65                      | -4.5                       |
| 7.18 | 29.6       | 28              | -1.6                  | 87.6              | 83                      | -4.6                       |
| 7.19 | 28.1       | 27              | -1.1                  | 70.4              | 68                      | -2.4                       |
| 7.20 | 28.9       | 27              | -1.9                  | 76.5              | 75                      | -1.5                       |
| 7.21 | 28.8       | 28              | -0.8                  | 69.6              | 66                      | -3.6                       |
| 7.22 | 28.3       | 27              | -1.3                  | 80.2              | 80                      | -0.2                       |
| 7.23 | 28.5       | 27              | -1.5                  | 77.3              | 74                      | -3.3                       |
| 7.24 | 29.8       | 28              | -1.8                  | 88.4              | 86                      | -2.4                       |
| 7.25 | 28.5       | 28              | -0.5                  | 68.5              | 65                      | -3.5                       |

The Temp error and humidity error has been given in TABLE1.According to the calculation formula of

standard deviation  $\sigma = \sqrt{\frac{\sum_{i=1}^n \delta_i^2}{n}}$ , we can calculate the

temp standard deviation and humidity deviation as follows:

$$\sigma_{temp} = \sqrt{\frac{\sum_{i=1}^{10} \delta_i^2}{10}} = 1.43 \quad \sigma_{humidity} = \sqrt{\frac{\sum_{i=1}^{10} \delta_i'^2}{10}} = 2.90$$

## 6、 THE EPILOGUE

This paper puts forward the greenhouse temperature and humidity monitoring system based on GSM, on the basis of the overall design of the system software and hardware design in detail.The system is based on SIM900A SMS transceiver module, based on microcontroller STC89C51 control core, has realized the remote monitoring of greenhouse temperature and humidity.This device has the local temperature and humidity remote monitoring alarm, temperature and humidity monitoring alarm, temperature and humidity automatic adjustment, etc.Test results show that the system is simple to use, easy to maintain, with low power consumption, low cost, the characteristics of small volume, light weight, further improve the level of the automation management of greenhouses, convenient for people's production and living.

## References

- [1] Jones, Ian S. F. Engineering Strategies for Greenhouse Gas Mitigation. Cambridge University Press, 2011.06.
- [2] Greenhouse, Lucia.Fathermothergod:My Journey Out of Christian Science. CROWN PUB INC.2011.08
- [3] NI Tian-long. Application of single bus sensor DHT11 in temperature humidity measure and control system[J].Microcontrollers & Embedded Systems, 2011 (4) :45-46.
- [4] HAN Ying-mei, ZHAO Jian-ping. Desiggn of temperature humidity wireless sensor network node based on DHT11 [J].Journal of Jinggangshan University (Natural Science), 2011, 32 (1) :67-70.
- [5] CHITRAPU, PRABHAKAR. Evolution of GSM into the Next Generation Wireless World [C]. IEEE Long Island Systems, Applications and Technology Conference, LISAT, 2007:63-72.
- [6] ZHAO YAN-BO, YE ZHAO-HUI. A Low Cost GSM/GPRS Based Wireless Home Security System [J]. IEEE Transactions on Consumer Electronics, 2008, 54(2): 567-572.
- [7] JEICH MAR, JUN PING HUANG. The Complementary Use of 3G WCDMA and GSM/GPRS Cellular Radio Networks [J]. Wireless Personal Communications, 2009, 43(2): 511-531.
- [8] QU Shun,WANG Wei -hong,ZHANG Kan,et al. IOT SMSalarm system based on SIM900A [J].Modern Electronic Technology,2012,35(5):86-89.
- [9] GAN Zhi -wei,YAN Kai.Wireless data acquisition card's design and implementation based on SIM900A[J].Shanxi Electronic Technology ,2013(1):55-58.
- [10] HE Jinzhi hai-yan MAO, Zhou Guoyun. GSM remote temperature controller design based on single chip microcomputer [J]. Journal of manufacturing automation, 2012 (21) : 138-131.

# Design of portable noninvasive blood glucose instrument based on near infrared optics

LING Zhen-bao; HOU Yang; YANG Yue; ZHAO Peng-fei

(*jilin university instrument science and engineering institute, changchun, 130021*)

**Abstract**--At present, diabetes has become a major killer of human health. In order to detect the blood glucose of diabetic patients quickly and easily, make up for the use of invasive blood glucose meter which brings pollution and pain and so on, we have designed a noninvasive blood glucose measurement method, using a 1650nm infrared light source to irradiate the human fingertip to receive light signals and carry on the photoelectric signal conversion, through A/D acquisition and serial port communication, digital filter and the Fourier transform and so on to complete data processing, finally store the blood glucose value and output. Verified by the experiment, this method can realize the basic measurement of blood glucose concentration. At the same time, it has the characteristics of high speed, no pollution and high practicability. The blood glucose value can be detected in a noninvasive way, which avoid the pain caused by invasive detection.

**Key words**--Near infrared optical; Blood glucose measurement; Noninvasive; Portable

## I. INTRODUCTION

DIABETES is one of the four major diseases that endanger human health. Currently, about 10% of adults worldwide are suffering from the disease. There are about 40 million diabetes patients in our country, and the incidence rate showed an upward trend. Diabetes not only bring a lot of inconvenience and pain to the patients themselves, but also seriously affect the quality of their family life, to the state and society to increase the heavy burden[1-3]. Therefore, rapid and accurate detection of blood glucose, real-time monitoring of blood glucose levels in the human body and early prevention of diabetes is particularly important.

There has yet to find a cure for diabetes, Clinical monitoring of blood glucose concentration is mainly used to guide drug use. Now widely used blood glucose detection method is minimally invasive blood glucose detection, This method requires the collection of finger tip blood, bring pain and the risk of infection to the patient, which limits the frequency of measurement of blood glucose, blood glucose monitoring in diabetic patients can not achieve the desired[4-6].

In view of the above problems, The project is to design a portable non-invasive blood glucose meter based on near infrared spectroscopy, In this technique, the near infrared light sensitive sensor is used to

transmit the finger, and data transmission, processing and modeling of the pulse wave signal collected at the end of the finger is used to realize the display of the blood glucose value and the pulse wave waveform of the host computer. Compared with the traditional minimally invasive blood glucose detection technology, this method has the advantages of fast measurement, no pollution and no wound, and can be measured for many times.

## II. PRINCIPLE OF BLOOD GLUCOSE MEASUREMENT

### BASED ON NEAR INFRARED SPECTROSCOPY

#### A. Blood Glucose Signal Acquisition Principle

When light passes through the body tissue, it will be absorbed by the tissue, and accompanied by reflection, refraction, scattering and other physical phenomena[7]. In this design, we will use near infrared optical transmission principle to achieve blood glucose measurement. Near infrared light is the electromagnetic wave at the wavelength of 780-2500nm, Its penetration depth in biological tissue can reach several millimeters, which can reach the tissues containing blood[8]. The glucose absorption peak of the human finger is just in the wavelength range of near infrared light, so transmission the fingers with a certain wavelength near

infrared, the absorption in tissue of finger tip, obtain the transmission in different light intensity ,the light transmitted through the photoelectric receiving tube is converted into electrical signals, we can get the pulse wave signal carrying blood glucose.The feasibility of this research direction has been confirmed by previous studies.Abroad Robinson[9], etc.the first infrared spectrometer was used to carry out the transmission of the finger, and the non invasive blood glucose measurement was carried out.Shouhei Koyama[10] use PLS to correct the finger attenuated total reflectance spectra in the range of cm-1 1750-700 wave number,The results show that the finger attenuated total reflectance spectroscopy can be used to detect blood glucose in patients with diabetes mellitus.Figure 1 is a schematic diagram of the near infrared transmission finger model.

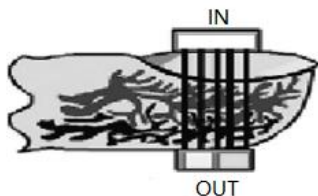


Fig.1 Schematic diagram of near infrared transmission finger

**B. Blood Glucose Concentration Calculation And Data Modeling**

**B1. Blood Glucose Concentration Calculation**

According to Longbow Bill's law,  $A = \lg \frac{I_0}{I} = \epsilon cb$

When the wavelength of the incident light is constant,The absorption degree of the sample material on the light path is only correlated with the concentration and sample material[11],among:

- A: the absorbance of blood glucose;
- I<sub>0</sub>: the incident light intensity, for the fixed value;
- I: transmitted light intensity;
- $\epsilon$  : absorbnacy index ;
- b: Optical path;
- c: Blood glucose concentration;

The relationship of blood glucose concentration can be deduced:

$$c = -\frac{1}{\epsilon b} \lg I + \frac{1}{\epsilon b} \lg I_0$$

Order,x=lgI,y=c,The function relation between Y and X can be obtained,By curve fitting to get the calculation formula of Y, the amount of blood glucose concentration C can be obtained.

**B2. Blood Glucose Data Modeling**

The integral calculation of pulse wave in the whole cycle(Quasi 3 periodic integration),The integral result is used as the independent variable x,Glucose concentration as a dependent variable y,Using the least square method to fit the curve obtained by X and Y,The blood glucose concentration curve is obtained, so that the blood sugar value can be calculated when the integral result is any value, thereby detecting the blood glucose value of different individuals in different physiological states.

**II. THE WHOLE DESIGN OF NON INVASIVE BLOOD**

**GLUCOSE METER**

**A. Hardware Design**

The hardware circuit includes: power supply module, blood glucose signal acquisition module, signal conditioning module, signal acquisition and transmission module.

Power module output constant voltage value  $\pm 12v$  and  $\pm 5v$  .The power supply ripple interference is small, the output voltage is stable, so as not to interfere with the signal acquisition process.

Blood glucose signal acquisition module includes two parts of signal transmitting and receiving.The signal transmitting part adopts the LED lamp with the wavelength of 1650nm as the infrared light source to illuminate the human finger tip,generating optical signal,the receiving part receives the transmitted light from the photodiode, and then converts it into a voltage signal output.

Signal conditioning module includes the amplification of the higher voltage value,filtering and changing polarity,output voltage value is weak signal,therefore, it needs to be amplified by the amplifier to facilitate the acquisition of the signal.Signal carries a large number of high-frequency noise and a large degree of impulse noise, the need for filtering, extraction of useful signal.The resulting voltage signal is bipolar, because the follow-up AD acquisition design for unipolar acquisition, so the need for a unipolar voltage signal processing, adding DC offset, to meet the requirements of the acquisition.

Signal acquisition and transmission module is to get the voltage signal AD acquisition.Using MSP430f449

low voltage, low power consumption, high analog digital conversion accuracy, select the main control chip, complete the blood glucose information to carry the voltage signal A/D collection, the collected data is transmitted to the host computer through the serial port communication, and the display of the data processing and the result is completed by the upper computer.

**B. Software Design**

Software design is divided into two parts, the reading of pulse wave signal and the design of MATLAB host computer interface. Figure 2 is the overall software flow path.

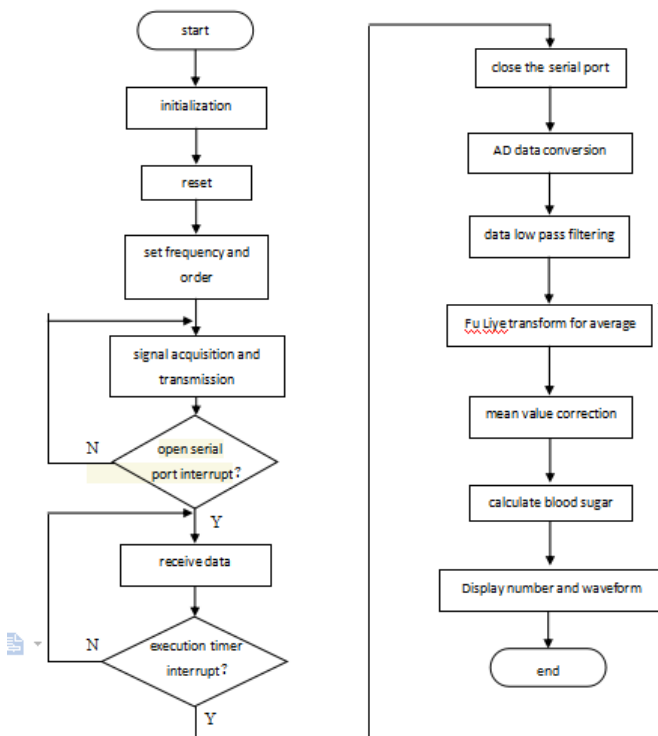


Fig.2 Software flow chart

In the Matlab host computer interface, there are buttons to control the blood glucose testing function, and the filter parameters can be directly set up. Due to the signal collected by the environment and the circuit itself and other factors, with a large number of noise and power frequency interference, and therefore need to be processed by filtering. When the test starts, first, the next bit machine and serial port initialization, and set the filter order and frequency, after the completion of the blood sugar signal acquisition and filtering processing, and through the FU Li-ye transform of the signal to the integral cycle, the integral value of blood sugar into the fitting algorithm, the obtained human blood glucose value is displayed in the upper computer interface and simultaneously displays the collected

pulse waveform. Figure 3 is an upper computer interface to finish the data acquisition and blood glucose detection process through the actual operation.

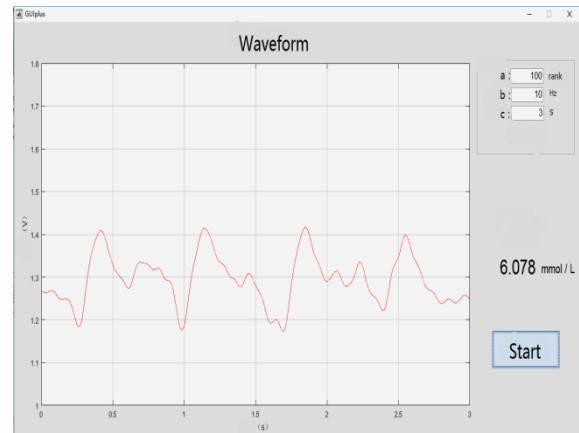


Fig.3 PC interface diagram

**III. SYSTEM TEST AND RESULT ANALYSIS**

**A. Blood Glucose Curve Fitting**

In order to fit the qualitative relationship between integral value  $x$  and the standard value of blood glucose  $f(x)$ , choose 18 physical condition good 20-22 years old men and women, in the fasting, after a meal 0.5-4 hours and other different physiological state, testing the standard value of blood glucose with Sannuo's domestic blood glucose tester, the measured standard values and blood glucose analog (whole period integral quantity) the least square method is used to fit, after fitting, obtain the function of the relationship between the value of blood glucose and the analog quantity is

$f(x) = 6.859x^2 + 9.69x + 7.59$ , the function was used as a blood glucose fitting algorithm to complete the measurement of blood glucose, figure 4 is blood glucose curve.

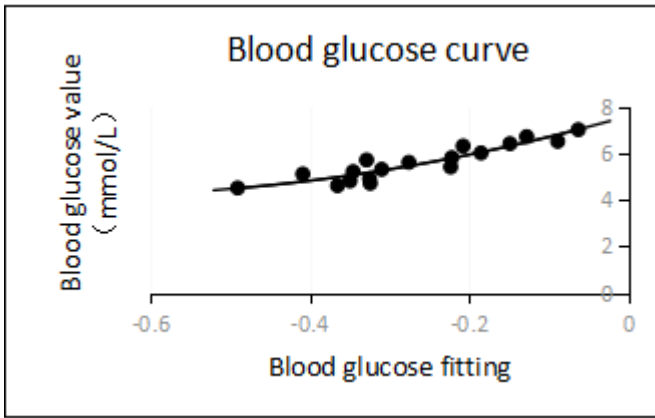


Fig.4 The blood glucose curve fitting

**B. System Test**

In order to carry out experiments on the near infrared measuring blood glucose theory and existing fitting algorithm, with the design of a good noninvasive blood glucose detector, the blood glucose levels were detected at different times, at the same time, the standard value of blood glucose was measured by the SAN NUO family of minimally invasive blood glucose tester (reference volume) compared with the measured value.

Test standard: 10 physical condition good 20-22 years old men and women, measurement of blood glucose levels in the fasting, postprandial 1H and 2H physiological state, ensure that the 10 volunteers in the test before strenuous exercise led to energy loss and emotional stability. The test results are reflected by the blood glucose data sheet and the broken line chart. Table 1 is the results of the comparison of the 10 groups of data measured by the non-invasive blood glucose detector prototype and minimally invasive blood glucose meter. A line graph made of table 1 is shown in Figure 5.

TABLE I NON INVASIVE AND STANDARD BLOOD GLUCOSE METER

TEST DATA ANALYSIS TABLE

| number<br>value  | 1     | 2     | 3     | 4     | 5     |
|------------------|-------|-------|-------|-------|-------|
| Real (mmol/L)    | 6.150 | 6.658 | 5.569 | 5.605 | 7.012 |
| Standad (mmol/L) | 6.4   | 6.0   | 4.9   | 5.3   | 8.0   |
| Error (mmol/L)   | 0.250 | 0.658 | 0.669 | 0.305 | 0.988 |
| Error (%)        | 3.9%  | 10.9% | 13.6% | 5.7%  | 12.3% |
| number<br>value  | 6     | 7     | 8     | 9     | 10    |
| Real (mmol/L)    | 5.463 | 6.356 | 6.133 | 4.787 | 4.224 |
| Standad (mmol/L) | 5.0   | 6.3   | 5.7   | 4.5   | 4.8   |
| Error (mmol/L)   | 0.463 | 0.056 | 0.325 | 0.287 | 0.576 |
| Error (%)        | 9.2%  | 0.1%  | 7.6%  | 6.4%  | 12.0% |

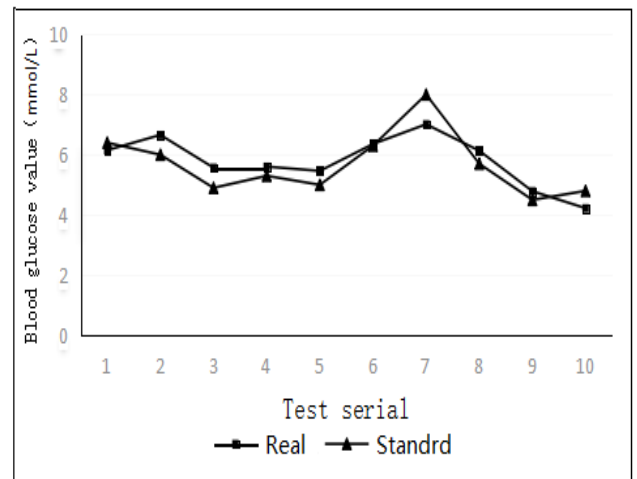


Fig.5 Non invasive and standard blood glucose meter test data comparison line chart

**C. test results analysis**

By calculating comparison, the error between the theoretical blood glucose value and the actual measured value is 0.056-0.988mmol/L in the ten groups of data, the maximum measurement error is 13.6%, and the correlation coefficient between the measured value and the standard value is 0.8503.

Therefore, verified by analysis, the non-invasive blood glucose measuring instrument can be used for the qualitative analysis of the blood sugar level of the human body and the detection of the blood sugar level. But for more accurate and more stable

measurement, it is necessary to further improve the device and algorithm.

## V. CONCLUSION

This study is based on the basic theory of near infrared optics, a non-invasive blood glucose detection device was designed based on Longbow Bill's law, prior to use should be the first to determine the status of the diet and health status of the detector, get the normal blood glucose concentration range and realize the detection process, qualitative analysis.

Because there are some defects in this research, for example, the measurement accuracy is not high enough, the blood of other tissue components on the measurement of interference and other issues. So in future research, the interference of other components in blood glucose signal acquisition should be further excluded, to improve fitting algorithm, to improve the theoretical basis, increasing the number of samples, so that the blood glucose measurement results would be more accurate and reliable.

## Reference:

- [1] Wen Jing, Chen Lili. Self-monitoring of blood glucose problems and nursing countermeasures [J]. *Modern nursing*, 2006, 25: 2393-2394.
- [2] Ma Jin Zi, Zhu Jianming, Chen Zhencheng. Based on the energy metabolism of conservation law of noninvasive blood glucose detector [J]. *Guilin University of Electronic Technology*, 2015, 01: 35-38.
- [3] Li Gang, Zhou Mei, Wu Hongjie, Lin Ling. Non-invasive blood glucose detection status of research and development of optical methods [J]. *Spectroscopy and Spectral Analysis*, 2010, 10: 2744-2747.
- [4] Zhu Jianming, Chen Zhencheng, Jin Xingliang, Wang Diya. Portable noninvasive blood glucose detection instrument based on DSP technology [J]. *Journal of electronic measurement and instrument*, 2009 practices: 108-112.
- [5] Chen Wenliang, Xu Kexin, Du Zhenhui, Liu Rong, Fan Shifu. Body non-invasive blood glucose monitoring technology [J]. *Journal of Scientific Instrument*, 2003, S1: 258-261 + 265.
- [6] Liu Guangda, Cai Jing, Sun Maolin, Song Qianli, Liu Mengwan, Wang Qingji. Based on the photoelectric volume pulse wave of noninvasive blood glucose measurement study [J]. *Journal of Jilin University (information science edition)*, 2015, 01: 52-56.
- [7] Lu Qipeng. Physiological background of non invasive blood glucose detection in near infrared spectroscopy [J]. *Optical mechanical and electrical information*, 2010, 12: 44-48.
- [8] Chen Xingdan, Gao Jing, Ding Haiquan. Theory of noninvasive blood glucose monitoring method of infrared spectrum (invited) [J]. *Chinese optics*, 2012, 317: 317-326.
- [9] Robinson M R, Eaton R P, Haaland D M, et al. Noninvasive glucose monitoring in diabetic patients: a preliminary evaluation [J]. *Clin. Chem.*, 1992, 38: 1618-1622.
- [10] Shouhei K, Yuki M, Takuro H, et al. Non-invasive Measurement of Blood Glucose of Diabetic Based on IR Spectroscopy [J]. *SICE Annual Conference 2010*, 18-21 Aug. 3425-3426.
- [11] Yang Xing. Blood glucose noninvasive detection system based on near infrared transmission method [D]. *Chongqing University*, 2012.